UNIVERSITY OF CALIFORNIA SAN DIEGO

Using the Einstein-Infeld-Hoffmann Equations to Determine the Equivalence of Rotational Frames with Gravitational Forces: A New Tool For Cosmological Investigation

A dissertation submitted in partial satisfaction of the
requirements for the degree
Doctor of Philosophy

in

Physics

by

Daniel Patrick Gonzales

Committee in charge:

Professor Thomas W. Murphy, Chair
Professor George M. Fuller, Co-Chair
Professor Adam Burgasser
Professor Jeffrey Rabin

2023

The dissertation of Daniel Patrick Gonzales is approved, and it is acceptable in quality and form for publication on microfilm and electronically.

University of California San Diego

2023

DEDICATION

If you take away all matter, there is no space.

If you take away Justine, there is no Dan.

TABLE OF CONTENTS

LIST OF FIGURES

LIST OF TABLES

ACKNOWLEDGEMENTS

My sincerest gratitude goes to Dr. Jeff Veal, whose enthusiasm for physics and astronomy was so great it helped me realize my passion for the subject. And of course, to Dr. Tom Murphy for being the most patient and engaged of mentors.

VITA

2023	Graduate Student Distinguished Teaching Award, University of California San Diego
2021-2022	Instructor of Record, Physics Department, University of California San Diego
2021-2023	Graduate Student Outreach Coordinator, Physics Department, University of California San Diego
2018-2023	Graduate Student Researcher, Murphy Gravitational Astrophysics Lab, University of California San Diego
2018	San Diego Fellowship, University of California San Diego
2014-2018	Research Scientist, Space and Naval Warfare Center, San Diego, CA
2014	B. S. in Physics with Specialization in Astrophysics *magna cum laude*, University of California San Diego
2014	John Holmes Malmberg Prize, Department of Physics, University of California San Diego
2014	Dean's Undergraduate Award of Excellence, Dean of Physical Sciences, University of California San Diego
2012-2014	DoD SMART Scholarship Award Recipient
2012	Lipp Foundation Astronomy/Physics Excellence Scholarship

PUBLICATIONS

N.R. Colmenares, J.R.R. Battat, D.P. Gonzales, T.W. Murphy Jr., S. Sabholk Fifteen-years of millimeter accuracy lunar laser ranging with APOLLO: data reduction and calibration Submitted to Publications of the Astronomical Society of the Pacific for review on 4/25/2023

J.R.R. Battat, E. Adelberger, N.R. Colmenares, M. Farrah, D.P. Gonzales, C.D. Hoyle, R.J. McMillan, T.W. Murphy Jr., S. Sabholk, C.W. Stubbs Fifteen years of millimeter accuracy lunar laser ranging with APOLLO: dataset characterization Submitted to Publications of the Astronomical Society of the Pacific for review on 4/25/2023

S. Sabholk, J.B.R. Battat, N.R. Colmenares, D.P. Gonzales, T.W. Murphy Jr. Examining the Full Moon Deficit in Lunar Laser Ranging with Simulation and Experiment (Forthcoming)

D.P. Gonzales, Z. Ritsema, C. Reinhardt, D. Tsintikidis, D. Talcott, K. Rutkowski, Target Acquisition Task Modeling for Small Vessels in Maritime Scenarios: Optical Zoom Performance Metrics Military Sensing Symposium, Battlespace Survivability and Discrimination Conference, 2016 (Distributed to Department of Defense and Contractors Only)

D.P. Gonzales, S. Lynch. Radiosonde data-based Cn2 Climatology. Military Communications Conference (MILCOM), 2015 IEEE (Restricted-Access Technical Program, Distributed to Department of Defense and Contractors Only)

C. Reinhardt, Z. Ritsema, D.P. Gonzales, D. Tsintikidis, B. Preece, T DuBosq Periscope Target Acquisition Simulation and Modeling Military Sensing Symposium, Battlespace Survivability and Discrimination Conference, 2016 (Classified Secret, Distributed to Department of Defense and Contractors Only)

ABSTRACT OF THE DISSERTATION

Using the Einstein-Infeld-Hoffmann Equations to Determine the Equivalence of Rotational Frames with Gravitational Forces: A New Tool For Cosmological Investigation

by

Daniel Patrick Gonzales
Doctor of Philosophy in Physics

University of California San Diego, 2023

Professor Thomas W. Murphy, Chair

In order to better understand the equivalence between gravitational forces of rotating bodies and rotating frames, I use the Einstein-Infeld-Hoffman equations to develop a cosmological appropriate integral for such study. I find that the ΛCDM model of cosmology along with General Relativity (GR) are enough to get a near equivalence between rotational frames and gravity. Then, using this integral and asserting an interpretation of Mach's Principle (MP), I examine what might need to change from the standard ΛCDM cosmology to make a perfect equivalence. One topic developed and tested is a modified ΛCDM cosmology with a time varying gravitational coupling. This model is compared with supernova distance modulus data against ΛCDM. I find that in some cases this modified cosmology can statistically outperform ΛCDM.

Chapter 1

Introduction

An undergraduate's first encounter with General Relativity is often accompanied by an image of an astronaut in a rocket with no windows. This lonely astronaut makes a number of observations that include projectiles making parabolic arcs with a constant acceleration $\boldsymbol{a}$. We teach the student that the astronaut, not being able to observe outside of the rocket's cabin, cannot determine whether they are on a planet's surface with its mass and radius such that $\boldsymbol{a} = -GM/r^2\hat{\boldsymbol{z}}$, or if they are far away from any massive body with their rocket accelerating at $-\boldsymbol{a}$. We would state that both these situations are in principle equivalent, and no experiment the astronaut can make will distinguish between the two. If the astronaut were in fact on a planet, we would attribute the parabolic arcs to the force of gravity. If they were in the second case, we could state that the arcs are caused by the straight line—inertial—trajectories of the projectiles being observed in an accelerating—non-inertial—frame. The ability to make the equivalence between a uniform gravitational[1] field and an

[1]It should be noted that the gravitational field at the planet's surface is *not* uniform, but is in fact divergent. As a result, an astronaut in a sealed cabin can in principle with very precise measurements tell the difference between the two situations described. Implicit in the setup is an assumption that the astronaut's equipment cannot make measurements precise enough to differentiate elliptical trajectories from perfect parabolas. However, this is a common scenario when introducing these

accelerating frame is a foundational concept in our modern understanding of gravity.

Now let's consider not simply linear accelerations but rotations. For any child on a merry-go-round (MGR) they understand that the way things move on the merry-go-round is dramatically different from their everyday experiences. The most apparent difference is that they seem to be forced away from the center of the MGR, despite the lack of another object to provide this force. Some particularly observant kids might notice that—even in the absence of wind—projectiles follow paths that are curved in the horizontal direction as well as the vertical. We could provide an explanation to the children that these unusual experiences are caused by the straight line—inertial—trajectories of the objects being observed in a rotating—non-inertial—frame. In fact, if our astronaut from the previous paragraph were to make similar observations of projectile trajectories, they would know without a doubt that their rocket was rotating relative to the fixed stars—even *without* making any observations outside of their rocket. However, in the case of rotation, we don't try to draw an equivalent picture where the curved trajectories are caused by gravity. This is not because they are children and the equivalence might be difficult to explain to them. It might even be rare to draw attention to this equivalence in a graduate level General Relativity course. Why is that? Is there a gravitational–inertial equivalence to be made between trajectories observed in rotating frames? Or rather, is there something that is fundamentally different between rotation and linear acceleration? These questions along with others will be explored in this work.

concepts in General Relativity to illustrate the equivalence of gravitational fields and accelerations.

1.1 General Relativity and the Einstein-Infeld-Hoffman Equations

General Relativity (GR) is a geometric theory of gravity developed by Albert Einstein in 1915. It is widely regarded as the best and most accurate theory of gravity. It generalizes special relativity and Newton's theory of universal gravity into a unified framework. Specifically, GR relates the curvature of space-time to local energy-momentum distribution. In turn, bodies within the curved space-time follow straight lines (geodesics). The fact that space and time are coupled and can in fact be curved can be quite perplexing to many people. Nevertheless, GR makes testable predictions for a remarkable range of phenomena that are confirmed by experiment. Some of the most interesting of these predictions include; the perihelion shift of Mercury, light deflection by massive bodies, gravitational lensing effects, and gravitational waves from in-spiraling neutron stars and black holes.

The theory of GR is succinctly captured in the tensor equation:

$$G_{\mu\nu} = \frac{8\pi G}{c^4} T_{\mu\nu} - \Lambda g_{\mu\nu}. \tag{1.1}$$

These are known as Einstein's Field Equations. Broadly speaking, the left-hand side of the equation is a description of the geometry of space-time while the right-hand side describes the energy and momentum distribution through the so called energy-momentum tensor $T_{\mu\nu}$. Λ in the equation is called the cosmological constant and is the energy density of space or the vacuum energy.

This elegant framing can hide the true complexity of the theory. Tucked into this equation are ten coupled second-order partial differential equations. Because of this complexity, only a handful of exact solutions to the Field Equations have been found. And all of those that have been found have utilized symmetries of the energy and momentum distribution of the system to drastically reduce the number of coupled differential equations to a manageable number. Some of these solutions include the

Schwarzschild Exterior Solution for points outside a non-rotating spherically symmetric body (used to describe trajectories of bodies exterior to a slowly rotating body like a planet or star); The Kerr Exterior Solution for points outside an axially symmetric rotating body (used to describe trajectories outside a rapidly rotating body like a black hole or neutron star); and the Friedman-Lemaître-Robertson-Walker (FLRW) solution which describes a homogeneous and isotropic expanding perfect fluid (used as the basis for cosmological models).

Because no general solution exists to the Einstein Field Equations, working with systems that present no apparent symmetry can be nearly impossible to analyze using the full tensor theory of GR. Because of this, a common technique for solving the Einstein Field Equations in a weak field limit is to introduce "Nearly Lorentz" coordinate systems (pp. 189 [Sch09], pp. 435 [MTW73]) with metric components:

$$g_{\alpha\beta} = \eta_{\alpha\beta} + h_{\alpha\beta}, \quad \text{where, } |h_{\alpha\beta}| \ll 1. \tag{1.2}$$

In Equation 1.2 $\eta_{\alpha\beta}$ are the components of the flat Minkowski metric, and $h_{\alpha\beta}$ are the components of a linearized gravitational field. Given these components for the metric tensor, one can expand Einstein's Field Equations to powers of $h_{\alpha\beta}$ using a coordinate frame in which Eq. 1.2 holds. This technique has been applied to many situations. Two better known cases are gravitational waves (ch. 9 [Sch09], part VIII [MTW73]) and the equations of motion for massive bodies (ch. 39 [MTW73], pp. 149 [Wil95]).

In general, any metric theory of gravity can utilize this technique of having a "Nearly Lorentz" coordinate system, not just GR. The equations of motion for any theory of gravity can be written in the so called Parameterized-Post-Newtonian formalism (PPN). The "Post-Newtonian" part of PPN refers to the fact that these are corrections to Newton's universal theory of gravity, usually in terms of $(v/c)^2$. The "Parameterized" part of PPN refers to 10 parameters: γ related to the amount of spatial curvature generated by mass; β related to the degree of non-linearity in the

gravitational field; ξ and three α parameters related "preferred frame" effects; four ζ parameters related to "breakdowns in global conservation laws" ([Wil11], box 39.5 [MTW73]). In GR both γ and β are equal to one. All other parameters are equal to zero. Many local experiments of gravity have been made that tightly constrain the parameters of the framework to coincide with the GR values.

Even though spacetime is curved, the PPN coordinates provide a natural "3+1" split of spacetime into space plus time. We can then treat that split using the notation of three-dimensional, flat-space vector analysis [MTW73] pp. 1074. This treatment of curved spacetime might seem fundamentally incorrect, PPN has been very well tested by experiment and observation. Clifford Will sums it up nicely in the title of his 2011 paper "On the Unreasonable Effectiveness of the post-Newtonian Approximation in Gravitational Physics" [Wil11]. Experiments have determined the PPN parameters to be consistent with GR. Table 1.1 summarizes the degree to which we have experimentally verified the parameters to their values in GR.

In GR the equations of motion for massive bodies are referred to as the Einstein-Infeld-Hoffman Equations (EIH) [EIH38]. These equations determine the accelerations on a particle labeled with the subscript, A, that are imparted on it by the gravitational interactions of the distribution and motions of particles summed over with labels B, and in cases where double sums are required C. The EIH Equations contain, as I present them,[2] twelve vector terms.

[2]Various sources represent the EIH Equations with slightly different conventions, usually in how the sums over the B and C particles are grouped together or using different vector conventions (such as expanding out a BAC-CAB rule).

Table 1.1: Parameters in the general PPN framework. For GR, the γ and β parameters in the top two lines are equal to one, while all others are equal to zero. The second column in the table gives the experimental limits of the various parameters. The third column gives a short description of the experiments that best constrain those particular parameters. This table is reproduced from [Wil11] (LLR indicates Lunar laser ranging).

Parameter	Limit	Remarks
$\gamma - 1$	2.3×10^{-5}	Cassini spacecraft tracking
	4×10^{-4}	VLBI radio deflection
$\beta - 1$	3×10^{-3}	perihelion of Mercury
	2.3×10^{-4}	no Nordtvedt effect, LLR
ξ	10^{-3}	no anomalous Earth tides
α_1	10^{-4}	no anomalies in lunar, binary-pulsar orbits, LLR
α_2	4×10^{-7}	alignment of sun and ecliptic
α_3	2×10^{-20}	no pulsar "self" accelerations
ζ_1	2×10^{-2}	combined PPN bounds
ζ_2	4×10^{-5}	no binary "self"-accelerations
ζ_3	10^{-8}	no Lunar "self"-acceleration, LLR

$$
\begin{aligned}
\boldsymbol{a}_A = & \sum_{B\neq A} \frac{Gm_B}{r_{AB}^2}\hat{\boldsymbol{n}}_{BA} \\
& + \frac{1}{c^2}\sum_{B\neq A}\frac{Gm_B}{r_{AB}^2}\Bigg[v_A^2 + 2v_B^2 - 4(\boldsymbol{v}_A\cdot\boldsymbol{v}_B) - \frac{3}{2}(\hat{\boldsymbol{n}}_{BA}\cdot\boldsymbol{v}_B)^2 \\
& \qquad\qquad - \frac{Gm_A}{r_{AB}} - 4\frac{Gm_B}{r_{AB}}\Bigg]\hat{\boldsymbol{n}}_{BA} \\
& - \frac{1}{c^2}\sum_{B\neq A}\frac{Gm_B}{r_{AB}^2}[\hat{\boldsymbol{n}}_{BA}\cdot(4\boldsymbol{v}_A - 3\boldsymbol{v}_B)](\boldsymbol{v}_A - \boldsymbol{v}_B) \\
& - \frac{1}{c^2}\sum_{B\neq A}\sum_{C\neq A,B}\frac{Gm_B}{r_{AB}^2}\left[4\frac{Gm_C}{r_{AC}} + \frac{Gm_C}{r_{BC}}\right]\hat{\boldsymbol{n}}_{BA} \\
& + \frac{1}{c^2}\frac{1}{2}\sum_{B\neq A}\frac{Gm_B}{r_{AB}}\Big[\hat{\boldsymbol{n}}_{BA}(\hat{\boldsymbol{n}}_{BA}\cdot\boldsymbol{a}_B) + 7\boldsymbol{a}_B\Big] \\
& + O(c^{-4})
\end{aligned}
\tag{1.3}
$$

A quick point to make before getting into the details of this equation, one may recognize the first term as Newton's Law of Universal Gravitation. All other terms are GR corrections of order v^2/c^2. You may notice that the numerical coefficients in front of all the terms are simple rational numbers. This is a result of the fact that the PPN parameters in GR are either one or zero.

A list of the various symbols used in the equations and their meanings is presented as follows:

1. G and c are the typical physical parameters for the gravitational constant and speed of light, respectively. Their values in SI units being $G = 6.67 \times 10^{-11}$ $\mathrm{Nm^2/kg^2}$ and $c = 3.00 \times 10^8$ m/s. Because of the nature of this work, it is also worth mentioning that c is also the speed of gravity.

2. m_X is the mass of particles X $(X = A, B, C)$.

3. Vectors $\boldsymbol{r}_X$, $\boldsymbol{v}_X$, and $\boldsymbol{a}_X$ represent the barycentric position, velocity and acceleration vectors of particle X.

4. r_{XY} is the scalar distance between the X and Y particles.

5. $\hat{\boldsymbol{n}}_{XY}$ is the unit vector pointing from the X mass to the Y mass, $\hat{\boldsymbol{n}}_{XY} = (\boldsymbol{r}_Y - \boldsymbol{r}_X)/r_{XY}$.

Even though these equations are a simplification of the ten coupled partial differential equations GR begins with, they are still complicated. Handling such a large equation can be quite daunting and confusing to discuss. Given that, I will introduce the following labeling convention for each of the terms. Each term will be labeled in roughly alphabetical order using script capital roman letters in the following way:

$$\begin{aligned}\mathbf{a}_A = &\boldsymbol{\mathcal{N}} \\ &+ [\boldsymbol{\mathcal{A}} + \boldsymbol{\mathcal{B}} + \boldsymbol{\mathcal{C}} + \boldsymbol{\mathcal{D}} \\ &\qquad + \boldsymbol{\mathcal{E}} + \boldsymbol{\mathcal{F}}] \\ &+ \boldsymbol{\mathcal{G}} \\ &+ [\boldsymbol{\mathcal{H}} + \boldsymbol{\mathcal{I}}] \\ &+ [\boldsymbol{\mathcal{J}} + \boldsymbol{\mathcal{K}}].\end{aligned} \tag{1.4}$$

This was typeset in such a way as to make it easier for the reader to pair the letter label of each term in the second equation with its more explicit pair in the Equation 1.3.[3]

[3]If you spend a lot of time with these equations, you feel like they are your children and may want to name them. May I suggest the following names Newton, Albert, Banesh, Charles, Daniella, Ernst, François, Galileo, Hermann, Isaac, John and Kip. Only two of these are not named after scientists that have contributed to topics discussed in this thesis. Sadly, these are mostly boys names, not for want of attempting to include some diversity in this list. Hopefully by the time Daniella and Isaac are ready to write their PhD dissertations, if like their old man they want to include a silly list of names in theirs, they will have a more diverse pool of names to choose from.

Though the equation may seem complicated and exotic, those familiar with physics at various levels may find a few familiar faces within the equations. As a reminder, the first term, $\boldsymbol{\mathcal{N}}$, is simply Newton's Law of Universal Gravitation or the inverse square law of gravitation. The next two terms ($\boldsymbol{\mathcal{A}}$ & $\boldsymbol{\mathcal{B}}$) and part of term $\boldsymbol{\mathcal{C}}$ account for kinetic energy and their difference for both the A and B particles. It can be noted that all terms except for the $\boldsymbol{\mathcal{G}}$ and $\boldsymbol{\mathcal{K}}$ terms are parallel (or antiparallel) to the ray joining particle A to particle B. These two terms then can help to partially account for the phenomenon known as frame dragging. Additionally, it can be shown that parts of the $\boldsymbol{\mathcal{C}}$ and $\boldsymbol{\mathcal{G}}$ terms are the result of expanding out the vector triple product BAC-CAB rule. The origin of that vector triple product is the phenomenological effect of gravitomagnetism. Gravitomagnetism is the gravitational analogue to magnetism. In electromagnetism, where moving charges create magnetic fields, so to do moving masses create gravitomagnetic fields. And again, just like a moving charge in a magnetic field has its trajectory deflected by magnetic force, a moving mass in a gravitomagnetic field will be deflected by a gravitomagnetic force.

It is worth noting that lunar laser ranging (LLR), has played a large role in tightening the constraints on some of these parameters. Of course, much of the resent progress in LLR has been performed here at UCSD under Tom Murphy. Thus working from the EIH Equations of motion, as this dissertation does, provides a firm footing in tested GR.

1.2 Inertial Forces

In this section we turn away from GR and discuss inertial forces in terms of classical Newtonian mechanics. If we consider two frames, one an inertial frame labeled A, and another non-inertial rotating frame labeled B, the rotation of the noninertial frame is characterized by the vector quantity $\boldsymbol{\omega}$. The acceleration of a body observed in the rotating frame is given by the formula:

$$\boldsymbol{a}_B = \boldsymbol{a}_A - 2\boldsymbol{\omega} \times \boldsymbol{v}_B - \boldsymbol{\omega} \times (\boldsymbol{\omega} \times \boldsymbol{x}_B). \tag{1.5}$$

In this formula, the kinematic variables with subscript B are what an observer rotating with the noninertial frame would measure. The acceleration $\boldsymbol{a}_A$ is due to *real external* forces acting on the body in the inertial frame. The two additional terms in the formula are the so-called *fictitious* or inertial forces. It is important to emphasize that $\boldsymbol{\omega}$ is the rotation rate of frame B relative to A. Observers in B would characterize the rotational motion of A as $-\boldsymbol{\omega}$.

A general derivation for these (or any other fictitious forces) can be done by considering a non-inertial frame B whose origin relative to the inertial one is given by $\boldsymbol{X}_{AB}(t)$. Let the position of a particle with mass m in the B frame be given by $\boldsymbol{x} = \Sigma_{j=1}^{3} x_j \hat{\boldsymbol{u}} j$. Here $\hat{\boldsymbol{u}}_j$ are the unit vectors in the $j = 1, 2, 3$ directions. An interesting note, naturally $\hat{\boldsymbol{u}}_j$ cannot change in magnitude, so their time derivatives can only represent a rotation of frame B. Additionally, $\boldsymbol{X}_{AB}$ is only a relationship between the origins of A and B and therefore can only represent a translation. We can then write down the position of the particle in A's frame in terms of it's position in B and $\boldsymbol{X}_{AB}$:

$$\boldsymbol{x}_A = \boldsymbol{X}_{AB} + \sum_{j=1}^{3} x_j \hat{\boldsymbol{u}}_j. \tag{1.6}$$

To determine accelerations and thus forces, we only need to differentiate this equation twice with respect to time. We get:

$$\boldsymbol{a}_A = \boldsymbol{A}_{AB} + \boldsymbol{a}_B + 2\sum_{j=1}^{3} v_j \frac{d\hat{\boldsymbol{u}}_j}{dt} + \sum_{j=1}^{3} \frac{d^2\hat{\boldsymbol{u}}_j}{dt^2}. \tag{1.7}$$

The first term is the translational acceleration of frame B relative to A. By solving for $\boldsymbol{a}_B$ and multiplying by the particle's mass, we can write this as:

$$\boldsymbol{F}_B = \boldsymbol{F}_A + \boldsymbol{F}_{\text{fict}}, \tag{1.8}$$

where $\boldsymbol{F}_A = m\boldsymbol{a}_A$ are the real external forces as determined in the inertial frame. $\boldsymbol{F}_{\text{fict}}$ is the collection of other "force" terms that arise purely from the rotation and acceleration of B relative to A:

$$\boldsymbol{F}_{\text{fict}} = -m\boldsymbol{A}_{AB} - 2m\sum_{j=1}^{3} v_j \frac{d\hat{\boldsymbol{u}}_j}{dt} - m\sum_{j=1}^{3} \frac{d^2\hat{\boldsymbol{u}}_j}{dt^2}. \tag{1.9}$$

For non-inertial frames without any translational acceleration, the first term is naturally zero. The other two terms would lead to the Coriolis and centrifugal forces, respectively.

1.3 Mach's Principle

Mach's Principle is a philosophical concept that suggests the inertial properties of matter arise from the influence of all the matter in the universe. It was proposed by physicist and philosopher Ernst Mach in the late 19^{th} century as a possible explanation of inertia.

Perhaps more to the point: what are inertial frames? If these are the frames in which Newtonian mechanics works and bodies under no external forces follow straight lines, which frames are they? Is there an absolute frame which all other frames move relative to? Newton seemed to think so [Mau12]. However, because physics worked even in Galilean relativity, no observational evidence could be made to support such an idea. Whether absolute space and time existed was a moot point. So long as you are in a Galilean frame with respect to another inertial frame, physics experiments would agree with one another. Therefore, rather than having a single—absolute—inertial frame, an infinite number could be defined, so long as they were in relative constant motion with respect to one another. Still, some frames appeared to not be inertial. Any frame in which the fixed stars were rotating about a central axis was NOT an inertial frame, because Newton's laws did not work in those frames.

Then Albert Einstein formulated his special theory of relativity. His theory laid to rest any possibility of the existence of an absolute and fundamental space and time. His new space-time had novel and interesting properties, where the lengths of objects were not absolute but depended on a body's motion relative to an observer. Likewise, two identical and perfect clocks in relative motion to one another would disagree on how much time had passed between events. Even if one clock measures no time passing between two events, that is, the events are simultaneous, the same events would *not* be simultaneous according to the other clock. Despite this definitive argument against the notion of an absolute space and time, a condition still existed which needed to be met in order for a frame to be considered inertial: the distant stars should not be in relative rotation to that frame. The frame in which the distant stars are rotationally fixed was seemingly still an absolute and fundamental frame.

Why is this frame special? Are there reasons within our physical laws that make it special? Or is it just the way the universe is, existing with an infinite number of Minkowski inertial frames but only one rotational inertial frame? In all my reading of Mach's principle, I think these are the core questions that philosophers and scientists want to answer. Part of the motivation for this dissertation is to address some of these questions. Furthermore, I think that supporters and investigators of Mach's Principle hope that giving a physical reason for this seemingly singular inertial frame would yield deep insights into the nature of space-time, mass-energy, and gravity.

Despite the many scientists and philosophers that investigate MP, no clear consensus has been met on what *exactly* is MP.[4] Hermann Bondi and Joseph Samuel categorized and enumerated what they felt were the most common interpretations of MP in the literature. They came up with 11 classes of MP [BS97]:

- Mach0*: The universe, as represented by the average motion of distant galaxies, does not appear to rotate relative to local inertial frames.

[4]Or maybe non consensus exists *because* so many scientists and philosophers have investigated it.

- Mach1*: Newton's gravitational constant G is a dynamic field.
- Mach2: An isolated body in otherwise empty space has no inertia.
- Mach3*: Local inertial frames are affected by the cosmic motion and distribution of matter.
- Mach4: The universe is spatially closed.
- Mach5: The total energy, angular and linear momentum of the universe are zero.
- Mach6*: Inertial mass is affected by the global distribution of matter.
- Mach7: If you take away all matter, there is no more space.
- Mach8*: $\Omega \equiv 4\pi\rho GT^2$ is a definite number, **of order unity**, where ρ is the mean density of matter in the universe, and T is the Hubble time.
- Mach9: The theory contains no absolute elements.
- Mach10: Overall rigid rotations and translations of a system are unobservable.

It is important to note that this list of interpretations is not exhaustive, nor does the truth value of one imply the truth value of another. Items marked with asterisks (*) can be related to this work and will be addressed as we come across examples of them.

One modern experimental technique that can be used to verify Mach0 with increasing precision is the use of ring laser gyros (RLGs). RLGs are devices that use the Sagnac effect to measure rotations to high precision. In an RLG, a laser beam is split into two counter-propagating beams that travel around a closed loop in opposite directions. The two beams recombine at a detector, where they interfere with each other. If the loop is not rotating, the two beams will experience the same amount

of time delay and arrive at the detector at a static phase difference. However, if the loop is rotating, the path length of the beam traveling in the direction of rotation is shorter than the path length of the beam traveling in the opposite direction. This leads to a phase shift between the two beams. Naturally, this will cause an interference pattern at the detector. The shift in the interference pattern is proportional to the area enclosed by the loop and the angular velocity of the rotation, and is known as the Sagnac phase shift [DV20]. One promising experiment is the Gyroscopes IN General Relativity (GINGER) project, which aims to measure the Earth rotation rate relative to the International Earth Rotation Reference System with a sensitivity to a part in 10^{12}. Its prototype project, GINGERINO, has demonstrated its own capabilities to a part in 10^9 [ABB+23]. This makes GINGERINO as capable as another, longer running RLG experiment, the Wettzell "G" ring laser [BSG+19]. Better than 10^{-9} sensitivity in RLG experiments is necessary to test GR terms measuring Lense-Thirring and de Sitter precessions[5] on the Earth [VTB+22]. It is worth noting that while the 10^{-12} is impressive and useful for testing and constraining GR, this sensitivity is about 10^{-16} radians per second, which may not be *quite* cosmologically relevant yet, as it would allow about 30 radians of accumulation (5 wraps) over the age of the universe 13.8 Gyr.

1.4 Cosmology

Cosmology is a field of study that aims to understand the origins, evolution, and structure of the universe as a whole. Additionally, cosmology investigates the distribution of matter and energy throughout the universe. Our modern interpretation of cosmology is intimately intertwined with gravity and GR. Indeed, as we will see in the next subsection, the foundational principles of modern cosmology are rooted in one of the few exact solutions of Einstein's Field Equations. Furthermore,

[5]De Sitter precession is also commonly known as geodetic precession.

driven by observations, the simplest model for the evolution of our universe, known as Lambda-CDM, ΛCDM, predicts a mysterious form of mass-energy known as dark energy.

1.4.1 FLRW

The Freidmann-Lemaître-Robertson-Walker metric is an exact solution of Einstein's Field Equations. The symmetries used to simplify the field equations are that the universe is spatially homogeneous and isotropic. The FLRW metric makes no assumptions regarding the temporal nature of space-time or its overall spatial curvature. The line element for the FLRW metric is given by:

$$\mathrm{d}s^2 = -\mathrm{d}t^2 + a^2(t)[\mathrm{d}r^2 + r^2\mathrm{d}\Omega^2]. \tag{1.10}$$

FLRW describes the geometry of space-time in terms of scale factor, $a(t)$. The scale factor determines the size of the universe at any given time, with the typical convention that in the present epoch, t_0, $a(t_0)$ is equal to one. From this line element, the equations of motion for the scale factor in a flat universe are determined to be:

$$\left(\frac{\dot{a}}{a}\right)^2 \equiv H^2 = \frac{8\pi G}{3}\rho - \frac{kc^2}{a^2} + \frac{\Lambda c^2}{3}, \tag{1.11}$$

$$2\frac{\ddot{a}}{a} + \left(\frac{\dot{a}}{a}\right)^2 = 2\dot{H} + H^2 = -\frac{8\pi G p}{c^2} + \frac{\Lambda c^2}{3} - \frac{kc^2}{a^2}. \tag{1.12}$$

The top equation is known as the Friedmann Equation, and is found from the 0–0 component of the Einstein Equations. The second equation is found from the i–i components of the Einstein Equations. These two equations are not independent, and by subtracting Eq. 1.11 from Eq. 1.12, one can find an equation for the acceleration $\ddot{a}$ alone:

$$\frac{\ddot{a}}{a} = -\frac{4}{3}\left(\rho + \frac{3p}{c^2}\right) + \frac{\Lambda c^2}{3}. \tag{1.13}$$

The Friedmann Equation defines the Hubble parameter H, and it is simply the rate of expansion of the universe. It is a dynamical property of an evolving universe and thus changes in time. The expansion rate for the present epoch $t = t_0$ is defined as the Hubble Constant H_0. In the equation, G and c serve their usual purpose as the gravitational constant and the speed of light, while ρ is the mass-energy density of the universe and p is the pressure provided by the density. The curvature parameter, k, determines the overall spatial curvature of the universe. The magnitude of k is unimportant as it can be arbitrarily rescaled with a, however the sign of k is very important. The Λ in the equation is the cosmological constant and is the same constant from Einstein's Field Equations 1.1.

We will, as per convention, absorb the cosmological constant term into the definition of the overall density such that, $\rho \to \rho - \Lambda c^2/8\pi G$. Given this convention, Equation 1.11 reads:

$$\left(\frac{\dot{a}}{a}\right)^2 \equiv H^2 = \frac{8\pi G}{3}\rho - \frac{kc^2}{a^2}. \tag{1.14}$$

If we solve this equation for k and set the dynamical parameters H, ρ, and a to the current epoch values H_0, ρ_0 and 1 respectively, we get:

$$k = \frac{1}{c^2}\left(\frac{8\pi G}{3}\rho_0 - H_0^2\right) \tag{1.15}$$

Given this, we can define a quantity called the critical density ρ_c. It is the density at which the curvature vanishes, and is easily found to be $\rho_c = 3H_0^2/8\pi G$. By definition if, $\rho_0 = \rho_c$ then $k > 0$. Then the universe is flat, spatially open and infinite. The analogous two-dimensional structure is that of an infinite flat sheet. For $\rho_0 > \rho_c$, $k > 0$, the universe is spatially closed, finite and positively curved. The analogous two-dimensional space would be the surface of a sphere. Finally, for $\rho_0 < \rho_c$, $k < 0$ the universe is spatially open, infinite and negatively curved. An analogous two-dimensional shape often used to visualize this space is that of an infinite saddle.[6]

[6]An interesting fact to point out is that not every "infinite saddle" has constant negative cur-

With the definition of ρ_c, it will be useful to define the density parameters Ω_x. The density of species x of mass-energy given by ρ_x. The density parameter for that species is then simply the ratio of the density to the critical density:

$$\Omega_x = \frac{\rho_x}{\rho_x}. \tag{1.16}$$

Observationally, the universe is flat [KR22]. The driving observation for determining this is the Wilkinson Microwave Anisotropy Probe (WMAP) as well as observations of type-Ia supernovae from the Sloan Digital Sky Survey. WMAP measures the temperature fluctuations in the Cosmic Microwave Background radiation. Given this fact, this dissertation will only operate under an assumption of $k = 0$.[7] For a flat universe, the Friedmann Equation simplifies to:

$$\left(\frac{\dot{a}}{a}\right)^2 \equiv H^2 = \frac{8\pi G}{3}\rho. \tag{1.17}$$

This is the form of the Friedmann equation we will be working with for the remainder of the dissertation.

1.4.2 ΛCDM

The current, most well accepted theory of cosmology is known as ΛCDM. ΛCDM is a modification of the FLRW metric that proposes that the universe is mostly made up of two exotic forms of mass-energy: Dark Energy (the Λ in ΛCDM) and Cold Dark Matter (CDM), in about 68% and 27% ratios respectively to the total mass-energy content of the universe in the present epoch. The remaining 5% of the mass-energy is what we might call normal matter that is primarily made up of baryons and radiation. Nobel laureate Adam Riess, describes ΛCDM as the vanilla cosmological

vature. The pseudosphere is usually given as the example of a constant negative curvature surface, but such a surface cannot be completely embedded in three-dimensional space without a singularity somewhere. Special thanks to Jeff Rabin for this interesting insight.

[7] Though, it could be an interesting future endeavor to relax this constraint and perform a similar analysis as this thesis to a universe without $k = 0$.

model—as it is simple and only contains six independent parameters [RCY+19]. The set of six parameters used to define the model is open to choice. However, from those chosen parameters, a number of derived parameters can be determined. Included in these derived parameters that will be of interest to us are: the Hubble Constant H_0; the various density parameters $\Omega_{x,0}$; and the age of the universe t_0 [aPARAAAC+14].

Cold Dark Matter is a form of mass which interacts only through gravity and is invisible by electromagnetic means. Many observations support the idea of Dark Matter independent of cosmology. The main lines of evidence for the existence of dark matter include: Galaxy Rotation Curves, the Cosmic Microwave Background Radiation, gravitational lensing and Dark Matter Halos. Despite this overwhelming evidence for the existence of Dark Matter, no clear consensus has been met on what it is actually made of or how it might interact with normal matter through channels other than gravity. Bertone and Hooper provide a broad historical perspective on these observational discoveries and the theoretical arguments that led the scientific community to adopt Dark Matter as an essential part of cosmology [BH18].

Dark Energy is a very unusual kind of mass-energy. It is most often associated with the cosmological constant Λ (the same Λ appearing in Einstein's field equations (Eq. 1.1), which would give it the equation of state $p = w_\Lambda \rho$, with the equation of state parameter $w_\Lambda = -1$. This equation of state is quite unusual in that w is negative. For comparison, the equation of state parameters for matter and radiation are $w_M = 0$ and $w_R = 1/3$.

One common way to describe how a negative equation of state parameter works is to consider a spring. Normally, if you try to compress a spring, the spring would impart a force in the opposite direction of compression. Likewise, if you attempt to stretch a spring, it will impart a force in the opposite direction of stretching. This is captured in the negative sign in Hooke's Law $\boldsymbol{F} = -k\boldsymbol{x}$. Now let us consider a Dark Energy Spring. If you try to compress this exotic spring, it will not resist the compression, in fact it will begin to compress further on its own accord. Likewise, if

you try to stretch it, it will create a force that will increase the stretched length. If we were to mathematically describe this force like Hooke's law, the biggest difference would be in the sign of the RHS, $\boldsymbol{F}_\Lambda = +k\boldsymbol{x}$.

The observational evidence for dark energy comes from a variety of cosmological observations, which suggest that the universe is accelerating in its expansion. In a flat universe when G is constant, this acceleration cannot be explained by the gravitational attraction of matter alone, and requires the existence of a repulsive force that counteracts gravity. This repulsive force is believed to be due to the presence of dark energy.

One of the earliest pieces of evidence for dark energy came from studies of distant supernovae in the late 1990s. These studies found that the light from distant supernovae was dimmer than expected. This observation was consistent with the idea of an accelerating universe, and was interpreted as evidence for the existence of dark energy [RFC+98][PAG+99]. Follow-up observations of supernovae have confirmed the initial results, providing more evidence for an accelerating universe and the need for dark energy [KRA+08].

Despite its success, a number of observations have been made that are in tension with the ΛCDM model. Perhaps the most well known of these is the Hubble tension, which refers to a discrepancy between measurements of the expansion rate of the universe obtained using independent methods. "Early" methods of determining the Hubble constant primarily use observations of the Cosmic Microwave Background (CMB) and spatial fluctuations in galaxy distributions. These observations have determined its value to be in the range $H_0^{\text{early}} = 67 - 68\,\text{km/s}\,\text{Mpc}$. While "late" methods use recessional velocities of nearby galaxies and the distances to those galaxies to directly measure the Hubble constant. These late methods give a higher range for the Hubble constant in the range $H_0^{\text{late}} = 70 - 75\,\text{km/s}\,\text{Mpc}$. The accepted weighted mean of each of these measurements with their uncertainties are reported as $H_0^{\text{early}} = 67.4 \pm 0.5\,\text{km/s}\,\text{Mpc}$ and $H_0^{\text{late}} = 73.0 \pm 1.0\,\text{km/s}\,\text{Mpc}$—a 5-

sigma discrepancy. Several theoretical hypotheses have been proposed to account for this large discrepancy, some models include Early Dark Energy (EDE), changing the equation of state parameter for Dark energy with a value of $w < -1$ (wCDM), and modified gravity [KR22]. In 2022 Nils Schöneberg et al. proposed an "Olympics" for fairly ranking proposed modifications to ΛCDM against one another [SAS+22]. In this playful yet comprehensive and systematic comparison, they had 17 theories of cosmology compete to win the coveted gold medal.

While the Hubble tension is the most well known discrepancy of ΛCDM, additional challenges for ΛCDM have been enumerated by Perivolaropoulos and Skara [PS22]. Some of these tensions include:

1. Growth Tensions: in the context of GR, the Planck/ΛCDM parameters indicate stronger growth of the cosmological perturbations than are implied by observations.

2. CMB Anisotropy anomalies: statistical anomalies of the large angle fluctuations in the CMB.

3. Cosmic Dipoles: the presence of signals which indicate the violation of the cosmological principle[8].

4. Cosmic Birefringence: parity violating rotation of CMB linear polarization.

1.4.3 Cosmography: Distance Measures in Cosmology

Future chapters will rely heavily on various cosmological distance measures, which are laid out here. This section is largely taken from David Hogg's work [Hog99].[9]

[8]William Keel writes, "The *cosmological principle* is usually stated formally as: 'Viewed on a sufficiently large scale, the properties of the Universe are the same for all observers."' p. 1 [Kee02].

[9]Nearly every cosmology textbook will have some portion of it devoted to this topic. However, Hogg's work was very good at organizing this information and relieving confusion between the differences in these distances.

The Hubble time is defined as the inverse of the Hubble parameter $t_H = 1/H_0$. If we multiply the Hubble time by the speed of light, c, we get the Hubble Distance D_H. It is worth pointing out that these two quantities are *not* the age of the universe or its size, but they do provide decent scales for comparing cosmological distances and times. Their numerical values are $t_H = 14.5$ Gyr and $D_H = 4.4$ Gpc. The redshift, z, of an object is the fractional shift in its emitted wavelength of light $z = \frac{\lambda_o}{\lambda_e} - 1$, where λ_o is the observed wavelength and λ_e is the emitted wavelength. It is similar to the Doppler shift of an object with an outward radial motion from an observer. However, it is probably more accurate to consider it as the *gravitational* redshift produced by an expanding universe. The redshift of an object is related to the scale length of the universe at the time it emitted its light to the scale length of the universe today. Defining the scale length in the present epoch to be one, the scale length at redshift z is given by:

$$1 + z = \frac{1}{a(t)}. \tag{1.18}$$

It is very important to note that the redshift of a distant object is a directly measurable quantity—unlike the distance to that object or the time it emitted its light. Because of this, redshift will be used as a coordinate to past events rather than time, with higher values of z corresponding to events further back in time.

A note on notation: at times it will be important for us to juggle various redshift quantities at a time. I will use a lower case z as the independent variable in a function such as $a(z) = (1 + z)^{-1}$. Often, a function of z might have the redshift as the upper limit on an integral. In such cases, I will use the Greek letter zeta, ζ, as an integration variable over redshift. On occasion, I may need to speak about a specific redshift, sometimes in the context of a hypothetical astronomer at some redshift relative to us, in these cases I will use a capital Z. Lastly, sometimes it may be necessary for me to refer to a redshift relative to this hypothetical astronomer at redshift Z. In those cases, I will add a "rel" subscript to the redshift z_{rel}. The

relationship between Z and z (both measured from the current epoch) and z_{rel} is:

$$1 + z_{\text{rel}} = \frac{1+z}{1+Z}. \tag{1.19}$$

The density of the universe is a dynamical property of an expanding universe. As can be clearly seen in Equation 1.17 it affects the time evolution of the metric. The density of our universe is naturally the sum of partial densities of the different species of mass-energy in our universe, $\rho = \Sigma\rho_x$. In terms of the density parameters, the density in the present epoch is, $\rho_0 = \rho_c \Sigma\Omega_{x,0}$. If the universe is measured to be flat today, then that means that the closure parameter defined as $\Omega_0 = \Sigma\Omega_{x,0} = 1$. Additionally, if the universe is flat today, then it has always been flat. This means that the density at *any* epoch is equal to the critical density at that epoch $\rho(z) = 3[H(z)]^2/8\pi G$. If we define the function $E(z)$, such that $H(z) = H_0 E(z)$, we can see that the density at redshift z is given by $\rho(z) = \rho_c[E(z)]^2$. Which means that the square of the $E(z)$ function is simply the sum of the density parameters at that epoch $[E(z)]^2 = \Sigma\Omega_x(z)$. This makes the density as a function of z equal to:

$$\rho(z) = \frac{3H_0}{8\pi G}[E(z)]^2. \tag{1.20}$$

The density of each species of mass-energy reacts differently to changes in the scale length. In particular, each one will scale like $a^{-d_x} = (1+z)^{d_x}$, where d_x is known as the dilution parameter of that species. The dilution parameter is related to the equation of state for that species. Given the equation of state $p = w\rho_x$, $d_x = 3(1+w)$. For radiation, matter and dark energy w is $1/3$, 0 and -1 respectively, leading to dilution parameters of 4, 3 and 0 respectively. With this, we are ready to fully define the $E(z)$ function as:

$$E(z) = \sqrt{\sum_x \Omega_{x,0}(1+z)^{d_x}}. \tag{1.21}$$

The 0 subscript in the Ω parameters indicates that those are the density parameters as measured in the present epoch. For ΛCDM $E(z)$ is explicitly given as:

$$E(z) = \sqrt{\Omega_{\Lambda,0} + \Omega_{M,0}(1+z)^3 + \Omega_{R,0}(1+z)^4}, \tag{1.22}$$

where the Λ, M and R subscripts refer to dark energy, matter (including both baryons and dark matter), and radiation (including photons and high energy massive particles like neutrinos) respectively.

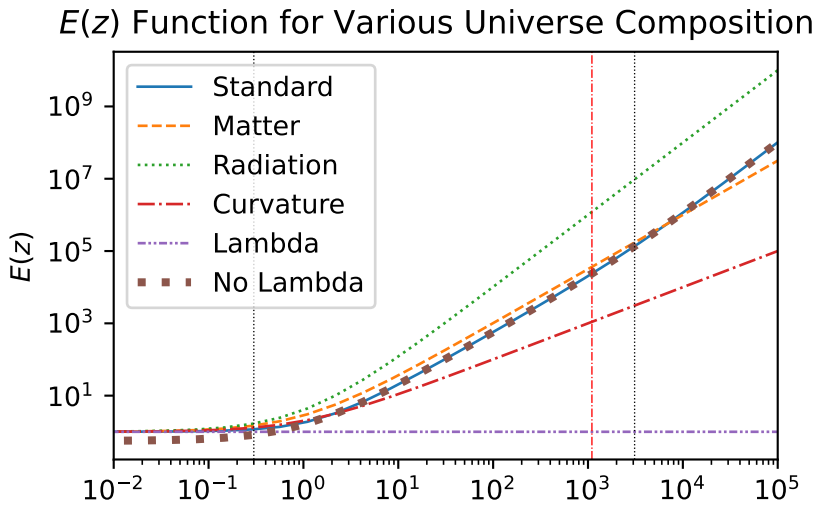

Figure 1.1: $E(z)$ function for various basic flat models of the universe. The models differ only in their current density parameters $\Omega_{x,0}$. The values for the density parameters are provided in Table 1.2.

Figure 1.1 presents the evolution of $E(z)$ with differing values of the density parameters $\Omega_{x,0}$. The density parameters used for the different models plotted are provided in Table 1.2. These basic models will be used to make various comparisons throughout this work. You'll notice in the table references to curvature only models $\Omega_{K,0} = 1$, even though it was explicitly state that the universe is flat and the curvature parameter k is zero. I include the curvature only model because the equation of state yields a dilution parameter of $d_K = 2$ which sits nicely on the other side of

Table 1.2: Density parameters for various basic flat models for the universe. The "Standard" case uses the values for ΛCDM as determined from the 2018 Planck experiment release [AAA+20]. The subscripts Λ, M, R and K refer to dark energy, matter (including both baryons and dark matter), and radiation (including photons and high energy massive particles like neutrinos), and curvature respectively. The subscript of 0 refers to the fact that these are the density parameters in the current epoch $t = t_0$.

Case	$\Omega_{\Lambda,0}$	$\Omega_{M,0}$	$\Omega_{R,0}$	$\Omega_{K,0}$
Standard	0.6889	0.3111	10^{-4}	
Lambda	1			
Matter		1		
Radiation			1	
Curvature[10]				1
No Lambda[11]		0.3111	10^{-4}	

matter's dilution parameter, $d_M = 3$ from radiaiton's, $d_R = 4$. In this sense, plotting the curvature only model can at times give a sense of how some results might "fit" between simple cases, for example in the results plotted in Figure 3.3.

Plugging the definition of $E(z)$ in Eq. 1.21 into Equation 1.20 we get our full formula for the density as a function of redshift to be:

$$\rho(z) = \frac{3H_0}{8\pi G}[E(z)]^2 = \frac{3H_0}{8\pi G}\sum_x \Omega_{x,0}(1+z)^{d_x}. \tag{1.23}$$

The general expression of $E(z)$ also leads us to define the rate of change of the scale length in terms of it as:

$$\frac{\dot{a}}{a} = H(z) = H_0 E(z). \tag{1.24}$$

[10]Because the sum of the density parameters is not equal to one, various cosmographic values and other values we will introduce will have very different forms that can include $\sin(r)$ and $\sinh(r)$ functions, where r is the radius of curvature of the universe. However, often the purpose of these comparisons will be more a demonstration of how those values behave when the density parameters are changed, and not necessarily for situations in which the k parameter is not equal to 0.

[11]Same note as the "Curvature" case.

Table 1.3: These are the three redshifts for which the given density parameters are equal. The arrows indicate when increasing z leads to a change from one dominant species to another. The two values where the dominant species changes will be plotted with vertical dotted lines in most of the figures as an aid for comparisons between the different dominated epochs. When $\Omega_\Lambda = \Omega_R$ matter remains the dominant species.

Transition	Z_{trans}
$\Omega_\Lambda \rightarrow \Omega_M$	0.30
$\Omega_\Lambda = \Omega_R$	5.1
$\Omega_M \rightarrow \Omega_R$	3100

Two things we might want to know are: what are the density parameters at some redshift Z; and what is $E(z_{\text{rel}})$ as measured from some redshift Z? It can be easy to relate these two quantities:

$$\Omega_{x,Z} = \frac{\Omega_{x,0}(1+Z)^{d_x}}{[E(Z)]^2}, \tag{1.25}$$

$$E(z_{\text{rel}}) = \frac{E(z)}{E(Z)}. \tag{1.26}$$

Figure 1.2 plots how the density parameters, $\Omega_{x,Z}$ evolve in time over the age of the universe.

Additionally, because the different mass-energy species scale differently with the size of the universe, there are times when two of the species' densities may be momentarily equal as one becomes more dominant than the other. The redshift of these epochs can be shown to be:

$$Z_{\text{eq}} = \left(\frac{\Omega_{x,0}}{\Omega_{y,0}}\right)^{1/(d_y - d_x)} - 1. \tag{1.27}$$

For ΛCDM these redshifts can be found in Table 1.3:

The comoving distance D_C is an important baseline distance measure in cosmology. The comoving distance we observe to a distant object is one that remains fixed

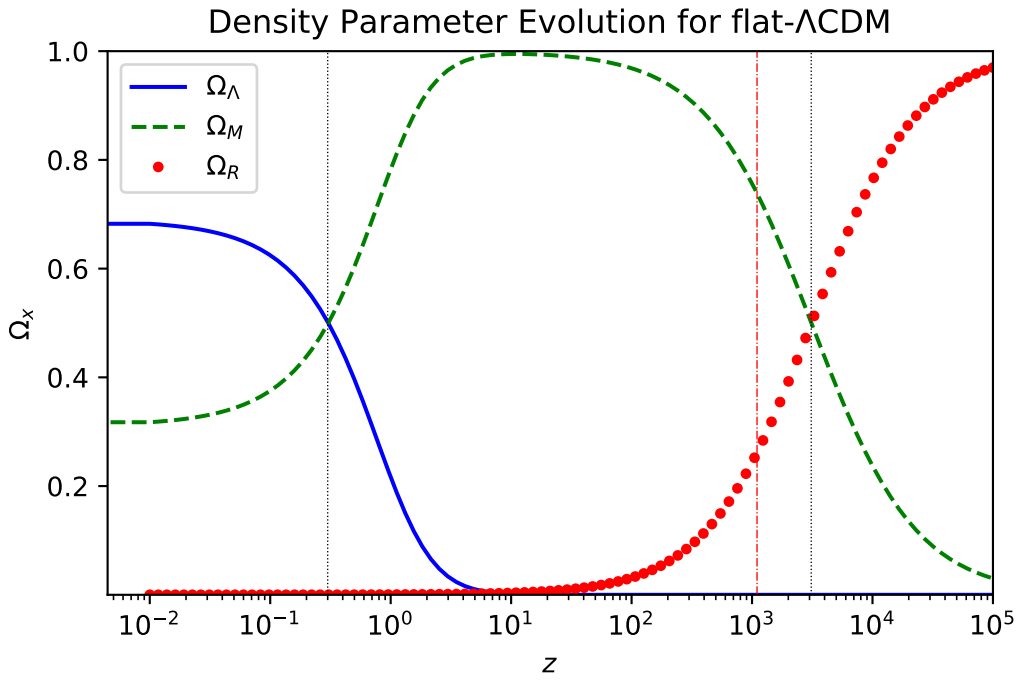

Figure 1.2: Plotted is the cosmological evolution of the density parameters. The values at the current epoch are given by the Planck experiment 2018 results $(\Omega_\Lambda, \Omega_M)$

in time, even though the *proper* distance—the distance you would measure with rulers—between the two objects will increase with the expansion of the universe. From Hogg:

> A small *comoving distance* δD_C between two nearby objects in the Universe is the distance between them, which remains constant with epoch if the two objects are moving with the Hubble flow. In other words, it is the distance between them which would be measured with rulers at the time they are being observed (the *proper distance*) divided by the ratio of the scale factor of the Universe then to now; it is the proper distance multiplied by $(1+z)$. The total line-of-sight comoving distance D_C from us to a distant object is computed by integrating the infinitesimal δD_C contributions between nearby events along the radial ray from $z = 0$ to the object.

The integral over time looks like this:

$$D_C = \int_{t_e}^{t_o} c\frac{\mathrm{d}t'}{a(t')}. \tag{1.28}$$

But recalling $(1+z) = a^{-1}$, differentiating this expression with respect to time gives, $dz/(\dot{a}/a) = -dt/a$. Plugging this into the integral above and replacing $\dot{a}/a$ with $H(z) = H_0 E(z)$ and c/H_0 with the Hubble distance, D_H, we get:

$$D_C = D_H \int_0^z \frac{\mathrm{d}\zeta}{E(\zeta)}. \tag{1.29}$$

Figure 1.3 plots how D_C (red solid line) as a function of redshift z along with other distance measures we will discuss.

Many other cosmographic distances are defined in terms of the line-of-sight comoving distance. The proper distance to any object is an observer specific quantity, as it is the distance between two events in the frame in which they occur at the same time. It is physically defined as the number of rulers that would span between two objects at any given instant in the observer's frame. In terms of cosmology, we, here on Earth, are implicitly defined as the observer. The proper distance not only requires identifying the two objects of interest, but also the time at which at which it is measured[12]. By definition, the comoving distance to any object at redshift z *today*, $t = t_0$, is the proper distance $D_C(z) = D_P(t_0)$. Remember, the comoving distance stays fixed in time. So, the proper distance to that same object when it emitted its light that we observe today, $t = t_e$, would be today's proper distance reduced by the scale factor when the light was emitted $a(t_e) = 1/(1+z)$. So the proper distance *at the time when light was emitted* to some object at redshift z is:

$$D_P(t_e) = \frac{D_C(z)}{1+z} = \frac{D_H}{1+z}\int_0^z \frac{\mathrm{d}\zeta}{E(\zeta)}. \tag{1.30}$$

[12]The act of laying out rulers and counting them is not meant to be a literal way to measure proper distance. By definition, it is the distance between two points at the same instant, and this would necessarily make the events of observing both points for measurement time-like separated. This is true not just for distances on the cosmic scale, but even holds for small terrestrial objects in a laboratory. Rather, this idea of laying our rules is simply used as a visualization device.

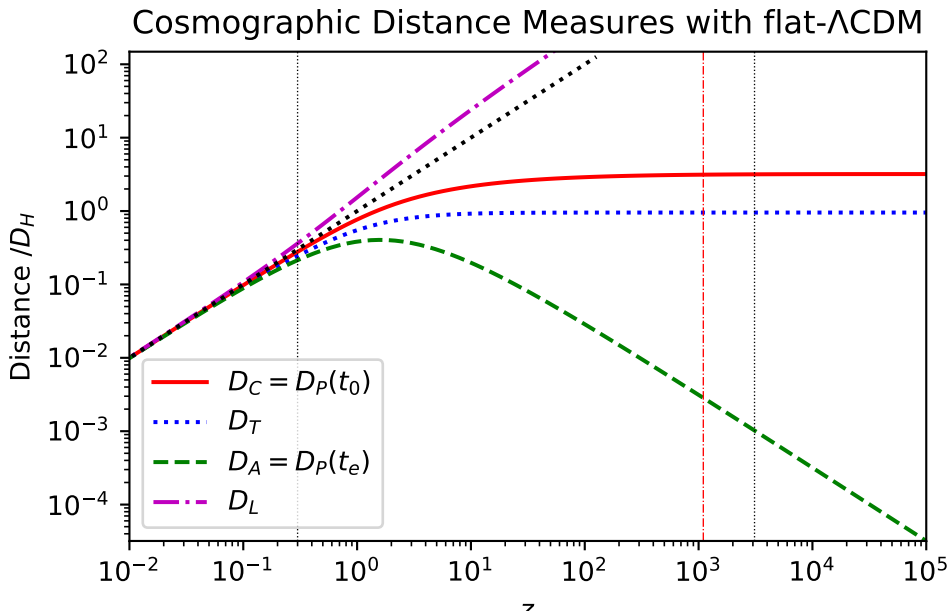

Figure 1.3: Distance measures in flat-ΛCDM cosmology. By definition, the proper distance today $D_P(t_0)$ is equal to the comoving distance D_C, (solid red line). In a flat universe, the proper distance between two objects at the time of emission, t_e, is equal to the angular diameter distance, $D_A = D_C/(1+z) = D_P(t_e)$, (dashed green line). The blue dotted line gives the look-back distance as determined by the look-back time $D_T = t_L/c$. The dotted black line has a slope of one in the plot and is used to show the departure of the other distance measures from a familiar Euclidean distance measure.

The transverse comoving distance, D_M, relates the comoving distance between two events at the same redshift but separated on the sky by some angle $\delta\theta$. The comoving distance between these two events is $\delta\theta D_M$. In a flat universe the transverse comoving distance, D_M is simply equal to the line-of-sight comoving distance D_C. The angular diameter distance D_A is the ratio of an object's physical transverse size to its angular size on the sky. It is commonly used to convert angular separations in telescopes into proper distances at the source. It is equal to the transverse comoving distance multiplied by the scale factor $D_A = aD_M = aD_C$. For a flat universe:

$$D_A(z) = \frac{D_C}{1+z}. \tag{1.31}$$

You'll notice that $D_A(z)$ is equal to $D_P(t_e)$. This is only true in a flat universe due to the fact that in a flat universe $D_M = D_C$. D_A is the one distance measure that begins to actually get smaller with high redshift, as can be seen in Figure 1.3 (green dashed line).

Hogg also talks about a lookback time. This is defined as the difference between the age of the universe now, t_0, and the age of the universe at the time the photons were emitted, t_e (according to the object). It is given by:

$$t_L = t_H \int_0^z \frac{\mathrm{d}\zeta}{(1+\zeta)E(\zeta)}. \tag{1.32}$$

Therefore, by multiplying by the speed of light, we can determine how "far" the light has traveled from the time it was emitted to observation:

$$D_T = D_H \int_0^z \frac{\mathrm{d}\zeta}{(1+\zeta)E(\zeta)}. \tag{1.33}$$

This then measures distance to events along our past light-cone. Furthermore, since gravity also travels at the speed of light, we can perhaps consider these events to be on our past gravitational-cone. I should point out that this is *not* a distance measure that Hogg defines. However, because it is the distance that a gravitational "signal" travels between two events, we will use this as the "gravitational distance" between two masses in Chapter 3. It is interesting to note that both D_C and D_T both approach constant values as $z \to \inf$, as can be seen in Figure 1.3. Additionally, those values are very near the value of D_H, at $D_T(\infty)/D_H = 0.95$ and $D_C(\infty)/D_H = 3.2$.

One last distance measure is the luminosity distance D_L. This distance is defined by the relationship between the bolometric (i.e., integrated over all frequencies) flux S and the bolometric luminosity L:

$$D_L \equiv \sqrt{\frac{L}{4\pi S}}. \tag{1.34}$$

It is related to the comoving distance and angular diameter distance by:

$$D_L = (1+z)^2 D_A = (1+z) D_C = D_H (1+z) \int_0^z \frac{\mathrm{d}\zeta}{E(\zeta)}. \tag{1.35}$$

As we can see in Figure 1.3, for ΛCDM the luminosity distance (purple dash-dotted line) is larger than the Euclidean distance. Because of this, distant supernovae look dimmer than expected from a simple inverse square law.

Cosmologists use the luminosity distance to directly measure H. They do this by recording the flux of "standard candles," objects with known intrinsic luminosity. By measuring the flux and knowing the luminosity, they are able to directly measure D_L via Equation 1.34. By also measuring the redshift z, they can fit $H(z)$ with the integral form of D_L in Equation 1.35. That is of course if $D_H = c/H_0$ is known. In practice, many standard candles are observed to constrain both H_0 and the density parameters $\Omega_{x,0}$ in $E(z)$.

Often, rather than reporting the luminosity distance directly, cosmologists will report the distance modulus μ. Therefore, a brief introduction to this quantity is necessary in order to be conversant with experimental results involving supernova data, as we will do in Chapter 4. The distance modulus is the magnitude difference between an object's observed bolometric flux and what its bolometric flux *would be* at a distance of 10 parsecs. The distance modulus is defined as:

$$\mu \equiv 5 \log \left(\frac{D_L}{10\,\mathrm{pc}} \right). \tag{1.36}$$

The absolute magnitude M is an astronomer's measure of luminosity, defined as the apparent magnitude the object would have if it were at 10 parsecs. The observed magnitude m of an object is:

$$m = M + \mu + K, \tag{1.37}$$

where K is the k-correction, and needs to be used if the magnitude is not measured at all wavelengths. The k-correction is given by:

$$K = -2.5 \log \left[(1+z) \frac{L_{(1+z)\nu}}{L_\nu} \right] = -2.5 \log \left[\frac{1}{(1+z) \frac{L_{\lambda/(1+z)}}{L_\lambda}} \right], \tag{1.38}$$

where L_ν is the differential luminosity at frequency ν over the band pass $\delta\nu$. It has units of energy per unit time per unit frequncy. Likewise, L_λ is the differential luminosity at wavelength λ over the band pass λ, with units of energy per unit time per unit wavelength. For this work, we won't be directly working with m or K, they are only provided to complete the discussion of the distance modulus.

The last cosmographic measures we will discuss are the comoving volume element and the proper volume element. The comoving volume V_C, is the volume in which the number densities of non-evolving objects locked into the Hubble flow are constant with redshift. The comoving volume element is the differential line-of-sight comoving distance, $\mathrm{d}D_C$, multiplied by two factors of the transverse comoving distance times a small solid angle element $\mathrm{d}\Omega D_M^2$. However, D_M is simply $(1+z)D_A$. Furthermore, from Eq. 1.29 we can see that $\mathrm{d}D_C$ is just $(D_H/E(z))\mathrm{d}z$. Altogether, the comoving volume element is given by:

$$\mathrm{d}V_C = D_H \frac{(1+z)^2 D_A^2}{E(Z)} \mathrm{d}\Omega \mathrm{d}z. \tag{1.39}$$

Recall that the comoving distances are fixed in time. That is to say, the comoving distance to a distant galaxy today is the same as it was at any point in the past, no matter how physically close it may have been at some earlier epoch. This would also mean that the comoving volume would remain fixed in time as well. If we are interested in real physical densities, clearly this notion of a volume that remains fixed in time is not sufficient. Recalling that the proper distance when the light

was emitted is simply the comoving distance multiplied by the scale factor at that redshift, in order to properly determine physical densities, what we want is the proper volume element. Which is the comoving volume element multiplied by the scale factor cubed. Given that, the proper volume element is:

$$\mathrm{d}V_P = D_H \frac{D_A^2}{(1+z)E(z)} d\Omega \mathrm{d}z. \tag{1.40}$$

But D_A in a flat universe is just $D_C/(1+z)$. So, the proper element is also:

$$\mathrm{d}V_P = D_H \frac{D_C^2}{(1+z)^3 E(z)} \mathrm{d}\Omega \mathrm{d}z \tag{1.41}$$

Chapter 2

Integration of EIH Over Rotating External Spherical Shells

An observer in what we would call a non-inertial frame is entitled by relativistic formulations to evaluate physics in that frame, in which the universe seems to wheel around their lab. Our question is: does the mass distribution of the universe, through GR, impose "fictitious forces" that collectively assert an inertial frame which is tied to the distant stars. To that end, this chapter will focus on evaluating the EIH Equations of motion for a test particle at the center of a thin shell of mass that can both move relative to the frame. We will then compare the accelerations imparted by the shell on the test particle to accelerations that would be observed should the observer change their frame to one that is fixed to the non-inertial shell.

2.1 The Spherical Shell

2.1.1 The Setup

In this section, we will consider a test particle at the center of a spherical shell with radius R and mass M in flat static space (not in an expanding FLRW universe,

to which we will return later). Because the coordinates in EIH are "Nearly Lorentz" and can be treated with a flat 3+1 space and time split, the coordinate radius R is simply the familiar Euclidean distance to the shell's surface. It will also have a uniform surface density σ such that $M = 4\pi R^2\sigma$. We will consider three cases with the following distinctions:

- Case:1 - Linear Acceleration Case - The shell will be momentarily at rest w.r.t the test particle, but it will have uniform linear acceleration, $\boldsymbol{a}_A$.
- Case:2 - Coriolis Case - The shell will be rotating uniformly with some angular frequency $\boldsymbol{\omega}$, while the particle has some velocity $\boldsymbol{v_A}$ in the equatorial plane.
- Case:3 - Centrifugal Case - The shell will be rotating uniformly with some angular frequency $\boldsymbol{\omega}$ about an axis that is displaced from the test particle by some distance $\boldsymbol{x}_A$. Additionally, the axis of rotation will be perpendicular to that displacement.

Because our shell is an extended mass and not a set of discrete point masses, we will need to convert the sums within the EIH Equations to integrals. For that, we will use the following transformations for all the cases:

$$m_B \to \mathrm{d}m = \rho(\boldsymbol{x})d^3x \to R^2\sigma\mathrm{d}\Omega, \tag{2.1}$$

$$r_{BA} \to \text{const} = R, \tag{2.2}$$

$$\hat{\boldsymbol{n}}_{BA} \to \hat{\boldsymbol{r}}, \tag{2.3}$$

$$\boldsymbol{v}_B \to \boldsymbol{v}(\boldsymbol{x}), \tag{2.4}$$

$$\boldsymbol{a}_B \to \boldsymbol{a}(\boldsymbol{x}), \tag{2.5}$$

$$\sum_{A\neq B} m_B f(\boldsymbol{r}_A, \boldsymbol{r}_B, \boldsymbol{v}_A, \boldsymbol{v}_B, \boldsymbol{a}_B) \to R^2\sigma \int_\Omega d\Omega f(R\hat{\boldsymbol{r}}, \boldsymbol{v}_A, \boldsymbol{v}(\boldsymbol{x}), \boldsymbol{a}(\boldsymbol{x})), \tag{2.6}$$

$$\int_\Omega \mathrm{d}\Omega = \int_0^{2\pi} \mathrm{d}\phi \int_0^{\pi} \sin\theta \mathrm{d}\theta. \tag{2.7}$$

2.1.2 Evaluation of Common Terms Between Cases

Before evaluating the integrals for each case, we can notice that the $\boldsymbol{\mathcal{N}}$, $\boldsymbol{\mathcal{E}}$, $\boldsymbol{\mathcal{F}}$, $\boldsymbol{\mathcal{H}}$, and $\boldsymbol{\mathcal{I}}$ terms do not contain any factors of $\boldsymbol{v}_A$, $\boldsymbol{v}_B$ or $\boldsymbol{a}_B$. Since all other factors are identical between each case, we can evaluate those terms once for all the cases.

With the substitutions from the previous section, the $\boldsymbol{\mathcal{N}}$ and $\boldsymbol{\mathcal{E}}$ terms become:

$$\boldsymbol{\mathcal{N}} = GR^2\sigma \int_\Omega \mathrm{d}\Omega \frac{\hat{\boldsymbol{r}}}{R^2}, \tag{2.8}$$

$$\boldsymbol{\mathcal{E}} = -5\frac{Gm_A}{c^2}R^2\sigma \int_\Omega \mathrm{d}\Omega \frac{\hat{\boldsymbol{r}}}{R^3}. \tag{2.9}$$

The integrals in both of these terms are identical and simply $\int_\Omega d\Omega\hat{\boldsymbol{r}}$. This isotropic integral is equal to zero, with Appendix A.1 detailing the the integration steps. Therefore, $\boldsymbol{\mathcal{N}} = \boldsymbol{\mathcal{E}} = 0$ for all cases. Naturally, the $\boldsymbol{\mathcal{N}}$ term is more generally zero for any location inside a shell, according to Newton's Shell theorem.

The integral of the $\boldsymbol{\mathcal{F}}$ term is a bit trickier to set up because the m_B^2 factor carries two powers of $\mathrm{d}\Omega$, while we need only integrate over one. For clarity in the integration I will label one of the differential elements as $\delta\Omega$, while we integrate over $\mathrm{d}\Omega$. The integral will then look like this:

$$\boldsymbol{\mathcal{F}} = -4\frac{G^2}{c^2R}\sigma \int_\Omega \mathrm{d}\Omega(R^2\sigma\delta\Omega)\hat{\boldsymbol{r}}. \tag{2.10}$$

Now, this term has the same form of isotropic integral as $\boldsymbol{\mathcal{N}}$ and $\boldsymbol{\mathcal{E}}$. Therefore, the $\boldsymbol{\mathcal{F}}$ term is also equal to zero.

Finally, the $\boldsymbol{\mathcal{H}}$ and $\boldsymbol{\mathcal{I}}$ integrals contain double sums. One thing we can note about these two terms is that because of the spherical symmetry of the setup, those inner sums/integrals will be constant over the surface of the sphere. For the moment, let's simply call them $\boldsymbol{\mathcal{H}}_{\text{inner}}$ and $\boldsymbol{\mathcal{I}}_{\text{inner}}$. Plugging these in and the substitutions from the previous section, we get:

$$\boldsymbol{\mathcal{H}} = -4\frac{G^2}{c^2}R^2\sigma\int_\Omega \mathrm{d}\Omega\frac{\boldsymbol{\mathcal{H}}_{\mathrm{inner}}}{R^2}\hat{\boldsymbol{r}}, \tag{2.11}$$

$$\boldsymbol{\mathcal{I}} = -\frac{G^2}{c^2}R^2\sigma\int_\Omega \mathrm{d}\Omega\frac{\boldsymbol{\mathcal{I}}_{\mathrm{inner}}}{R}\hat{\boldsymbol{r}}. \tag{2.12}$$

Once again, these are both isotropic integrals equal to zero. So in summary, the following terms are equal to zero for all of the cases:

$$\boldsymbol{\mathcal{N}} = \boldsymbol{\mathcal{E}} = \boldsymbol{\mathcal{F}} = \boldsymbol{\mathcal{H}} = \boldsymbol{\mathcal{I}} = \mathbf{0}. \tag{2.13}$$

2.1.3 Linear Acceleration Case:1

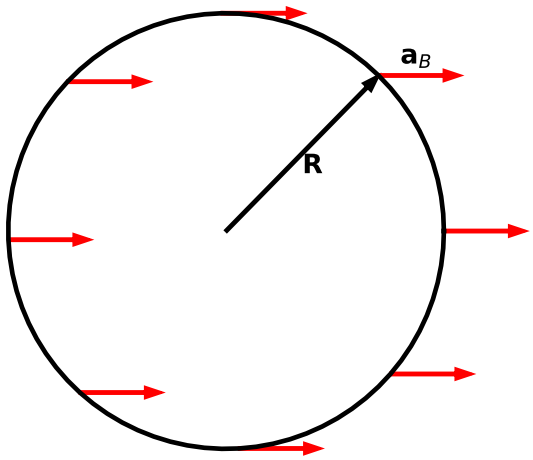

Figure 2.1: Diagram for the linear acceleration Case:1. The shell and test mass are momentarily at rest with respect to each other. The test mass is located at the center of the shell. The shell is accelerating uniformly with acceleration $\boldsymbol{a}_B$ indicated with the red arrows.

For the linear acceleration case, all the velocities are zero everywhere, $\boldsymbol{v}_A = \boldsymbol{v}(\boldsymbol{x}) = \mathbf{0}$. Therefore, the $\boldsymbol{\mathcal{A}}$ through $\boldsymbol{\mathcal{I}}$ terms can readily be set to $\mathbf{0}$. This leaves the

$\boldsymbol{\mathcal{J}}$ and $\boldsymbol{\mathcal{K}}$ terms as the only ones requiring explicit evaluation. Furthermore, $\boldsymbol{a}_B$ is equal to a constant for all points on the sphere. To give it a direction, the integrals are easiest if we choose its direction to be in the $\hat{\boldsymbol{x}}$ direction, $\boldsymbol{a}_B = a\hat{\boldsymbol{x}}$. Using the substitutions from Section 2.1.1 the $\boldsymbol{\mathcal{J}}_1$ and $\boldsymbol{\mathcal{K}}_1$ integrals look like this[1]:

$$\boldsymbol{\mathcal{J}}_1 = \frac{1}{2}\frac{G}{c^2}R^2\sigma\int_\Omega \mathrm{d}\Omega\frac{\hat{\boldsymbol{r}}(\hat{\boldsymbol{r}}\cdot\boldsymbol{a})}{R}, \tag{2.14}$$

$$\boldsymbol{\mathcal{K}}_1 = \frac{7}{2}\frac{G}{c^2}R^2\sigma\int_\Omega \mathrm{d}\Omega\frac{\boldsymbol{a}}{R}. \tag{2.15}$$

The $\boldsymbol{\mathcal{J}}_1$ term is evaluated to (see Appendix B.1 for a detailed solution):

$$\boldsymbol{\mathcal{J}}_1 = \frac{2}{3}\frac{G}{c^2}R\sigma\pi a\hat{\boldsymbol{x}}. \tag{2.16}$$

Putting this in terms of $M = 4\pi\sigma R^2$ and $\boldsymbol{a} = a\hat{\boldsymbol{x}}$ it looks like this:

$$\boldsymbol{\mathcal{J}}_1 = \frac{1}{6}\frac{MG}{c^2R}\boldsymbol{a}. \tag{2.17}$$

The $\boldsymbol{\mathcal{K}}_1$ term is much simpler. We can notice that everything in the integral is constant. Since the integral of $\int_\Omega \mathrm{d}\Omega$ is equal to 4π, we get:

$$\boldsymbol{\mathcal{K}}_1 = \frac{7}{2}\frac{G}{c^2}\sigma 4\pi R\boldsymbol{a}. \tag{2.18}$$

Again, putting this in terms of the mass of the shell M, we get:

$$\boldsymbol{\mathcal{K}}_1 = \frac{7}{2}\frac{GM}{c^2R}\boldsymbol{a}. \tag{2.19}$$

Adding the $\boldsymbol{\mathcal{J}}_1$ and $\boldsymbol{\mathcal{K}}_1$ terms together, we get our final solution for the linear acceleration Case:1 as:

$$\boxed{\boldsymbol{a}_{A,1} = \frac{11}{3}\frac{GM}{c^2R}\boldsymbol{a}}. \tag{2.20}$$

[1] I'm introducing numerical subscripts to the terms to label the case they are evaluated for.

2.1.4 The Coriolis Case:2

The Coriolis case dynamic and coordinate parameters can be defined:

$$\boldsymbol{v}_A = v_A\hat{\boldsymbol{x}}, \tag{2.21}$$

$$\boldsymbol{\omega} = \omega\hat{\boldsymbol{z}}, \tag{2.22}$$

$$\boldsymbol{v}(\boldsymbol{x}) = \boldsymbol{\omega} \times \boldsymbol{R} = \omega R(\hat{\boldsymbol{z}} \times \hat{\boldsymbol{r}}) = \omega R \sin\theta\hat{\boldsymbol{\phi}}, \tag{2.23}$$

$$\boldsymbol{a}(\boldsymbol{x}) = \boldsymbol{\omega} \times \boldsymbol{v} = -\omega^2 R \sin\theta(\hat{\boldsymbol{z}} \times \hat{\boldsymbol{\phi}}) = -\omega^2 R \sin\theta\hat{\boldsymbol{\rho}}, \tag{2.24}$$

$$\hat{\boldsymbol{r}} = \sin\theta\cos\phi\hat{\boldsymbol{x}} + \sin\theta\sin\phi\hat{\boldsymbol{y}} + \cos\theta\hat{\boldsymbol{z}}, \tag{2.25}$$

$$\hat{\boldsymbol{r}} = \sin\theta\hat{\boldsymbol{\rho}} + \cos\theta\hat{\boldsymbol{z}}. \tag{2.26}$$

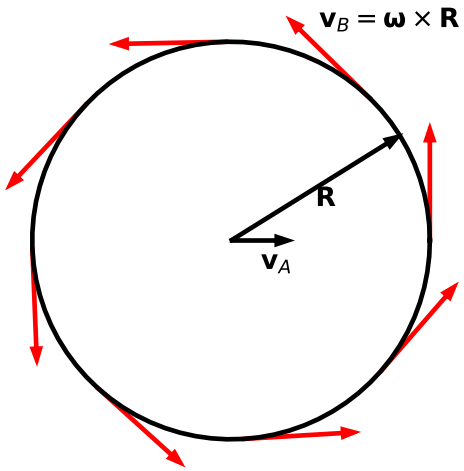

Figure 2.2: Diagram for the Coriolis Case:2. The shell is rotating uniformly with velocity $\boldsymbol{v} = \boldsymbol{\omega} \times \boldsymbol{b}$ and indicated by the red arrows. The test particle is located at the center of the shell and has velocity $\boldsymbol{v}_A$.

As already noted in Section 2.1.2 the $\boldsymbol{\mathcal{N}}$, $\boldsymbol{\mathcal{E}}$, $\boldsymbol{\mathcal{F}}$, $\boldsymbol{\mathcal{H}}$, and $\boldsymbol{\mathcal{I}}$ terms have already been evaluated to $\mathbf{0}$. Because $\boldsymbol{v}_A$, $\boldsymbol{v}(\boldsymbol{x})$, and $\boldsymbol{a}(\boldsymbol{x})$ are non-zero for this case, none of the remaining terms can quickly be dismissed.

The first term we come across is the $\boldsymbol{\mathcal{A}}_2$ term:

$$\boldsymbol{\mathcal{A}}_2 = \frac{G}{c^2}\sigma R^2 \int_\Omega \mathrm{d}\Omega \frac{v_A^2}{R^2}\hat{\boldsymbol{r}}. \tag{2.27}$$

However, this looks remarkably like the formula for $\boldsymbol{\mathcal{N}}$ (Eq. 2.8) with the exception of the constant $(v_A/c)^2$ factor. So just like the $\boldsymbol{\mathcal{N}}$ term, this one also evaluates to zero.

Next up, the $\boldsymbol{\mathcal{B}}_2$ term looks like this after plugging everything in:

$$\boldsymbol{\mathcal{B}}_2 = 2\frac{G}{c^2}R^2\sigma \int_\Omega \mathrm{d}\Omega \frac{(\omega R\sin\theta)^2}{R^2}\hat{\boldsymbol{r}}. \tag{2.28}$$

We can use Appendix A.2 that covers powers of the sine function over the solid angles to evaluate this term to also be zero.

The $\boldsymbol{\mathcal{C}}_2$ term turns out to be non-zero. So let's come back to it. Next up, let's evaluate the $\boldsymbol{\mathcal{D}}_2$ term. But for this term, we require evaluating $\hat{\boldsymbol{r}} \cdot \boldsymbol{v}(\boldsymbol{x})$. But since $\boldsymbol{v}(\boldsymbol{x}) = -\omega R\sin\theta\hat{\boldsymbol{\phi}}$, and $\hat{\boldsymbol{r}} \cdot \hat{\boldsymbol{\phi}} = 0$, this term is also equal to zero.

The $\boldsymbol{\mathcal{G}}_2$ term is also non-zero and a real pain to evaluate. Let's skip to the final two $\boldsymbol{\mathcal{J}}_2$ and $\boldsymbol{\mathcal{K}}_2$ terms, and then we can come back to $\boldsymbol{\mathcal{C}}_2$ and $\boldsymbol{\mathcal{G}}_2$.

For the $\boldsymbol{\mathcal{J}}_2$ term, we need to evaluate $\hat{\boldsymbol{r}} \cdot \boldsymbol{a}$. We can write $\hat{\boldsymbol{r}}$ in cylindrical coordinates as $\hat{\boldsymbol{r}} = \sin\theta\hat{\boldsymbol{\rho}} + \cos\theta\hat{\boldsymbol{z}}$ and $\boldsymbol{a} = -\omega^2 R\sin\theta\hat{\boldsymbol{\rho}}$, the inner product between the two is quickly evaluated to be $\hat{\boldsymbol{r}} \cdot \boldsymbol{a} = -\omega^2 R\sin^2\theta$. Converting the sum to an integral and plugging all this in the term looks like:

$$\boldsymbol{\mathcal{J}}_2 = -\frac{1}{2}\frac{G}{c^2}R^2\sigma \int_\Omega \mathrm{d}\Omega \frac{\omega^2 R}{R}\sin^2\theta\hat{\boldsymbol{r}}. \tag{2.29}$$

Again, using the Appendix for powers of sine over the solid angles A.2, this integral also evaluates to zero.

Now we turn our attention to the $\boldsymbol{\mathcal{K}}_2$ term. Converting the sum to an integral, it looks like this:

$$\boldsymbol{\mathcal{K}}_2 = -\frac{7}{2}\frac{G}{c^2}R^2\sigma\int_\Omega \mathrm{d}\Omega\frac{\omega^2 R\sin\theta}{R}\hat{\boldsymbol{\rho}}. \tag{2.30}$$

This integral evaluates to zero. Appendix A.5 details this conclusion.

As a brief recap, we have evaluated all but the $\boldsymbol{\mathcal{C}}_2$ and $\boldsymbol{\mathcal{G}}_2$ terms in the Coriolis case, and every one so far has evaluated to $\mathbf{0}$. Both the remaining $\boldsymbol{\mathcal{C}}_2$ and $\boldsymbol{\mathcal{G}}_2$ terms are equal to each other and evaluate to:

$$\boldsymbol{\mathcal{C}}_2 = \boldsymbol{\mathcal{G}}_2 = \frac{16}{3}\frac{Gv_A\sigma\omega\pi R}{c^2}\hat{\boldsymbol{y}}. \tag{2.31}$$

See appendices B.2 and B.3 for details on how these terms can be evaluated. After all is said and done, the acceleration on the test particle A is:

$$\boldsymbol{a}_{A,2} = 2\left(\frac{16}{3}\frac{Gv_A\sigma\omega\pi R}{c^2}\right)\hat{\boldsymbol{y}}, \tag{2.32}$$

where the 2 subscript denotes the acceleration of particle A in Case:2. We can also note that:

$$\boldsymbol{\omega}\times\mathbf{v_A} = \omega v_A(\hat{\boldsymbol{z}}\times\hat{\boldsymbol{x}}) = \omega v_A\hat{\boldsymbol{y}}. \tag{2.33}$$

Furthermore, a careful evaluation of other cases where $\boldsymbol{v}$ is not necessarily in the equatorial plane validates this general form. Additionally, replacing σ with $M/4\pi R^2$, we can rewrite our solution as:

$$\boxed{\boldsymbol{a}_{A,2} = 2\frac{4}{3}\frac{GM}{Rc^2}\boldsymbol{\omega}\times\mathbf{v_A}}. \tag{2.34}$$

2.1.5 The Centrifugal Case:3

The integration of this case was saved for last because the nature of it makes it a little more difficult to perform than the previous cases. The primary reason for this is that while the shell is rotating uniformly, its axis of rotation is not through its

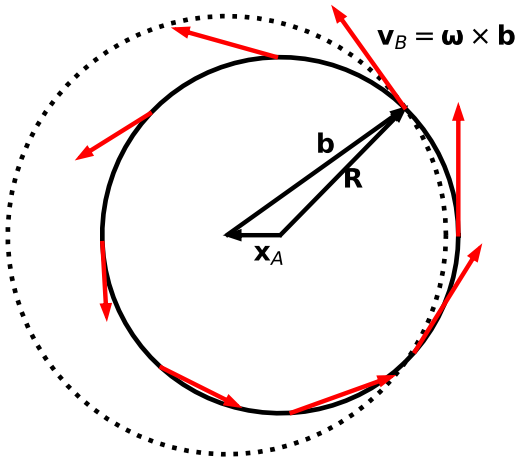

Figure 2.3: Diagram for the centrifugal Case:3. The shell (black solid circle) is centered on the test particle. The center axis of rotation is displaced by vector $\boldsymbol{x}_A$ from the test particle and is perpendicular to that displacement. Defining the displacement of points on the shell from the axis of rotation as $\boldsymbol{b}$ the velocity at any point is given by $\boldsymbol{v} = \boldsymbol{\omega} \times \boldsymbol{b}$, represented by the red arrows. The velocity vectors are therefore not necessarily tangent to the shell. Rather, they are tangent to an imaginary sphere centered on the axis of rotation. One of these imaginary spheres is represented by the dotted circle. You'll notice the velocity vectors at the points where the solid and dotted circles intersect are tangent to the dotted circle. Additionally, you'll notice the velocity vectors are not equal in magnitude. The red arrows toward the left side of the diagram are shorter than those on the right side.

center. In this case, the shell's axis of rotation is offset from the particle by the vector $-x_A\hat{\boldsymbol{x}}$. The vector from the test particle to a point on the shell is still $\mathbf{R} = R\hat{\boldsymbol{r}}$. We now need to define the displacement vector from the center of rotation at $(-x_a, 0, 0)$ to a point on the shell. This vector will be defined as $\mathbf{b}$. We have the simple formula $-x_A\hat{\boldsymbol{x}} + \boldsymbol{b} = \boldsymbol{R}$. So for the vector $\boldsymbol{b}$ we get:

$$\boldsymbol{b} = \boldsymbol{R} + x_a\hat{\boldsymbol{x}}. \tag{2.35}$$

To get the velocity of each point on the sphere, we simply need to use the formula

$\boldsymbol{v} = \boldsymbol{\omega} \times \boldsymbol{b}$. We will introduce a quantity s which is simply the ratio of x_A/R. Additionally, it will be useful to note the cross product of some of the unit vectors. Specifically, we will use: $\hat{\boldsymbol{z}} \times \hat{\boldsymbol{x}} = \hat{\boldsymbol{y}}$ in a rectilinear right-handed coordinate system, and $\hat{\boldsymbol{z}} \times \hat{\boldsymbol{r}} = \sin\theta\hat{\boldsymbol{\phi}}$ mixing cylindrical and spherical coordinate unit vectors. Given all this, we can write the velocity for each point on the sphere as:

$$\boldsymbol{v}(\boldsymbol{x}) = \omega R(\sin\theta\hat{\boldsymbol{\phi}} + s\hat{\boldsymbol{y}}). \tag{2.36}$$

To know the acceleration of all the points on the sphere we need to use a similar formula for acceleration of rotating points, $\boldsymbol{a} = \boldsymbol{\omega} \times \boldsymbol{v}$. For this, we will need more relationships for the cross products of unit vectors. In a rectilinear coordinate system we have $\hat{\boldsymbol{z}} \times \hat{\boldsymbol{y}} = -\hat{\boldsymbol{x}}$, and in a cylindrical coordinate system we know $\hat{\boldsymbol{z}} \times \hat{\boldsymbol{\phi}} = -\hat{\boldsymbol{\rho}}$, where $\hat{\boldsymbol{\rho}}$ is the radial unit vector in a cylindrical coordinate system centered on the test particle. Given these relationships, we have the acceleration as:

$$\boldsymbol{a}(\boldsymbol{x}) = -\omega^2 R(\sin\theta\hat{\boldsymbol{\rho}} + s\hat{\boldsymbol{x}}). \tag{2.37}$$

It is worth pointing out here that the velocity and acceleration of points on the sphere for Case:2 are the same for Case:3 with an additional constant offset $s\hat{\boldsymbol{y}}$ for the velocity and $-s\hat{\boldsymbol{x}}$ for the acceleration. This fact will make it easier to evaluate some of the terms in the EIH Equations.

One thing to note, is that this particular arrangement for the centrifugal case is not the only way we could have set up a rotating shell. We could have easily chosen the shell's axis of rotation to make a diameter with the shell and simply have the test particle offset from the center of the shell by the same displacement. This method would have been simpler to integrate, as the velocities and accelerations for points on the shell would be easier to handle. However, with the end goal of using this solution to integrate over a volume of the universe, it makes better sense to set up this case as described above. This is done so that we may evaluate a positional displacement from the rotation axis while maintaining a mass distribution

that is symmetric around the test particle. Furthermore, as we will see in the next chapter, when density is a function of radial distance from the particle, these simpler velocities and accelerations would be traded for more complex density distributions and an asymmetric upper limit to the radial integration. Additionally, within the context of cosmology, every particle is at the center of its universe. So again, it makes better sense to center the shell on the test particle.

Beginning the integration of the terms, we already noted in Section 2.1.2 the $\boldsymbol{\mathcal{N}}$, $\boldsymbol{\mathcal{E}}$, $\boldsymbol{\mathcal{F}}$, $\boldsymbol{\mathcal{H}}$, and $\boldsymbol{\mathcal{I}}$ terms have already been evaluated to $\mathbf{0}$. Furthermore, in this case $\boldsymbol{v}_A = \mathbf{0}$. This makes the $\boldsymbol{\mathcal{A}}$ and $\boldsymbol{C}$ terms vanish as well. Because $\boldsymbol{v}(\boldsymbol{x})$ and $\boldsymbol{a}(\boldsymbol{x})$ are non-zero for this case, none of the remaining terms can quickly be dismissed.

For the $\boldsymbol{\mathcal{B}}_3$ term we need to evaluate $\boldsymbol{v}\cdot\boldsymbol{v}$. For our setup, this becomes $\omega^2 R^2(\sin^2\theta + 2s\sin\theta(\hat{\boldsymbol{\rho}}\cdot\hat{\boldsymbol{x}}) + s^2)$. But $\hat{\boldsymbol{\rho}}$ is equal to $\cos\phi\hat{\boldsymbol{x}} + \sin\phi\hat{\boldsymbol{y}}$. Therefore, $\hat{\boldsymbol{\rho}}\cdot\hat{\boldsymbol{x}}$ is simply equal to $\cos\phi$. So, after converting to an integral and substituting all the necessary values it looks like this:

$$\boldsymbol{\mathcal{B}}_3 = 2\frac{G}{c^2}R^2\sigma\int_\Omega \mathrm{d}\Omega\frac{\omega^2R^2(\sin^2\theta + 2s\sin\theta\cos\phi + s^2)}{R^2}\hat{\boldsymbol{r}}. \tag{2.38}$$

Here we can note two things. For one, the first term in the above expression is identical to the $\boldsymbol{\mathcal{B}}_2$ term from Case:2 (Eq. 2.28). Recall that term vanished in Case:2, so the first term in this equation will also vanish. Second, the last term in the integral is made up of only constant factors, with the exception of the $\hat{\boldsymbol{r}}$. By symmetry (and Appendix A.1) that term also vanishes. What's left is only to evaluate the integral over the center term. Details of how this is performed can be found in Appendix B.4. The final result for this term is:

$$\boldsymbol{\mathcal{B}}_3 = \frac{16\pi}{3}\frac{G\sigma\omega^2Rx_A}{c^2}\hat{\boldsymbol{x}}. \tag{2.39}$$

For the $\boldsymbol{\mathcal{D}}_3$ term we need to evaluate the product $\hat{\boldsymbol{r}}\cdot\boldsymbol{v}$. The first term in the expression for $\boldsymbol{v}$ is the $\hat{\boldsymbol{\phi}}$ direction which is orthogonal to $\hat{\boldsymbol{r}}$. The second term is in

the $\hat{\boldsymbol{y}}$ direction, so this picks out only the $\hat{\boldsymbol{y}}$ term of $\hat{\boldsymbol{r}}$ which is $\sin\theta\sin\phi$. Given this substitution, we get:

$$\boldsymbol{\mathcal{D}}_3 = -\frac{3}{2}\frac{G}{c^2}R^2\sigma\int_\Omega \mathrm{d}\Omega\frac{(s\omega R\sin\theta\sin\phi)^2}{R^2}\hat{\boldsymbol{r}}. \tag{2.40}$$

This will evaluate to $\boldsymbol{\mathcal{D}}_3 = \mathbf{0}$. For details on the calculations, see Appendix B.4.

In the $\boldsymbol{\mathcal{G}}_3$ term the fact that $\boldsymbol{v}_A = \mathbf{0}$ simplifies it a bit. This leaves the term to look like this:

$$\boldsymbol{\mathcal{G}}_3 = -3\frac{G}{c^2}R^2\sigma\int_\Omega \mathrm{d}\Omega\frac{\hat{\boldsymbol{r}}\cdot\boldsymbol{v}}{R^2}\boldsymbol{v}. \tag{2.41}$$

But we also know what $\hat{\boldsymbol{r}}\cdot\boldsymbol{v}$ is, so we can plug that right in to get:

$$\boldsymbol{\mathcal{G}}_3 = -3\frac{G}{c^2}\sigma\int_\Omega \mathrm{d}\Omega s\omega R\sin\theta\sin\phi\boldsymbol{v}. \tag{2.42}$$

As nicely as this simplifies, there remains much work to be done to fully work it out. For details see Appendix B.6 the result of which gives:

$$\boldsymbol{\mathcal{G}}_3 = 4\pi\frac{G\sigma\omega^2 R x_A}{c^2}\hat{\boldsymbol{x}}. \tag{2.43}$$

For the $\boldsymbol{\mathcal{J}}_3$ term we need to know $\hat{\boldsymbol{r}}\cdot\boldsymbol{a}$. This turns out to be $\hat{\boldsymbol{r}}\cdot\boldsymbol{a} = -\omega^2 R(\sin^2\theta\cos^2\phi + s\sin\theta\cos\phi + \sin^2\theta\sin^2\phi)$. But the first and third terms have a common factor of $\sin^2\theta$ and the sum of $\cos^2\phi + \sin^2\phi$ is of course equal to one. This leaves the integral to be solved as:

$$\boldsymbol{\mathcal{J}}_3 = -\frac{1}{2}\frac{G}{c^2}R^2\sigma\int_\Omega \mathrm{d}\Omega\frac{\omega^2 R(\sin^2\theta + s\sin\theta\cos\phi)}{R}\hat{\boldsymbol{r}}. \tag{2.44}$$

However, once again from Appendix A.2 we can conclude that the first term is simply 0. Leaving the final integral as:

$$\boldsymbol{\mathcal{J}}_3 = -\frac{1}{2}\frac{G}{c^2}R^2\sigma\omega^2 s\int_\Omega \mathrm{d}\Omega\sin\theta\cos\phi\hat{\boldsymbol{r}}. \tag{2.45}$$

For details of the rest of the integration, see Appendix B.7. It evaluates to:

$$\boldsymbol{\mathcal{J}}_3 = -\frac{2\pi}{3}\frac{G\sigma\omega^2 R x_A}{c^2}\hat{\boldsymbol{x}}. \tag{2.46}$$

Finally, we can turn to the last term $\boldsymbol{\mathcal{K}}_3$. We only need to insert our value of $\boldsymbol{a}$ to get:

$$\boldsymbol{\mathcal{K}}_3 = -\frac{7}{2}\frac{G}{c^2}R^2\sigma\int_\Omega \mathrm{d}\Omega\frac{\omega^2 R(\sin\theta\hat{\boldsymbol{\rho}} + s\hat{\boldsymbol{x}})}{R}. \tag{2.47}$$

Appendix A.5 has details on why the term with the $\hat{\boldsymbol{\rho}}$ is zero. The remaining integral is simply:

$$\boldsymbol{\mathcal{K}}_3 = -\frac{7}{2}\frac{G}{c^2}R^2\sigma\omega^2 s\int_\Omega \mathrm{d}\Omega\hat{\boldsymbol{x}}. \tag{2.48}$$

But the $\hat{\boldsymbol{x}}$ factor is simply a constant, and the integral of solid angle over a whole shell is simply 4π. This and plugging $s = x_A/R$ leaves our $\boldsymbol{\mathcal{K}}$ term to be:

$$\boldsymbol{\mathcal{K}}_3 = -14\pi\frac{G\sigma\omega^2 R x_A}{c^2}\hat{\boldsymbol{x}}. \tag{2.49}$$

All of our terms now contain the same factors of all the parameters of the setup:

$$\pi\frac{G\sigma\omega^2 R x_A}{c^2}\hat{\boldsymbol{x}}. \tag{2.50}$$

We can again use the fact that $M = 4\pi R^2\sigma$ to rewrite this as:

$$\frac{GM\omega^2 x_A}{4Rc^2}\hat{\boldsymbol{x}}. \tag{2.51}$$

Additionally, we can rewrite the ω's and $x_A\hat{\boldsymbol{x}}$ to be:

$$\boldsymbol{\omega}\times(\boldsymbol{\omega}\times\boldsymbol{x}_A) = -\omega^2 x_A\hat{\boldsymbol{x}}. \tag{2.52}$$

As a quick demonstration of the above fact, consider this double cross product, $\boldsymbol{c}\times(\boldsymbol{c}\times\boldsymbol{d})$ between two arbitrary orthogonal vectors $\boldsymbol{c} = c\hat{\boldsymbol{z}}$ and $\boldsymbol{d} = x\hat{\boldsymbol{x}} + y\hat{\boldsymbol{y}}$. The

cross product inside the parenthesis will yield $\boldsymbol{c} \times \boldsymbol{d} = -c(y\hat{\boldsymbol{x}} + x\hat{\boldsymbol{y}})$. Now the outer cross product will look like this $c[\boldsymbol{c} \times (-y\hat{\boldsymbol{x}} + x\hat{\boldsymbol{y}})]$ and this will equal $c^2(-x\hat{\boldsymbol{x}} - y\hat{\boldsymbol{y}})$. But the parenthetical factor is simply $-\boldsymbol{d}$. We are then justified to rewrite the double product as $\boldsymbol{c} \times (\boldsymbol{c} \times \boldsymbol{d}) = -c^2\boldsymbol{d}$. It is interesting to note that the double cross product of two orthogonal vectors has the effect of reversing the right-most vector and scaling it by the square magnitude of the left vector.

Given these two substitutions the common factor for each term can be written as:

$$\frac{1}{4}\frac{GM}{c^2R}\boldsymbol{\omega} \times (\boldsymbol{\omega} \times \boldsymbol{x}). \tag{2.53}$$

Now all we need to do is add the terms by their rational prefactors. Those prefactors factors are summarized here:

$$\boldsymbol{\mathcal{B}}_3 \to \frac{16}{3}, \tag{2.54}$$

$$\boldsymbol{\mathcal{G}}_3 \to 4, \tag{2.55}$$

$$\boldsymbol{\mathcal{J}}_3 \to -\frac{2}{3}, \tag{2.56}$$

$$\boldsymbol{\mathcal{K}}_3 \to -14. \tag{2.57}$$

The sum of these is simply $-16/3$. All told, the final form of the acceleration in this Case:3 is:

$$\boxed{\boldsymbol{a}_{A,3} = \frac{4}{3}\frac{GM}{c^2R}\boldsymbol{\omega} \times (\boldsymbol{\omega} \times \boldsymbol{x}_A)}. \tag{2.58}$$

2.1.6 Comparison with Inertial Cases

Looking back at the results from the previous three sections, we can notice a common factor of $4GM/3c^2R$. To simplify notation, I'll introduce the dimensionless quantity Θ.

$$\Theta \equiv \frac{4}{3}\frac{GM}{c^2 R}. \tag{2.59}$$

Summarizing our results from the previous three sections, we have:

$$\boldsymbol{a}_{A,1} = \frac{11}{4}\Theta \boldsymbol{a}, \tag{2.60}$$

$$\boldsymbol{a}_{A,2} = 2\Theta \boldsymbol{\omega} \times \mathbf{v}_A, \tag{2.61}$$

$$\boldsymbol{a}_{A,3} = \Theta \boldsymbol{\omega} \times (\boldsymbol{\omega} \times \boldsymbol{x}_A). \tag{2.62}$$

So far in this chapter, we have assumed the shell is moving relative to an observer in an inertial frame. That setup made the accelerations on the test particle come from "real" gravitational forces. Now we will analyze the situation from the opposite standpoint, in which the shell is static relative to an inertial frame but the observer is in a non-inertial frame. In each case, the relative motion of the shell to the observer frame must be maintained. For Case:1 the frame would be accelerating in the opposite direction of the shell's original acceleration, $\boldsymbol{a}_{\text{frame}} = -\boldsymbol{a}_{\text{shell}}$. For cases 2 and 3—the rotational ones—the observer's non-inertial frame would rotate in the opposite direction as shell's original rotation, $\boldsymbol{\omega}_{\text{frame}} = -\boldsymbol{\omega}_{\text{shell}}$.

With these new non-inertial frames set up, we can ask what will the test particle's apparent acceleration will be *without* any external forces. The results would simply be the *fictitious* forces of the centripetal, Coriolis and linear acceleration as established in Chapter 1.

$$\boldsymbol{a}^{\text{non}}_{A,1} = -\boldsymbol{a}_{\text{frame}} \tag{2.63}$$

$$\boldsymbol{a}^{\text{non}}_{A,2} = -2\boldsymbol{\omega}_{\text{frame}} \times \boldsymbol{v}^{\text{non}}_A \tag{2.64}$$

$$\boldsymbol{a}^{\text{non}}_{A,3} = -\boldsymbol{\omega}_{\text{frame}} \times (\boldsymbol{\omega}_{\text{frame}} \times \boldsymbol{x}^{\text{non}}_A) \tag{2.65}$$

Note in the above set of equations I replace the "B" subscript that was used in the

original definition of the fictitious forces with a "non" superscript. Now substituting in $\boldsymbol{\omega}_{\text{shell}} = \boldsymbol{\omega} = -\boldsymbol{\omega}_{\text{frame}}$, and $\boldsymbol{a}_{\text{shell}} = \boldsymbol{a} = -\boldsymbol{a}_{\text{frame}}$ we get:

$$\boldsymbol{a}_{A,1}^{\text{non}} = \boldsymbol{a}, \tag{2.66}$$

$$\boldsymbol{a}_{A,2}^{\text{non}} = 2\boldsymbol{\omega} \times \boldsymbol{v}_{A}^{\text{non}}, \tag{2.67}$$

$$\boldsymbol{a}_{A,3}^{\text{non}} = -\boldsymbol{\omega} \times (\boldsymbol{\omega} \times \boldsymbol{x}_{A}^{\text{non}}). \tag{2.68}$$

Now we are able to make some very interesting comparisons between gravitational forces of a rotating/accelerating sphere vs. its observationally equivalent[2] static counterpart in a non-inertial frame. First, each case is proportional[3] to the dimensionless quantity Θ. Second, the vector relationships are the same under both considerations. Finally, cases 2 and 3 have the same numerical proportionality for both considerations (1 and 2, respectively).

For now, let's focus on Case:2, the Coriolis case. Since the gravitational solution is completely in line with the fictitious solution apart from the Θ factor, what does that factor mean? For one, we can note that the Schwarzschild radius of a body, R_S, is equal to $2GM/c^2$, which forms the event horizon for a black hole. Θ then is equivalent to $(2/3)R_S/R$. So, unless the test particle is in a black hole $R > R_S$, and Θ must be less than one. But in fact Θ is typically *really* small for most conceivable shells. G is on the order of 10^{-11} and c^2 on the order of 10^{17} in SI units. Any M/R configuration needs to reach an order of magnitude of about 10^{27} for Θ to be of order unity. As an example, for a spinning basketball Θ is roughly 8×10^{-27}. However, more relevant to the topic at hand is Θ sets the amount that the shell drags the inertial frame of the particle. It may be helpful to consider a gyroscope at the center of the shell rather than a free particle. Without the spinning shell the gyroscope

[2]To make this truly observationally equivalent, the shells would have to have the same characteristics of an "Einstein Cabin." That is to say, the observer cannot be able to view anything outside the shell.

[3]Admittedly, I've shoehorned that factor out of the linear acceleration case.

would naturally remain fixed in its orientation with respect to the distant stars and galaxies. However, once we introduce the spinning shell, the gyroscope will slowly drift in its orientation in the direction of the shell's rotation. And, after Θ^{-1} full rotations of the shell, the gyroscope will have made one full rotation with respect to the distant stars and galaxies. This effect is better known as "frame dragging," as it appears to drag the inertial frame of the gyroscope relative to stars.

It is worth pointing out again that these kinds of effects have been tested very well with experiments like GINGERINO, Gravity Probe B, and Lunar Laser Ranging. Additionally, I am not the first to theoretically determine this result of Θ. In Misner, Thorne and Wheeler's (MTW) massive textbook on "Gravitation" they attribute Lense and Thirring to first determining this drag [MTW73]:

$$\omega_{drag} = k\frac{G}{c^2}\frac{M_{\text{shell}}}{R_{\text{shell}}}\omega_{\text{shell}}, \tag{2.69}$$

with k being a coefficient depending on the location of the experiment relative to the shell, and $k = 4/3$ anywhere inside the shell, as is the case in Θ (Eq. 2.59). However, Lense, Thirring and other authors have determined this coefficient by detailed calculations using weak field limit within GR. Additionally, Okamura, Ohta, Kimura and Hiida computed accelerations within a rotating shell to order $(v/c)^4$ to determine $\omega_{\text{drag}}/\omega_{\text{shell}}$ [OOKH75]. They found the same result for the Coriolis case as was found in Section 2.1.4. However, their result for the centrifugal case included two terms. The first was is identical to the result found in Section 2.1.5. The second term represents an acceleration toward the axis of rotation at the order of ω^2. Based on the two centrifugal terms, they concluded that the quantity GM/R needed to be equal to both 3/4 *and* 1260/3737 in order to satisfy "Mach's thought," thus exposing a critical contradiction and thereby rejecting the Machian premise.

Okamura et al. treat the centrifugal case differently than I did in Section 2.1.5, by putting the test particle away from the shell center, while I required the shell to be symmetric about the particle—instead displacing the rotation axis. When I

originally approached the problem in the common way (as Okamura et al. did), I also saw unexpected axial acceleration. Reasoning that the universe is not asymmetrically distributed around the test particle, I switched to the centered approach and found that the centrifugal term survived while the unexpected acceleration disappeared. It seems to me that the inconsitiency noted by Okamura et al. is an artifact of their choice of shell de-centering. An asymmetric mass distribution is not physically consistent with the universe, and produces a spurious acceleration in the EIH terms when invoked.

One question we should ask is, what happens when Θ is equal to one? As mentioned above, since Θ is also equal to $(2/3)(R_S/R)$, for a single shell the test particle would be within the shell's event horizon. But, what if there were two concentric shells each rotating at the same rate? If these shells had different radii and mass such that both their ratios of R_S/R were equal to 3/4, then $\omega_{\text{drag}} = \omega_{\text{shell}}$. This would mean that the inertial frame of the gyroscope would be totally dragged by the shells. We might call this frame "locking," as for every full rotation of the shells we would expect a full rotation of the gyroscope. If these shells made up the Einstein cabin in which our lonely astronaut was sealed within, they might conclude that their rocket was *not* rotating relative to the fixed stars. In this case, their inertial frame would be tied, not to the fixed stars, but to their rocket's cabin. This implies that the gravitational forces of their rotating cabin would supply the inertial forces if they were to do experiments in a frame rotating relative to their cabin.

Chapter 3

Volume Integration of Shells

In the previous chapter we integrated the EIH Equations over the surface of a shell to determine the net gravitational accelerations it imparted on a test particle at its center. We did this under three different cases to compare with well known "fictitious" forces. They were the linear acceleration Case:1, the Coriolis Case:2, and the centrifugal Case:3. The results from each case contained a common factor of $\Theta \equiv 4GM/3c^2R$. Additionally, the vector nature of each result was in line with its fictitious counterpart. In this chapter we extend the previous integration in the radial direction to get a volume integral. The question will be whether the universe as a whole has the right amount of $\int M/R$ to lock our inertial frame to the fixed stars—providing fictitious forces from gravitational coupling to any frame that is not fixed wrt the stars.

If one moves to a rotating frame, then the whole universe is in relative rotation to the frame. For this reason, we want to understand what the total gravitational contributions would be from every bit of mass-energy in the test particle's past light-cone. Our integral will then need to cover a volume that includes the whole observable universe. We will then compare this again with the fictitious counterparts.

3.1 Solid Sphere

For a spherical solid, to get a volume integral from the shells, we simply need to integrate over Θ, by redefining the mass to be a mass element $M \to dM(r)$:

$$I = \int \frac{4}{3}\frac{G\mathrm{d}M}{c^2 R}. \tag{3.1}$$

Naturally, we will define this in terms of the density, ρ, as a function of r, $dM = \rho(r)dV(r) \to 4\pi r^2\rho(r)dr$. We will then need to integrate from $r = 0$ to some upper limit R. Again, the distance measures will be Euclidean. The integral will then look like this:

$$I = \frac{4}{3}\frac{G}{c^2}\int_0^R \frac{4\pi\rho(r)r^2}{r}\mathrm{d}r = \frac{4}{3}\frac{G}{c^2}4\pi\int_0^R r\rho(r)\mathrm{d}r. \tag{3.2}$$

This integral would be perfectly valid for any sphere where one might be interested in these sorts of accelerations. In cases where the density is constant, and the sphere has mass M, I simply reduces to

$$I = \frac{2}{3}\frac{G}{c^2}(4\pi\rho R^2) = \frac{2GM}{c^2 R} \tag{3.3}$$

This result is equivalent to R_S/R. For those with easily retrievable knowledge on the Schwarzschild radius of certain bodies, this result can be quite useful to estimate I. For instance, R_S for the Sun and Earth respectively are about 3 km and 1 cm. While their radii are about 7×10^5 km and $6,000$ km respectively. This puts their values at $I_{\mathrm{Sun}} \approx 4\times10^{-6}$ and $I_{\mathrm{Earth}} \approx 2\times10^{-9}$. If we look at some other astrophysical objects, a white dwarf is about the size of Earth but with a density that is a factor of about 200,000 greater than the Earth, resulting in $I_{\mathrm{WD}} \approx 4 \times 10^{-4}$. A neutron star's mass is on the order of a solar mass, but its radius is only $20\,\mathrm{km} \approx 3 \times 10^{-5}\,R_{\mathrm{Sun}}$. This makes the integral for a neutron star to be about[1] $I_{\mathrm{NS}} \approx 0.1$. For a black

[1]The strong gravitational field of the interior of a neutron star would very likely be a case

hole $R = R_S$, making $I_{\rm BH} = 1$. If we wanted to consider what we might get for a terrestrial construction, lead has a density of about 11,000 kg/m^3. A ball of lead 2 meters across would have the integral come out to $I_{\rm lead} \approx 7 \times 10^{-23}$.

3.2 Naïve Integral

Turning back to our original goal of integrating over the volume of the universe, let's first take a naïve but simple setup for the universe to get a sense of scale for this integral. In this setup, we will assume the universe has constant density and extends out to some finite horizon. In addition to this, we will assume a non-evolving FLRW universe where space is not expanding. Given that condition, we can still use Euclidean distance measures in this integration. Later, we will take greater care in setting up the density and distance relationships in a more cosmologically relevant manner. For now, however, let's use the fact that this universe is observationally flat to determine an appropriate density for this naïve integral. Recall, a flat universe has its overall density parameter, Ω, equal to 1. This in turn determines the density to be equal to the critical density $\rho_c = 3H_o^2/8\pi G$. In terms of the radial limits, we know the Hubble distance $R = D_H = c/H_0$ sets the scale for the size of the universe and all other relevant radial cosmographic distances. Using this as the upper limit then sets a natural scale for our integral. Another facet we should be careful about is the rotation rate. Recall that EIH carries terms to order $(v/c)^2$. The speed of a particle in circular motion is given by $v = \omega r$. Even a modest rotation rate can provide superluminal velocities at fairly short distances[2]. To ensure there are no superluminal speeds on account of the rotation, we require $\omega \ll 1/t_H$. Even though this rotation rate is *incredibly* slow, a demonstration of $I \sim 1$ would be a

where the EIH approximation would not hold. So this value should only be really used as a first approximation.

[2]Consider the Earth, and its angular frequency of $2\pi \times 365\,{\rm yr}^{-1}$. Given $c = 1\,{\rm ly\,yr}^{-1}$, the superluminal distance, is merely 4×10^{-4} ly or about 25 AU. It isn't even passed Neptune's orbit.

significant result, in that even trivially small relative rotation rates would impose inertial effects that would "lock" the inertial frame to the universe. We can give this particular implementation of the cosmological integral a subscript of N to remind us that it is a naïve first step toward understanding the general integral. This integral then results in:

$$I_N = \frac{2}{3}\frac{G}{c^2}(4\pi\rho_c D_H^2) = \frac{2}{3}\frac{G}{c^2}\left(4\pi\frac{3H_0^2}{8\pi G}\right)\left(\frac{c}{H_0}\right)^2 = 1. \tag{3.4}$$

The fact that this integral comes out to unity is quite a remarkable result. This means that the gravitational accelerations from this rotating sphere are *exactly* equal to their fictitious counterparts. These accelerations being equal makes it so that any two frames that observe the same relative rotation of the distant stars are equivalent. This equivalence means that like our lonely astronaut who cannot tell whether they are on a planet's surface or accelerating out in deep space, we cannot tell whether gravitational influences from a rotating universe are producing our "fictitious" forces or whether we're rotating with respect to some absolute frame. In other words, the only frame in which we see no "fictitious" forces is the one that is not rotating relative to the mass distribution of the universe. Likewise, the only rotation we would be able to determine from experiment would be a rotation *relative* to the fixed stars. All this is consistent with three interpretations of Mach's principle. Restating them from page 12:

- Mach0: The universe, as represented by the average motion of distant galaxies, does not appear to rotate relative to local inertial frames.
- Mach3: Local inertial frames are affected by the cosmic motion and distribution of matter.
- Mach8: $\Omega \equiv 4\pi\rho G T^2$ is a definite number, of order unity, where ρ is the mean density of matter in the universe, and T is the Hubble time.

All of this implies that our local inertial frame is "locked" to that of the distant stars. Or put another way, **General Relativity asserts the universe as a "natural" frame**, allowing the detection of rotation relative to the fixed stars, whether you can see them or not.

Furthermore, because all experiments we have done imply that our natural inertial frame is the one that is tied to the fixed stars, I strongly believe that this integral *must* be equal to unity. To substantiate this belief, it may be helpful to consider what would happen should the integral be close—but not equal—to one. Suppose we analyze a situation in two frames, both of which observe the same relative rotation to the distant stars. The first frame A asserts that their frame is not rotating while the universe rotates about it. The second frame, B, asserts that the distant stars are not moving, but that its frame is non-inertial (rotating). Observationally, A is indistinguishable from B. The integral relates the gravitational accelerations from frame A, $\boldsymbol{a}_A = \boldsymbol{a}_{\text{grav}}$, to the accelerations from the fictitious forces in frame B, $\boldsymbol{a}_B = \boldsymbol{a}_{\text{fict}}$, by the relationship $\boldsymbol{a}_{\text{grav}} = I\boldsymbol{a}_{\text{fict}}$. Naturally, observables in one frame should not contradict observables in the second. But, if $I \neq 1$, then $\boldsymbol{a}_A \neq \boldsymbol{a}_B$. If this were the case, we would need to invent some other force to make $\boldsymbol{a}_A = \boldsymbol{a}_B$.

Figure 3.1 gives another illustration of what happens should $I \neq 1$. The figure plots trajectories for particles in a rotating frame with accelerations $\boldsymbol{a} = I\boldsymbol{a}_{\text{fict}}$, where $\boldsymbol{a}_{\text{fict}}$ is equal to the Coriolis acceleration and centrifugal accelerations. The axis of rotation is through the origin of the figure and perpendicular to the x-y plane. In the rotating frame all these trajectories will produce inward spirals. When plotted in the rotating frame it is difficult to qualitatively analyze. For this reason, the trajectories have been "un-rotated" back to a non-rotating frame. The initial conditions for each trajectory are identical with $\boldsymbol{x}_0 = (1, 0)$ and $\boldsymbol{v}_0 = (-1, 0)$. The time span for the trajectories is set to $t = [0, t_f]$, where $t_f = |x_0/v_0| = 1$. The initial position and final positions of each trajectory are marked with a star and diamond, respectively. The rotation rate used in the fictitious accelerations is $\omega = 1$. We clearly notice when

$I \neq 1$ the trajectories make large deviations from the straight line trajectory given by $I = 1$. What is more interesting however is that the curved trajectories never reach the origin. Suppose we placed some sort of detector at the origin that will beep if our projectile strikes it. This means that if we analyze this situation like we would in cases A and B from the previous paragraph and if $I \neq 1$ we would get different testable results.

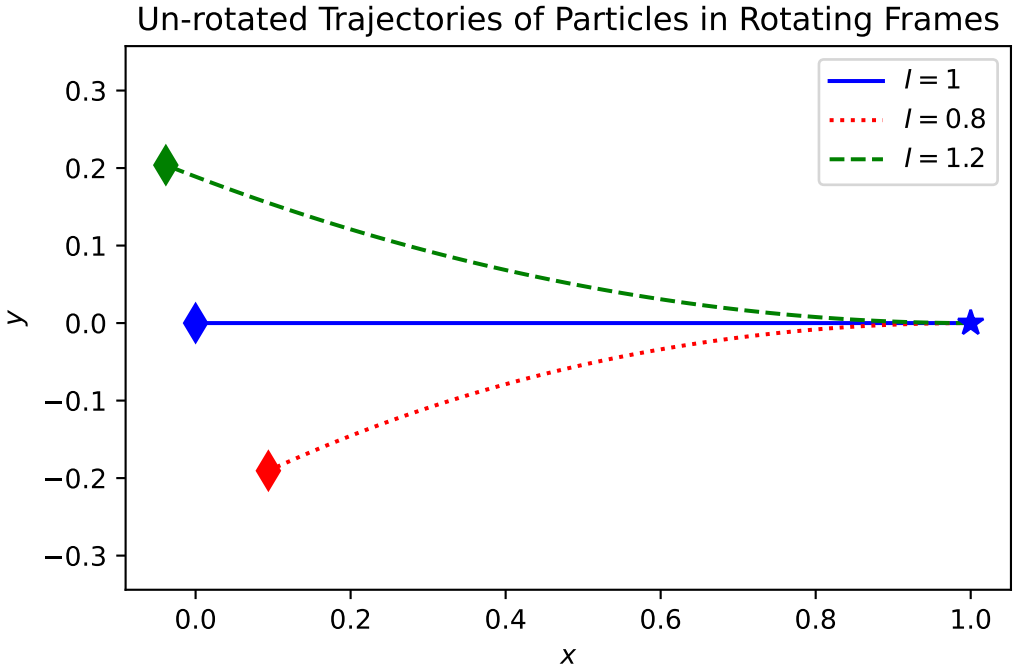

Figure 3.1: Projectiles following accelerations in a rotating frame equal to $I\boldsymbol{a}_{\text{fict}}$, with $\boldsymbol{a}_{\text{fitct}} = -2\boldsymbol{\omega}\times\boldsymbol{v} - \boldsymbol{\omega}\times(\boldsymbol{\omega}\times\boldsymbol{x})$ and $\boldsymbol{\omega} = 1\hat{\boldsymbol{z}}$. The initial conditions are $\boldsymbol{x}_0 = (1, 0)$ and $\boldsymbol{v}_0 = (-1, 0)$. The time is run for a span of $|x_0/v_0|$. The initial and final positions are marked with a star and diamond, respectively. These trajectories are "un-rotated" and viewed from a frame that is fixed relative to the rotating frame.

Another way to look at this is to say that the inertial properties of a body, given by its inertial mass, are dictated by gravitational coupling to the universe and proportional to the gravitational (coupling) mass of the body in question. Thus, this

relationship provides a mechanism for the inertial mass of a body to be equal to its gravitational mass. This is in line with Mach6: inertial mass is affected by the global distribution of matter. This mechanism also explains the success of equivalence principle measurements: if an object's *inertial* mass is produced by gravitational coupling of its *gravitational* mass to the mass distribution of the universe, then no experiment will be able to produce anything but strict proportionality between these two mass types.

It is worth pointing out that in 2017 Braek, Grøn and Farup made a similar integration to find the Cosmic Causal Mass. However, their method simply sought to find the ratio r_{SD0}/r_{ph0}, where r_{SD0} is the Schwarzschild radius of the total amount of matter in the observable universe and r_{ph0} is the particle horizon distance for the current epoch. The particle horizon is the proper distance today to the particles at redshift $z = \infty$. Recalling that the comoving distance is defined as the proper distance today, the particle horizon is simply given as $D_C(\infty)$. The value they get is $r_{SD0}/r_{ph0} = 1.05$, [BGF17]. What they don't do is integrate over shells the quantity M/R. While the interest and motivation are similar, the technique in this work of integrating over shells is fundamentally different.

3.3 Cosmological Integral

In the previous section, we found that the naïve integral of shells over a constant-density universe resulted in a value for I_N exactly equal to unity. However, for an expanding and evolving universe composed of multiple species of mass-energy (such as matter, radiation, and dark energy) it is clear that the assumption of constant density is far from realistic. This section will focus on a more careful handling of the integral with respect to a cosmological model of the universe. Recalling the expression we want to integrate:

$$I = \int \frac{4}{3} \frac{G \mathrm{d}M}{c^2 R}. \tag{3.5}$$

The parameters we will need to consider in cosmological terms include the density of the universe at its various epochs, the appropriate distance to the mass-energy at those epochs, as well as the volume element at those epochs. We will also need to consider the upper limit to the integral, as it is not a truncated edge as was handled in the naïve integral.

As noted in Section 1.4, cosmologists have defined a number of distance measures to effectively handle questions of distance related to the evolving geometry of the universe. Each of these distance measures is related to redshift, z. Redshift, you may recall, is an actual observable that astronomers can measure. For this reason, it makes more sense to shift our integration over distance to one over redshift rather than a radial coordinate. The use of redshift will provide a natural upper limit to the integral of $z \to \infty$.

Schutz remarks that "the most convenient ways to measure the range to a distant object is [with light]" [Sch09]. This is the fundamental principle of determining the distance to the Moon in Lunar laser ranging. Within the Solar system, as well as terrestrially, this is performed by sending a light signal out to an object, which reflects it back to the sender. The time is measured for the signal to go out and return. By multiplying that time by the speed of light and dividing by two, we can determine the distance to that object. For cosmological distances, we cannot send a light signal out and back, but we do have a way to determine the time it takes for the light to leave a distance source and reach us. It is the look-back time. By multiplying that time by the speed of light, we can define the distance we will need for our integral. Recall from Section 1.4 that the light travel distance is given by:

$$D_T(z) = D_H \int_0^z \frac{\mathrm{d}\zeta}{(1+\zeta)E(\zeta)}. \tag{3.6}$$

Defining the mass of our shell, as we did in the naive integral, as $dM = \rho(z)dV$ we simply need to determine the volume elements and density of a shell at redshift z. We do have expressions for these two values. Reprinting them from Section 1.4 we have:

$$\rho(z) = \frac{3H_0^2}{8\pi G}[E(z)]^2 = \frac{3H_0^2}{8\pi G}\sum_x \Omega_{x,0}^{d_x}, \tag{3.7}$$

$$\mathrm{d}V_P = D_H \frac{D_C^2}{(1+z)^3 E(z)}\mathrm{d}\Omega\mathrm{d}z. \tag{3.8}$$

But because the universe is flat, the integration over the solid angle will simply return 4π. Combining all this together, we get the mass element to be:

$$\mathrm{d}M = \rho(z)dV_P(z) \to \frac{3H_0^2[E(z)]^2}{8\pi G} \cdot \frac{4\pi D_H D_C^2}{(1+z)^3 E(z)}\mathrm{d}z. \tag{3.9}$$

This reduces to:

$$\mathrm{d}M \to \frac{3H_0^2 E(z) D_H D_C^2}{2G(1+z)}\mathrm{d}z. \tag{3.10}$$

We have now satisfactorily defined dM and R as functions of redshift. So it may seem like we are ready to plug everything in and start integrating, but we aren't quite done yet. We can note that in EIH there are five terms that depend on the velocity or acceleration of the B particles—the points on the shell in our integrations. These are the $\boldsymbol{\mathcal{B}}$, $\boldsymbol{\mathcal{C}}$, $\boldsymbol{\mathcal{G}}$, $\boldsymbol{\mathcal{J}}$, and $\boldsymbol{\mathcal{K}}$ terms. Additionally, scrolling through Chapter 2 you may notice that all the other terms were zero for all three cases. This leaves a factor in the numerator of each term with a dimensionality of length. But because the universe was smaller when the shell at redshift z left its mark on the local gravity fields, we also need to modify and reduce these velocities and accelerations by the scale factor, $a = (1+z)^{-1}$. This means we need an extra factor of $(1+z)^{-1}$ in our integrand along our expressions for R and dM.

All together, our integral will be:

$$I = \frac{4}{3}\int_0^\infty \frac{G}{c^2}\left[\frac{3H_0^2 E(\zeta) D_H D_C^2}{2G(1+\zeta)^3}\right]\frac{\mathrm{d}\zeta}{(1+\zeta)D_T}. \tag{3.11}$$

After some canceling of factors, it reduces to:

$$I = 2\int_0^\infty \frac{H_0^2}{c^2}\left[\frac{E(\zeta)}{2G(1+\zeta)^4}\right]\left[\frac{D_H D_C^2}{D_T}\right]\mathrm{d}\zeta. \tag{3.12}$$

As a reminder the Hubble time, D_H, is equal to c/H_0, and the comoving distance, D_C, is given by:

$$D_C = D_H \int_0^z \frac{\mathrm{d}\zeta}{E(\zeta)}. \tag{3.13}$$

This makes the factor of $D_H D_C^2/D_T$ equal to:

$$\frac{D_H D_C^2}{D_T} = \frac{c^2}{H_0^2}\frac{[\int_0^z \mathrm{d}\zeta/E(\zeta)]^2}{\int_0^z \mathrm{d}\zeta/(1+\zeta)E(\zeta)}. \tag{3.14}$$

Plugging this in we get our final integral:

$$\boxed{I = 2\int_0^\infty \frac{d\zeta E(\zeta)}{(1+\zeta)^4}\frac{[\int_0^\zeta \mathrm{d}\zeta'/E(\zeta')]^2}{\int_0^\zeta \mathrm{d}\zeta''/(1+\zeta'')E(\zeta'')}}. \tag{3.15}$$

In order to simplify the notation a little I'll collect the ratio of the inner integrals into the factor:

$$D_I(z) = \frac{[\int_0^z d\zeta/E(\zeta)]^2}{\int_0^z d\zeta/(1+\zeta)E(\zeta)}. \tag{3.16}$$

I will also wrap the whole integrand up into the following function:

$$\mu(z) = \frac{E(z)}{(1+z)^4} D_I(z). \tag{3.17}$$

Thus, our integral will simply look like this:

$$I = 2\int_0^\infty \mathrm{d}\zeta\mu(\zeta). \tag{3.18}$$

3.4 Integration Results

Now that we have a carefully considered the integral under cosmological conditions, what does it integrate to? The $E(z)$ function—which contains all the evolutionary behavior for any cosmological model—can be found in the integral three times. This makes the integral—and *its* evolutionary behavior—depend on the model used. Because ΛCDM is the accepted standard (vanilla) cosmological model, it makes sense to first evaluate the integral using it. For ΛCDM, this integral evaluates to:

$$I^{\Lambda\text{CDM}} = 0.94 \tag{3.19}$$

It is rather remarkable that this is of order unity. The universe seems to have nearly enough mass to supply what we call inertial mass and have our inertial frames tied to the distant galaxies. If my assertions are correct that this integral should be unity, then ΛCDM does a good job at getting most of the way there. But, just as ΛCDM already has some observable issues as outlined in Section 1.4, perhaps this is another "tension" that could be resolved by adjusting the model of ΛCDM. Indeed, as we will explore in the next chapter, maybe this "discrepancy" can shed light on how one might approach a more self-consistent gravitational and cosmological model.

It is helpful to see how the integral grows as we lower its upper bound. Plotted in Figure 3.2 is the integral I but truncated at an upper limit of z, marked on the horizontal axis. The curves in the plot represent the same set of alternate universe compositions as described in Table 1.2. This figure has a few features that are worth mentioning.

First, each case is asymptotic to some constant value—indicating that the integral is well-behaved as $z \to \infty$. Those values are the numbers printed in the legend next to each label. This should be fairly intuitive for all but the Λ-only case, because D_C and D_T will approach finite constant values as $z \to \infty$. Then the integrand is simply $E(z)/(1+z)^4$. Since the highest dilution parameter is 4 for radiation the

integrand will go like $(1+z)^{-2}$ or smaller as $z \to \infty$. Naturally, integrals of those types will be finite. For the Λ-only case, it is easy to show that the integrand is $z^2/(1+z)^4 \ln(1+z)$, which will also produce a finite result. Furthermore, all the values they integrate to are of order unity.

Second, the largest contribution to the integral in each scenario made is between $z = 1$ to $z = 10$. I find it quite interesting that these integrals have their greatest contribution during this epoch regardless of their make-up. Additionally, it seems like the overall initial sum of the Ω parameters does not have an overall impact on the integral's trajectory in the plot. Take for instance the matter only case and the "No Lambda" case. Both are very much matter dominated (one of them by definition). However, the total density Ω for the two cases is 0.3112 and 1 respectively. Despite this fairly large difference between the two initial conditions, their values are identical to a few parts in 10^3. They are so close, it is difficult in the figure to even notice the orange line tucked under the brown line.

3.5 Integral for Observer at Arbitrary Z

We've made the argument that this integral should be of order unity. But, that argument should not just be true for the current epoch. Indeed, if there were sufficient reason for this integral to be equal to one today, then the same arguments should hold for any epoch. In this vein, another thing we should look at is how this integral changes if it starts out at some other epoch Z. The most straightforward way to do this is to simply update the $\Omega_{x,0}$ parameters in the integral to $\Omega_{x,Z}$. Recalling Equation 1.25, the updated density parameters are given by:

$$\Omega_{x,Z} = \frac{\Omega_{x,0}(1+Z)^{d_x}}{[E(Z)]^2}. \tag{3.20}$$

We can then update the E function to be:

$$E_Z(z_{\rm rel}) = \sqrt{\sum_x \Omega_{x,Z}(1+z_{\rm rel})^{d_x}}, \tag{3.21}$$

where $z_{\rm rel}$ is the redshift an observer would make from their epoch Z. By simply plugging this into the original integral in place of $E(z)$ we get a new integral I_Z. The limits of the new integral will be the same, and the integrating variable will simply be over $z_{\rm rel}$. For clarity, any parameter, function, etc. that is relative to some epoch Z will be labeled with its epoch as a subscript. One way we can imagine this is as if some other graduate student at redshift Z were trying to do a similar calculation, they would use the results from their Planck satellite for $\Omega_{x,0}$ to initialize their integral. Their $\Omega_{x,0}$ would simply be equal to our $\Omega_{x,Z}$.

Figure 3.3 show the results of these I_Z integrals for the same $\Omega_{x,0}$ values as given in Table 1.2. This plot has a few notable features. First, all single component universes' integrals, I_Z, are constant[3] for all Z. This should make some sense if we refer to Equation 3.20. For any single component universe with X species of mass-energy, $\Omega_{X,0}$ is equal to one, while all the others are equal to zero. Therefore, $[E(Z)]^2$ is simply equal to the numerator $\Omega_{X,0}(1+Z)^{dX}$, which is constant. A less mathematical but more physics-minded approach to understand this is that single component universes never encounter a time when their behavior changes because of a swap in the dominant species.

Something else we can notice is that for the mixed universes, they remain fairly constant to the far right and left of the plot. The small evolution at high redshift, z well into the radiation dominated epochs, makes it so that any adjustments to cosmology to flatten out the curves need not be drastic. They take on the most change near and between the transitions of the dominant species. These transitions are given by the two dotted vertical lines in the plot. The left-most is the Λ-Matter transition, while the other is the Matter-Radiation transition. It is also interesting

[3]The small bump on the radiation line near $Z = 10^4$ appears to be an artifact from the numerical integration.

to note that the "Standard" universe matches up very well with the "No Lambda" universe to the right of the Λ-Matter transition. Then both those compositions match up with the "Radiation" universe.

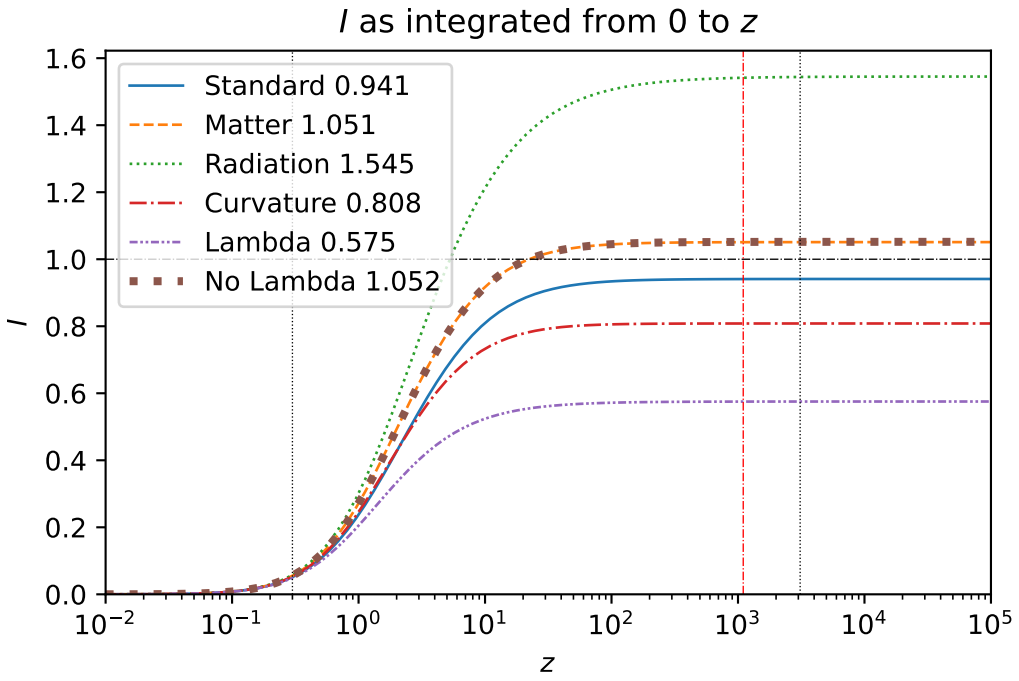

Figure 3.2: This is the integral I but truncated on its upper limit from ∞ to z. Each curve represents a different model with differing compositions of mass-energy at the current epoch. These models and their compositions are enumerated in Table 1.2. In the legend are the full values I integrates to with the proper upper limit of $z \to \infty$. The orange curve for the "Matter" universe is plotted, however it is nearly identical to the brown dotted "No Lambda" curve and can be difficult to see. The horizontal dash-dotted line is used to mark a line for $I = 1$. The vertical dotted lines represent the transitions from radiation to matter dominated epochs (right line) and matter to dark energy dominated epochs (left line). The red vertical line is the redshift of the CMB, $z_{ls} = 1100$.

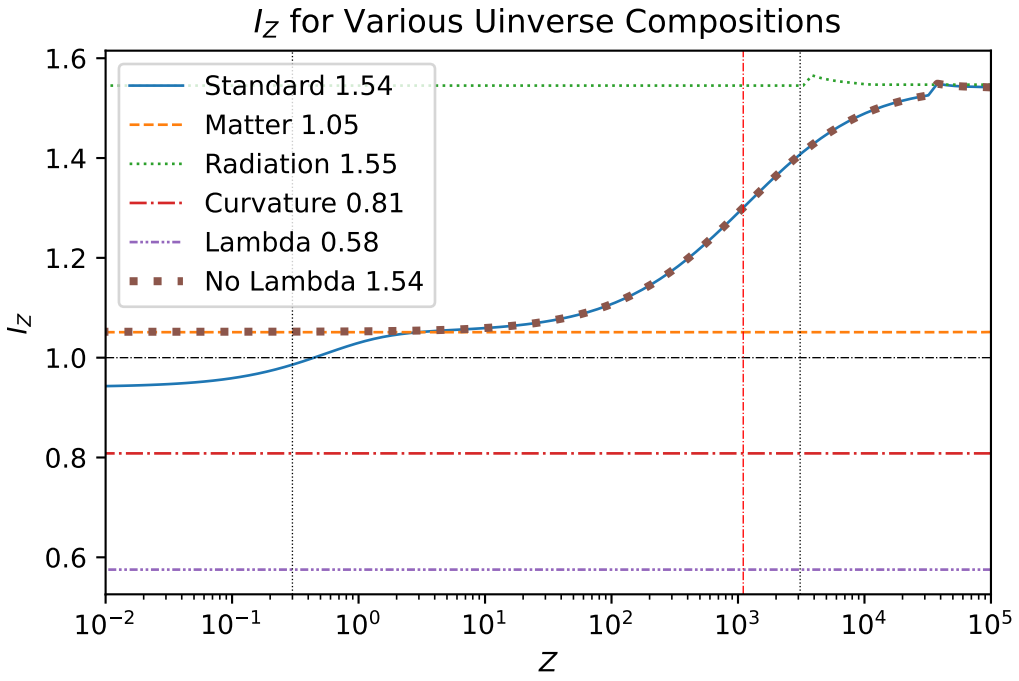

Figure 3.3: This is a plot of I as evaluated from the epoch Z. This plot essentially demonstrates how I evolves in time from high Z to the present epoch. Each curve represents a different model with differing compositions of mass-energy at the current epoch. These models and their composition are enumerated in Table 1.2. In the legend the values I_Z as $Z \to \infty$ are reported. At $Z \approx 1$ the blue "Standard" curve joins and then becomes nearly identical with the brown dotted "No Lambda" curve. The "Standard," "No Lambda," and "Radiation" curves all evaluate to the same value as $Z \to \infty$. The vertical black dotted lines represent the transition epochs from matter to dark energy (left line) and radiation to matter (right line). The red vertical line is the redshift of the CMB, $z_{ls} = 1100$.

Chapter 4

Investigation of a Possible "Correction" to the Cosmological Integral

In the previous chapter we determined that the integration of the important quantity $\Theta \equiv 4GM/3c^2R$ over the volume of the universe is of order unity under the assumptions of ΛCDM. At every turn, I've also been quick to point out that the fact that these integrals come out to order unity is very important. It is also important to note that in the previous chapters, we were simply working within the context of GR and ΛCDM—two theories that are well-supported by experiment and observation. This chapter will ask "what modifications are needed to make the integral *equal to* one, as we strongly suspect it must be?" Moreover, we will explore ways to ensure that this integral evaluates to unity for all epochs.

4.1 Changes to $E(z)$

One of the first places we can look to change this integral is by changing the $E(z)$ function. A natural first step might be simply to change one of the density parameters Ω_x or a dilution parameter d_x. Tweaking any single one of these parameters or any combination to give $I = 1$ for the current epoch is certainly a straightforward task. One alternative theory to ΛCDM is wCDM. Simply put, this theory hypothesizes that the equation of state parameter for dark energy is not equal to -1, as in ΛCDM, but has some value $w \neq -1$. In 2021 D'Amico, Senatore and Zhang using early and late epoch observations set limits on the equation of state parameter to $w = -1.02 \pm 0.03$ [DSZ21]. Using this value for w in the integral yields nearly the same result as ΛCDM, and only increases the integral (in the correct direction) by about 2×10^{-4}. However, the failure of wCDM to *completely* fix the integral to unity is mostly due to the fact that this fix would only really affect the integration during Λ dominated epochs, $Z \leq 0.3$. Again referring to Figure 3.2, most of the contributions to the integral come from a redshift interval between 1 and 10—well before dark energy dominates. Therefore, making changes that really only effect $E(z)$ for $z < Z_{M \to \Lambda}$ won't contribute much to the interval. Setting the integral equal to one, we could numerically solve for w. Doing this yields a result of $w = -3.5$, nowhere close to D'Amico's result.

Another strategy might seek to modify the ratio of $\Omega_{\Lambda,0}/\Omega_{M,0}$. Noting that in Figure 3.2 the "No Lambda" Curve rises above unity we can expect that lowering the amount of dark energy relative to matter in the current epoch will raise the value I toward one. This does work, but to get the integral to unity $\Omega_{\Lambda,0}/\Omega_{M,0}$ would have to be lowered from the Planck experiment's value of 2.214 ± 0.008 [AAA$^+$20] to 0.74. A value that low would mean that we are in a matter dominated era, which is simply not consistent with observation under ΛCDM's framework.

Even if either of these adjustments to $E(z)$ were aligned well—or even close—

to observation, they would both suffer from the problem that they are fixes to the current epoch's value of I. What we truly want is an integral that is equal to one *and* invariant relative to the epoch for which it is integrated for. A simple fix or correction to any static value within $E(z)$ will fail in a universe with multiple types of mass-energy. But, from Figure 3.3 and some analytic solutions we can infer that single component universes satisfy the condition that the integral is a constant for all initiating epochs. So we can ask "for what constant equation of state parameter, w, in the context of a single component universe will the integral I be equal to one?" Noting from Figure 3.3 that matter alone gives a constant integral value of 1.05 and Λ alone gives a value of 0.58, we can expect w to be between $w_M = 0$ and $w_\Lambda = -1$. Testing single component universes between these values finds that an equation of state parameter of $w = -0.05$ will accomplish this goal to a part in 10^4. This would give a dilution parameter of $d = 2.85$. This would have to be a substance that is very much like matter. But, a matter filled universe was already inconsistent with observations of nearby supernovae—so much so that ΛCDM was developed to account for the discrepancy. But, at least matter is a substance we are familiar with, to some extent, and this test isn't producing an equation of state parameter for something truly exotic.

4.2 Changing the Gravitational Coupling Between Epochs

Referring to our original setup of a test mass at the center of a thin shell, one thing we may want to adjust is the gravitational coupling strength between them. For this, I propose to introduce a dimensionless function $\xi(t)$. Normally, the gravitational interaction is mediated by Newton's constant G_N. But for massive bodies separated by cosmic distances, this may not be fully correct. It has long been recognized

that the dark energy (and/or dark matter) may be an artifact of misunderstanding how gravity works at cosmic scales. The proposed replacement for the gravitational coupling between two masses at epochs z_1 and z_2 is:

$$G = \xi(z_1)\xi(z_2)G_N, \tag{4.1}$$

where G_N is our familiar Gravitational constant from Newton's theory.

It is also worth pointing out that Brans and Dicke note that models with variable gravity are fundamentally identical to models with variable gravitational mass [BD61]. The variable mass they are referring to is a more fundamental notion of mass, like say the proton mass. Not a mass change by other more mundane means such as accretion. This means that in the quantities $\xi(z_1)$ and $\xi(z_2)$ could be interpreted as scaling factors of the gravitational masses of the bodies at the different redshifts. In a more fundamental sense, this leads to a realization that the quantity we measure and use as G is simply chosen in such a way as to make gravitational mass and inertial mass equal to each other. From this point of view, the value of G is empirically determined: any experimenter would assign its value based on the inertial properties of mass. If the inertial properties vary cosmologically, in order to keep our integral equal to one, then local assignments of G would simply follow along. Then in a very real sense, having the gravitational coupling change within the integral to generate inertial forces could be a natural way to invoke Mach's Principle with our integral, as G has no fundamental connection to quantities like the electron charge, Planck's constant, the speed of light, etc.

I can appreciate that some may be hesitant splitting a constant by taking the square root of G. But it is worth pointing out that $\sqrt{G}$ is a common quantity, particularly in defining the "natural" Planck units. The Planck length l_p, mass m_p, and time t_p, all contain a factor of $\sqrt{G}$ in their formulation. Often the Planck mass is simply defined as $M_P^2 = 1/G$, by setting c and $\hbar$ both to one. Rewriting the expression as $\sqrt{G}M_P = 1$, it becomes more clear that G is more of a proportionality

constant chosen such that this product is equal to one (or $\hbar c$ if you don't set them to one).

Now back to the integral, if we plug our new expression for the gravitational coupling between epochs into our integral we get:

$$I' = 2\int_0^\infty \mathrm{d}\zeta \xi(0)\xi(\zeta)\mu(\zeta) = 1. \tag{4.2}$$

The prime on the I' is simply to note that this is not our original integral, I, instead it is one constructed so that *by definition* it is equal to one. The function $\xi(t)$ is a scalar value varying with epoch. Since we want our integral to be equal to one for any epoch, Z, we can write this integral more generally as:

$$I' = 2\xi(Z)\int_0^\infty \mathrm{d}\zeta_{\mathrm{rel}} \xi(\zeta_{\mathrm{rel}})\mu_Z(\zeta_{\mathrm{rel}}), \tag{4.3}$$

where ζ_{rel} is the redshift relative to Z and $\mu_Z(\zeta_{\mathrm{rel}})$ is in terms of $E_Z(\zeta_{\mathrm{rel}})$. For visual clarity, I will drop the rel subscript from the ζ variables for the remainder of this text.

The natural question now is, how can we determine this function? One helpful first step is to recall that for any single component universe the integral without this correction factor is constant across redshift (see Figure 3.3). Furthermore, for mixed universes we know that beyond some transition redshift the universe will remain dominated by a single species. For ΛCDM radiation dominates at high z. So beginning at some redshift of $Z_0 \gg Z_R$, with Z_R the redshift where radiation becomes subdominant, the $\xi(z)$ function becomes constant: $\xi(Z_0)$ =const.= $\xi(z > Z_0)$.

$$I'_R = 2\xi(Z_0)\int_0^\infty \xi(Z_0)\mathrm{d}\zeta\mu_Z(\zeta) = 1. \tag{4.4}$$

But this integral is simply equal to our original integral I—in the context of constant G—multiplied by two factors of $\xi(Z_0)$. Labeling the original integral for a radiation dominated epoch as I_R, no prime, we get:

$$I'_R = [\xi(Z_0)]^2 2 \int_0^\infty \mathrm{d}\zeta \mu_Z(\zeta) = [\xi(Z_0)]^2 I_R = 1. \tag{4.5}$$

Again by construction this is equal to one, so for some redshift $Z_0 \gg Z_R$ we get:

$$\xi(Z_0 \gg Z_R) = \frac{1}{\sqrt{I_R}}. \tag{4.6}$$

With this information we can pin the high z behavior of ξ. Now let's make a small step forward in time δt to some later epoch $Z_1 = Z_0 - \delta Z$. The integral will be identical to Equation 4.3, but we will have some knowledge about $\xi(\zeta)$ for $\zeta > Z_0$. Given this, we can break up the integral into two parts:

$$I'_{Z_1} = \xi(Z_1)\left[2\int_0^{\delta Z} \mathrm{d}\zeta \xi(\zeta)\mu_Z(\zeta) + 2\int_{\delta Z}^\infty \mathrm{d}\zeta \xi(\zeta)\mu_Z(\zeta)\right]. \tag{4.7}$$

In the above equation we completely know everything in the second term, so we can simply perform that integral. I will introduce the quantity γ to hold it and simplify the notation:

$$\gamma = 2\int_{\delta Z}^\infty \mathrm{d}\zeta \xi(\zeta)\mu_Z(\zeta). \tag{4.8}$$

For this initial step $\xi(\zeta)$ in the γ expression simply equals $I_R^{-1/2}$, but for subsequent steps in determining the full ξ function this will not be the case. But more importantly, we will have determined the ξ function for all epochs covered by γ.

For the left term in Equation 4.7 if we choose δZ small enough such that $\xi(\zeta)$ doesn't change much on that interval we can set it equal to a constant $\xi(Z_1)$. This makes the left term equal to:

$$2\int_0^{\delta Z} \mathrm{d}\zeta \xi(Z_1)\mu_Z(\zeta) = 2\xi(Z_1)\int_0^{\delta Z} \mathrm{d}\zeta \mu_Z(\zeta) = \frac{\xi(Z_1)}{\beta}, \tag{4.9}$$

where I introduce the symbol β^{-1} to be equal to the integral in the above equation. Again, β is a completely known function and we can calculate it. Given this, our integral looks like this:

$$I'_{Z_1} = \xi(Z_1)[\xi(Z_1)\beta^{-1} + \gamma] = 1. \tag{4.10}$$

Again, β and γ are completely determined from the previous step of evaluating the integral from Z_0.

The above expression is simply a quadratic equation:

$$[\xi(Z_1)]^2 + \xi(Z_l)\beta\gamma - \beta = 0. \tag{4.11}$$

Taking the positive root, its solution is:

$$\xi(Z_1) = \frac{\beta\gamma}{2}\left[\sqrt{1 + \frac{4}{\beta\gamma^2}} - 1\right]. \tag{4.12}$$

We now have a way to make incremental steps in time from some radiation dominated epoch $Z_0 \gg Z_R$ to the present epoch. Given the density parameters at some epoch and their respective equation of state parameters[1], this process can be done to uniquely $\xi(z)$ for a given FLRW-like model of the universe. Performing this iterative building up of the $\xi(t)$ function for ΛCDM yields the curve found in Figure 4.1. In and of itself, this curve is very interesting. First, it is of order unity and only varies absolutely by about 25% across the age of the universe, increasing from 0.8 to 1.07. There are three flat regions—perhaps not surprising—when each species of mass-energy is fully dominant. The transitions between the flat regions happen around the epochs of transition. The function is monotonically increasing with time, decreasing in redshift. This implies that gravitational coupling was weaker in the past.

We can test if this function performs its required task of making the integral I' equal to one for any epoch. Figure 4.2 gives those results. In that figure we can see the function is very nearly unity for all epochs and only deviates from unity by a

[1]They don't necessarily need to be constant in time either, so long as you know how they evolve in time.

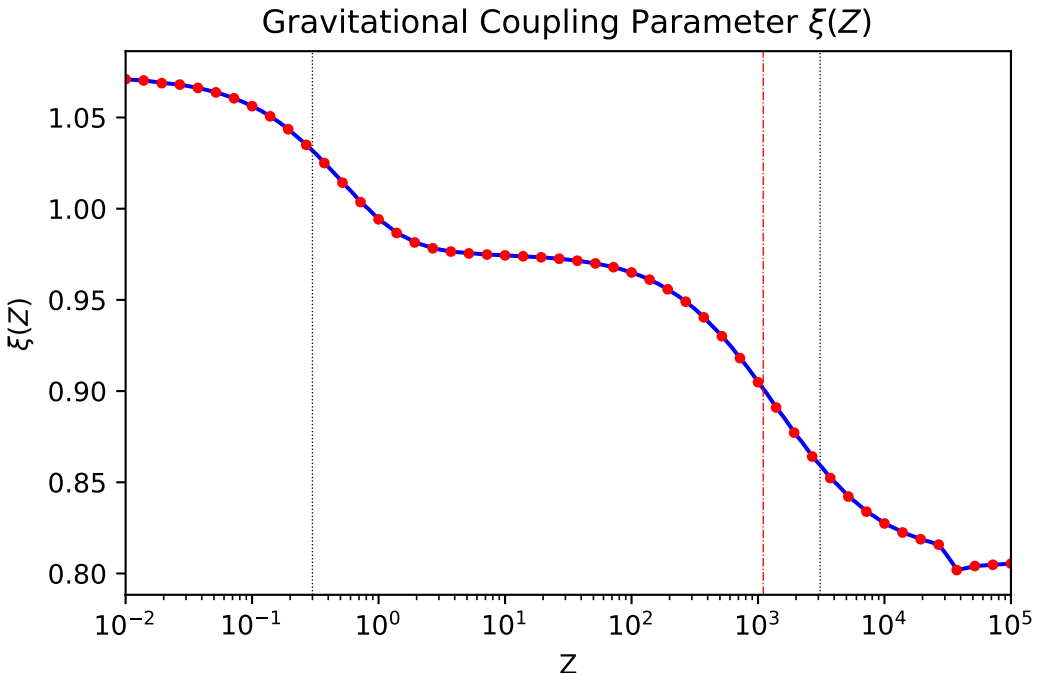

Figure 4.1: Numerically determined $\xi(z)$. The red points are the directly calculated values for $\xi(z)$, while the blue lines are interpolated values used for numerical integration of I'_Z in Figure 4.2. The vertical black dotted lines represent the transition epochs from matter to dark energy (left line) and radiation to matter (right line). The red vertical line is the redshift of the CMB, $z_{ls} = 1100$. The discontinuous bump at about $Z \sim 3500$ is suspected of being a numerical artifact and not representative of the model.

few tenths of a percent. This is better by up to two orders of magnitude from the uncorrected I integrals. The largest swings in the plot come from epochs where ξ is changing most rapidly.

In both Figures 4.2 and 4.1, we can also see a small bump in the curve at a redshift of $z \sim 3500$. This is likely not a real feature of the model, but rather a numerical artifact from the integration. It appears in roughly the same spot as the bump we saw in Figure 3.3 when looking at how I_Z (no prime) behaves in a radiation-only universe. You may recall in that case, I_Z was evaluated analytically to be a constant,

so its bump can only be explained by a numerical artifact. We believe this bump is similar in nature as it occurs at about the same epoch[2].

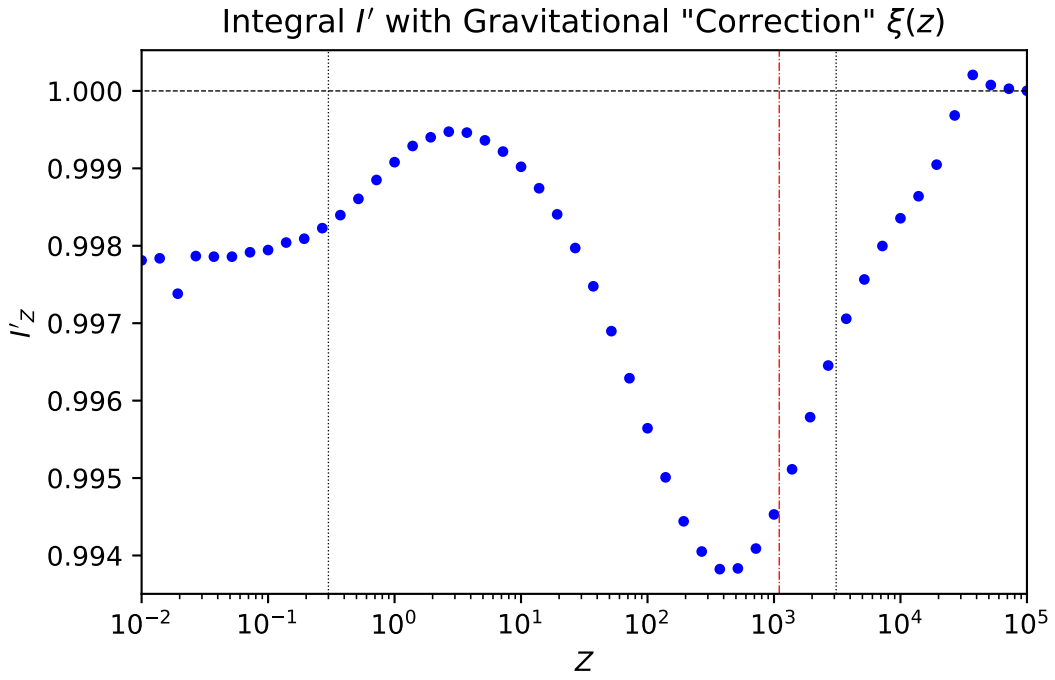

Figure 4.2: I'_Z with the gravitational coupling parameter $\xi(z)$ determined by numerical integration. I' by construction should be equal to one, indicated by the horizontal dashed line. The vertical black dotted lines represent the transition epochs from matter to dark energy (left line) and radiation to matter (right line). The red vertical line is the redshift of the CMB, $z_{ls} = 1100$. The discontinuous bump at about $Z \sim 3500$ is suspected of being a numerical artifact and not representative of the model.

While it may seem distasteful to vary the strength of gravity in this multistep way, recall the guiding idea: if mass-energy distribution of the universe determines inertial frames and inertial mass, and G is the emergent constant of proportionality, then transitions in the universe may be expected to imprint on G. Moreover, this

[2]All the calculations done use similar methods in Python. Other investigations have been performed to identify the cause of these bumps. While these efforts have obviously not solved the problem, they also don't reveal this to be a true property of the model.

dissertation is one of exploration, rather than asserting a new cosmology, completely rendered. Rather, I hope to introduce a tool by which other questions can be asked of any cosmological theory. If a scientist wants to test Mach's Principle, then they may be able to use the above technique to tease out new insights into a given cosmology, or perhaps provide an opportunity to question assumptions about any given cosmology. The assumption we brought into question was the concept of an unchanging gravitational coupling for all time, $G(t) = G_N$.

4.3 Comparison With Supernova Data

A natural next step after proposing this model with variable coupling parameter $\xi(z)$ is to compare this with observational data. While there are a number of ways astronomers probe cosmology, the classic comparison of cosmology in the nearby universe has been the use of type Ia supernovae. Type Ia supernovae are a type of standard candle in cosmology, a source with known intrinsic luminosity, L. Recall from Section 1.4.3, that by measuring the bolometric flux, S, of a standard candle it can be used to directly probe H by two luminosity distance relations:

$$D_L = \sqrt{\frac{L}{4\pi S}}, \tag{4.13}$$

and

$$D_L = (1+z)^2 D_A = (1+z) D_C = D_H (1+z) \int_0^z \frac{\mathrm{d}\zeta}{E(\zeta)}. \tag{4.14}$$

We can consider how an increasing gravitational parameter might influence these observations. I'll use subscripts v and c to distinguish between quantities with a variable G from those with it as a constant. If G was weaker in the past then $G_v(z) < G_c$. But the Hubble parameter is proportional to the square root of G, and thus proportional to the gravitational parameter ξ. So $H_v(z) < H_c(z)$. The same proportionality holds for the $E(z)$ function as well, $E_v(z) < E_c(z)$. But,

the comoving distance element δD_C is inversely proportional to $E(z)$. Therefore, $\delta D_{C,v}(z) > \delta D_{C,c}(z)$, which leads to $D_{C,v}(z) > D_{C,c}(z)$. And since the luminosity distance is simply the comoving distance multiplied by a factor of $(1 + z)$, finally:

$$D_{L,v}(z) > D_{L,c}(z). \tag{4.15}$$

To quantitatively modify this expression we will take out the gravitational parameter $\xi(z)$ (which remember is proportional to $\sqrt{G(z)}$) and multiply it by the density $\rho(z)$. Since $E(z)$ can be written as $\sqrt{\sum_x \rho_x(z)/\rho_c}$, multiplying the density by $\xi(z)$ has the effect of modifying E by a simple overall multiplication. Our *new* E function is simply:

$$E'(z) = \xi(z)E(z), \tag{4.16}$$

where I use the prime to denote that this is a modified E function that provides a modified I' integral. Thus, our modified luminosity distance will be:

$$D'_L = D_H(1 + z) \int_0^z \frac{\mathrm{d}\zeta}{\xi(\zeta)E(\zeta)}. \tag{4.17}$$

Figure 4.3 plots the distance modulus of type Ia supernova data up to 2006 as reported by Riess et al. in 2007, [RSC+07]. A fitted model of ΛCDM (green dotted line), and ΛCDM with a variable gravity (blue dashed line) are also plotted. The luminosity distance used for the variable gravity is that given by Equation 4.17, with the $\xi(z)$ function provided by the results plotted in Figure 4.1. The value of $\xi(0)$ is 1.07, and decreases overall by $\Delta\xi = 0.09$ for the redshift interval the supernovae span. Figure 4.4 plots the residuals of the supernova data with ΛCDM. The variable G model is also plotted with a blue dashed line.

The difference between ΛCDM and the variable G model is small. So small in fact that one might have trouble distinguishing between them in Figure 4.3. Referring to the more clear Figure 4.4 we can see that the variable G model is clearly above—if only by a small amount—ΛCDM. This confirms that D_L with an increasing gravi-

tational parameter would be greater than with constant gravity. The smallness of the change is rather remarkable, considering that ξ varies by about 8%. To compare some statistical measures between the two models, for ΛCDM $\chi^2_{\Lambda\text{CDM}}$=0.976, while the variable G model has $\chi^2_{\text{var}G} = 0.980$. With a difference between χ^2 values only in the thousandths place, this makes them statistically nearly identical. $1 - \text{CDF}(\chi^2)$ is 0.63 and 0.65 for the variable G and ΛCDM models, respectively. It is worth noting that H_0 is a fitted parameter to the data. The value of H_0 given by the variable G model was about 6% smaller than the ΛCDM fit. This is largely accounted for by the fact that $\xi(0)$ is 1.07 and not one.

Having a new tool in the integral I' gives us some room to play around with some parameters. One parameter to vary is the ratio $r = \Omega_\Lambda/\Omega_M$. The value of r for ΛCDM is 2.215. Recall from Section 4.1 the value of r to get the original integral I to be equal to one for the current epoch was 0.74. For this reason, various values of r between 2.215 and 0.74 were modeled. For each value, the supernova data were compared with the output from a constant gravity ΛCDM_r model with the given ratio, setting Ω_Λ and Ω_M while keeping Ω_R fixed. The supernova were also compared with a variable G model with the same value r, $\Lambda\text{CDM}_{\xi r}$. For $\Lambda\text{CDM}_{\xi r}$, $\xi(z)$ was determined in the same manner outlined as in Section 4.2. Table 4.1 shows the results from these tests. For all r values χ^2 was smaller when including a variable G compared to ΛCDM_r. More remarkable was that for a wide range of $r = 1$, $1 - \text{CDF}(\chi^2)$ was within a statistically acceptable range as to not rule out $\Lambda\text{CDM}_{\xi r}$ in and of itself. Additionally, as r decreased $\xi(0)$ became closer to one, and $\Delta\xi$ decreased. Indicating a more self-consistent initial value along with a smaller overall change in G, both nice things to have in a model. One thing that doesn't work out so well is eliminating dark energy. Setting r to zero gives a ξ^2 value of 2.02.

What the results of this section show us is that adding a variable G to cosmology can do some of the work dark energy was intended to cover, such as aligning with supernova magnitudes. A variable G also doesn't break from supernova observations—

Table 4.1: Table of results from modeling ΛCDM$_r$ and ΛCDM$_{\xi r}$ and comparing this with the supernova data set used in Figure 4.3. r is the ratio of the Λ and matter density parameters, $\Omega_{\Lambda,0}/\Omega_{M,0}$. $\xi(0)$ is the value of the gravitational parameter ξ in the current epoch. $\Delta\xi$ is the quantity $\xi(0) - \xi(z_{\max})$, where $z_{\max}$ is the highest value of redshift in the supernova data set. This quantity simply makes a measure of how much ξ changes over the span of the data set. Also reported are the χ^2 values with a variable gravity "w/ξ" and without "no ξ." The next column reports one minus the cumulative distribution function of χ^2 for the variable gravity model (the same quantity for constant gravity was examined but these values fell off quickly over the span of r explored and so were not reported).

r	$\xi(0)$	$\Delta\xi$	χ^2 w/ξ	χ^2 no ξ	$1 - \mathrm{CDF}(\chi^2)$ w/ξ
2.215	1.07	0.09	0.98	0.98	0.63
1.75	1.06	0.07	0.97	1.00	0.68
1.25	1.04	0.06	1.01	1.07	0.43
0.74	1.02	0.04	1.16	1.24	0.01
0	0.98	4×10^{-5}	2.02	2.02	0

anchors to our late time experimental probes of cosmology. In fact, variable G can do better than ΛCDM alone. For instance, the smallest χ^2 value in Table 4.1 is for a variable gravity with $r = 1.75$. One intriguing question we had at the beginning of this process was, could a variable gravity replace dark energy? Within the context of this work, I would say the answer is a solid no. Dark energy—what ever it may be—seems to still be required to account for supernova being dimmer than expected.

In this section, I can see how one might walk away with the impression that cosmologists have never considered the concept of a variable gravity. This is certainly not the case. Variable gravity in the context of cosmology is not a new concept. One theory that was attractive in the 1960s was Jordan-Brans-Dicke Theory (JBD) (Brans 2014 [Bra14]). In 1961 Brans and Dicke proposed—based on work by Jordan and his group—an alternative scalar–tensor theory to Einstein's General Relativity [BD61]). JBD contained a variable gravitational parameter based on the matter

distribution of the universe, and in 1968 Greenstein developed this theory into a cosmological model [Gre68a], [Gre68b]. MTW reference JBD cosmology and admit "[they] are qualitatively the same and quantitatively almost the same as the standard hot big-bang model. However, no motivation or justification is evident for abandoning general relativity" [MTW73]. In the past decade, the uncovering of the Hubble Tension under the ΛCDM model has given rise to a renewed interest in JBD to account for these tensions. As an example, Peracaula et al. find that JBD—a variable-strength gravity model, recall—combined with a cosmological constant can ease ΛCDM tensions [PGVdCPMP19]. Apart from JBD, other cosmologies with variable mass/gravity have been proposed. In fact, the gold medal winners of the H_0 Olympics mentioned in Section 1.4.2 are a pair of proposals by Sekiguichi and Takahashi that both include a time varying effective electron mass, m_e [ST21].

The point I am trying to make in this section is simply that a gravitational parameter that is increasing in time is consistent—at least qualitatively—with observations of an accelerating universe. I only do this because in the previous section I demonstrate a way to use Mach's Principle to tease out a possible function for $G(t)$ and it appears to be weaker in the past. I also don't want to make the claim that this is *THE* way to find $G(t)$, rather I think my method could provide useful insights into a more complete and self-consistent approach to developing or refining any theory of cosmology. I think exploring what the integral I evaluates to for some of the different models mentioned in this work could be very interesting. How close are the integrals to unity? If they aren't equal to unity, what parameters can be changed to bring it closer to unity? How might those changes affect comparisons with observations? Do the models that have made the podium in the H_0 Olympics evaluate I to be closer to unity? Maybe the integral I could be a new event!

4.4 Conclusion

In Chapter 2 I introduce a way to determine the acceleration of a test particle at the center of a thin shell of mass under the gravitational influence of the shell in three different kinds of motion. I do this only using the Einstein-Infeld-Hoffman Equations. I also show how the resulting accelerations are qualitatively—if not numerically—similar to the accelerations one would expect from an observationally equivalent non-inertial frame. Using the results from Chapter 2, in Chapter 3 I extend the shell integration to a volume filling the universe taking careful account of the density and distances involved from cosmology. I showed these result in accelerations that are near unity relative to inertial accelerations. It appears that no such integration has been performed yet in the literature. Finally, in Chapter 4, I invoke Mach's Principle by requiring the integral to equal unity. I explore different approaches to make this happen. In particular, I demonstrate a way to determine the gravitational coupling between two bodies at different cosmological redshifts. I then use this model of ΛCDM with a variable gravitational constant and compare this with supernova distance modulus data. I find that this modified model matches observations at least as well as ΛCDM and in some cases possibly outperforms it. My hope is that the methods outlined in this dissertation can be used to evaluate cosmological models and help to reveal new insights into improving them.

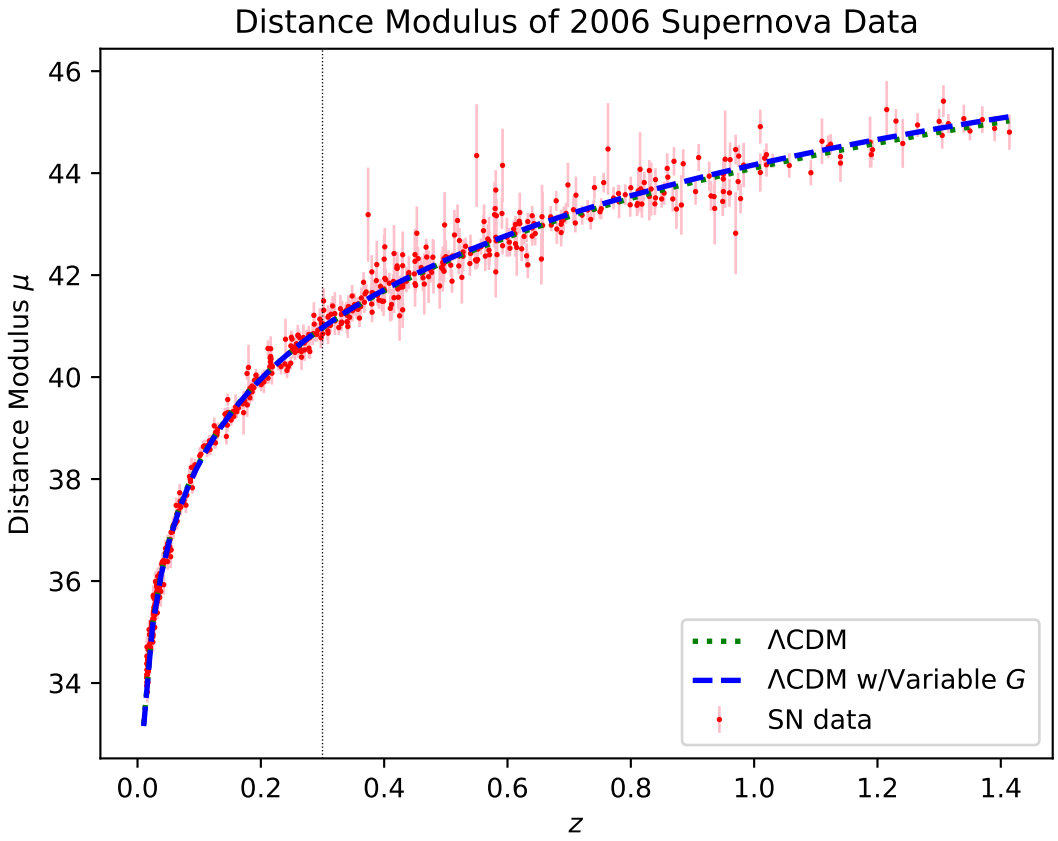

Figure 4.3: Supernova data prior to 2006 in comparison with ΛCDM model and a modified ΛCDM with variable G. The vertical axis represents the distance modulus μ. The red dots along with their error bars are the distance modulus of the supernova as reported by Riess et al. in 2007, [RSC+07]. The green dotted line is a model fit of ΛCDM with $(\Omega_\Lambda, \Omega_M, \Omega_R) = (0.6889, 0.3111, 0.0001)$. The blue dashed line represents a modified ΛCDM model using D'_L (Eq. 4.17) rather than D_L (Eq. 1.35) to fit $H(z)$. The $\xi(z)$ function used is that as provided in Figure 4.1. Note that the green dotted line is just barely visible under the below the dashed blue line. The thin vertical dotted line represents the transition from matter dominated epochs to Λ dominated epochs.

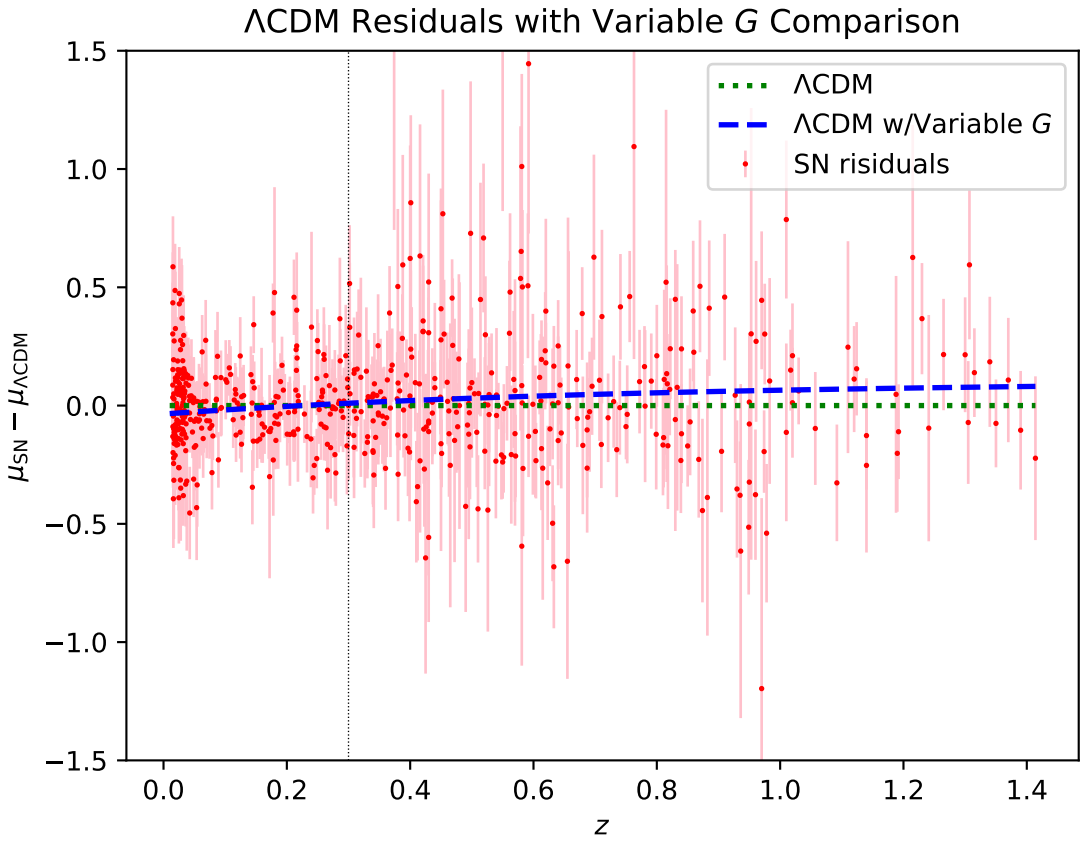

Figure 4.4: Residuals of supernova data prior to 2006 in comparison with ΛCDM model. A modified ΛCDM with variable G is also plotted as compared with vanilla ΛCDM. The red dots along with their error bars are the residuals of the distance modulus of the supernova as reported by Riess et al. in 2007, [RSC+07]. The green dotted line is a model fit of ΛCDM with $(\Omega_\Lambda, \Omega_M, \Omega_R) = (0.6889, 0.3111, 0.0001)$. The blue dashed line represents a modified ΛCDM model using D'_L (Eq. 4.17) rather than D_L (Eq. 1.35) to fit $H(z)$. The $\xi(z)$ function used is that as provided in Figure 4.1. The thin vertical dotted line represents the transition from matter dominated epochs to Λ dominated epochs. Note two data points around $z = 0.4$ and $z = 0.6$ are above the boundaries of the plotted region.

Appendix A

Useful Math and Worked out Integrals

A.1 Isotropic $\hat{\boldsymbol{r}}$ integral

This is an integral of the form:

$$\boldsymbol{I} = \int_{\Omega} \mathrm{d}\Omega f(r)\hat{\boldsymbol{r}} \tag{A.1}$$

Since $f(r)$ is only a function of the radial coordinate it can be pulled from the integral. Additionally, we can expand the following two parts of the integral:

$$\int_{\Omega} \mathrm{d}\Omega = \int_0^{\pi} \mathrm{d}\theta \int_0^{2\pi} \mathrm{d}\phi \sin\theta, \tag{A.2}$$

$$\hat{\boldsymbol{r}} = \sin\theta\cos\phi\hat{\boldsymbol{x}} + \sin\theta\sin\phi\hat{\boldsymbol{y}} + \cos\theta\hat{\boldsymbol{z}}, \tag{A.3}$$

Using those substitutions we can rewrite the integral as:

$$\boldsymbol{I} = f(r)\int_0^{\pi} \mathrm{d}\theta \int_0^{2\pi} d\phi[\sin^2\theta\cos\phi\hat{\boldsymbol{x}} + \sin^2\theta\sin\phi\hat{\boldsymbol{y}} + \sin\theta\cos\theta\hat{\boldsymbol{z}}]. \tag{A.4}$$

The first and second terms evaluate to zero, $\int_0^{2\pi} \mathrm{d}\phi \cos\phi = \int_0^{2\pi} \mathrm{d}\phi \sin\phi = 0$. This leaves the integral as:

$$\boldsymbol{I} = f(r) \int_0^{2\pi} \mathrm{d}\phi \int_0^{\pi} \mathrm{d}\theta \sin\theta \cos\theta \hat{\boldsymbol{z}}. \tag{A.5}$$

The integral over ϕ is simply 2π. A simple u substitution of $u = \sin\theta$ and $\mathrm{d}u = \cos\theta \mathrm{d}\theta$ yields:

$$\boldsymbol{I} = 2\pi f(r) \int_{\sin 0}^{\sin \pi} u \mathrm{d}u. \tag{A.6}$$

This of course is equal to zero. Therefore, we find the original integral to be equal to zero.

$$\boxed{\boldsymbol{I} = \int_\Omega \mathrm{d}\Omega f(r) \hat{\boldsymbol{r}} = \boldsymbol{0}} \tag{A.7}$$

This should be relatively intuitive in that for every direction there will be an equal magnitude vector in the integral in the opposite direction.

A.2 Powers of Sine

This involves integrals of the form:

$$\boldsymbol{I} = \int_\Omega \mathrm{d}\Omega \sin^n\theta \hat{\boldsymbol{r}}. \tag{A.8}$$

Substituting $\hat{\boldsymbol{r}} = \sin\theta\hat{\boldsymbol{x}} + \sin\theta\sin\phi\hat{\boldsymbol{y}} + \cos\theta\hat{\boldsymbol{z}}$ we get:

$$\boldsymbol{I} = \int_0^{2\pi} \mathrm{d}\phi \int_0^{\pi} \mathrm{d}\theta \sin\theta \sin^n\theta (\sin\theta\cos\phi\hat{\boldsymbol{x}} + \sin\theta\sin\phi\hat{\boldsymbol{y}} + \cos\theta\hat{\boldsymbol{z}}). \tag{A.9}$$

For the first and second terms, $\int_0^{2\pi} \mathrm{d}\phi \cos\phi = \int_0^{2\pi} \mathrm{d}\phi \sin\phi = 0$. Leaving:

$$\boldsymbol{I} = \int_0^{2\pi} \mathrm{d}\phi \int_0^{\pi} \mathrm{d}\theta \sin^{n+1}\theta \cos\theta \hat{\boldsymbol{z}}. \tag{A.10}$$

The integral over ϕ is simply 2π. And, a simple u substitution of $u = \sin\theta$ and $du = \cos\theta d\theta$ yields:

$$\boldsymbol{I} = 2\pi\hat{\boldsymbol{z}} \int_{\sin 0}^{\sin \pi} u^{n+1} \mathrm{d}u = \mathbf{0}. \tag{A.11}$$

And of course the upper and lower limits are equal to each other so the whole integral is equal to zero:

$$\boxed{\boldsymbol{I} = \int_\Omega \mathrm{d}\Omega \sin^n\theta \hat{\boldsymbol{r}} = \mathbf{0}}. \tag{A.12}$$

A.3 Definite Scalar Integrals of $\int d\theta \sin^3\theta$

Integral #297 from [Sel75] is:

$$I = \int (\sin^3 ax)\mathrm{d}x = -\frac{1}{3a}(\cos ax)(\sin^2 ax + 2). \tag{A.13}$$

For $a = 1$ and the limits of integration as $\theta = [n\pi, m\pi]$ with both n and m as integers:

$$I = -\frac{1}{3}[\cos\theta(\sin^2\theta + 2)|_{n\pi}^{m\pi}. \tag{A.14}$$

For the first term $\sin(m\pi) = \sin(n\pi) = 0$. Which leaves:

$$I = \frac{2}{3}[\cos(n\pi) - \cos(m\pi)]. \tag{A.15}$$

For limits of integration $[0, \pi]$ this yields:

$$I = \frac{2}{3}[1 - (-1)] = \frac{4}{3}. \tag{A.16}$$

For limits of integration $[0, 2\pi]$ this yields:

$$I = \frac{2}{3}[1 - 1] = 0. \tag{A.17}$$

A.4 Cosine Product with Phase

These are integrals of the form:

$$I = \int_0^{2\pi} \mathrm{d}\theta \cos(\theta + \delta) \cos\theta. \tag{A.18}$$

Using the product to sum rules for cosine, we can rewrite the first cosine and get:

$$I = \int_0^{2\pi} \mathrm{d}\theta [2\cos\theta\cos\delta - \cos(\theta - \delta)] \cos\theta \tag{A.19}$$

$$= 2\cos\delta \int_0^{2\pi} \mathrm{d}\theta \cos^2\theta - \int_0^{2\pi} \mathrm{d}\theta \cos(\theta - \delta)\cos\theta. \tag{A.20}$$

Above, the first integral on the left evaluates to $\pi/2$. For the second integral we can use a u substitution: $u = \theta - \delta$, $\mathrm{d}\theta = \mathrm{d}u$ and the limits become $0 \to -\delta$ and $2\pi \to 2\pi - \delta$.

$$I = \pi\cos\delta - \int_{-\delta}^{2\pi-\delta} \mathrm{d}u \cos(u + \delta)\cos u. \tag{A.21}$$

Now the second term on the RHS looks nearly identical to the original integral, save for the limits. But since the integrand is still periodic on the interval of 2π and the difference between the limits is still 2π, then the integral should still be equal to I. We then get:

$$I = \pi\cos\delta - I, \tag{A.22}$$

$$2I = \pi\cos\delta. \tag{A.23}$$

This makes the overall integral equal to:

$$\boxed{I = \int_0^{2\pi} \mathrm{d}\theta \cos(\theta + \delta) \cos\theta = \frac{\pi}{2} \cos\delta}. \tag{A.24}$$

When $\delta = \pi/2$ then this clearly is equal to zero. But in the original integral this would mean that the phase shifted cosine product would be $\cos(\theta + \pi/2)$, but this is of course equal to $\sin\theta$. We can then infer that the following integral is equal to zero:

$$\int_0^{2\pi} \mathrm{d}\theta \sin\theta \cos\theta = \frac{\pi}{2} \cos\left(\frac{\pi}{2}\right) = 0. \tag{A.25}$$

Thus:

$$I = \int_0^{2\pi} \mathrm{d}\theta \cos(\theta + \delta) \cos\theta = 0, \quad \text{with} \quad \delta = \frac{\pi}{2}. \tag{A.26}$$

A.5 Integral of cylindrical unit vector $\hat{\boldsymbol{\rho}}$ over a shell

These are integrals of the form:

$$I = \int_\Omega \mathrm{d}\Omega f(r, \theta) \hat{\boldsymbol{\varrho}}. \tag{A.27}$$

With $\hat{\boldsymbol{\rho}}$ being the radial unit vector in cylindrical coordinates. Expanding the surface element we get the double integral:

$$I = \int_0^{\pi} \sin\theta \mathrm{d}\theta f(r, \theta) \int_0^{2\pi} \mathrm{d}\phi \hat{\boldsymbol{\varrho}}. \tag{A.28}$$

We then convert the $\hat{\boldsymbol{\varrho}}$ into rectilinear coordinates with $\hat{\boldsymbol{\varrho}} = \cos\phi\hat{\boldsymbol{x}} + \sin\phi\hat{\boldsymbol{y}}$ to get:

$$I = \int_0^{\pi} \sin\theta \mathrm{d}\theta f(r,\theta) \int_0^{2\pi} \mathrm{d}\phi(\cos\phi\hat{\boldsymbol{x}} + \sin\phi\hat{\boldsymbol{y}}). \tag{A.29}$$

But the integral of cosine and sine over a full period is zero. So both terms in the second integral are zero. Thus:

$$I = \int_{\Omega} \mathrm{d}\Omega f(r,\theta)\hat{\boldsymbol{\varrho}} = 0. \tag{A.30}$$

A.6 Integral of $\sin\theta\cos\theta$

For integrals of the form:

$$I = \int_a^b \mathrm{d}\theta \sin\theta\cos\theta. \tag{A.31}$$

Using the following u substitution $u = \sin\theta$ and $du = \cos\theta d\theta$ we get:

$$I = \int_{\sin a}^{\sin b} u\mathrm{d}u. \tag{A.32}$$

This of course is simply equal to:

$$I = \left[\frac{u^2}{2}\right|_{\sin a}^{\sin b}. \tag{A.33}$$

Which is:

$$\boxed{I = \int_a^b \mathrm{d}\theta \sin\theta\cos\theta = \frac{1}{2}[\sin^2 a - \sin^2 b]}. \tag{A.34}$$

Since the integrals we deal with are either on the interval $\theta = [0,\pi]$ or $\theta = [0,2\pi]$, this makes the integrals simply equal to zero.

Appendix B

Detailed Integrations of Specific Terms

Many of the terms in the EIH integral require some detailed calculations that would distract from the flow of the thesis. For this reason, I have included some of the more complicated integrals in this appendix.

B.1 Linear Acceleration Case:1 $\mathcal{J}$ term

The $\boldsymbol{\mathcal{J}}_1$ term in the linear acceleration Case:1 is:

$$\boldsymbol{\mathcal{J}}_1 = \frac{1}{2}\frac{G}{c^2}R^2\sigma\int_\Omega \mathrm{d}\Omega\frac{\hat{\boldsymbol{r}}(\hat{\boldsymbol{r}}\cdot\boldsymbol{a})}{R}. \tag{B.1}$$

If we use the common substitution for $\hat{\boldsymbol{r}}$ as:

$$\hat{\boldsymbol{r}} = \sin\theta\cos\phi\hat{\boldsymbol{x}} + \sin\theta\sin\phi\hat{\boldsymbol{y}} + \cos\theta\hat{\boldsymbol{z}}. \tag{B.2}$$

The inner-product within the integral of $\boldsymbol{\mathcal{J}}_1$ simply becomes $\hat{\boldsymbol{r}}\cdot(a\hat{\boldsymbol{x}}) = a\sin\theta\cos\phi$. Plugging this into $\boldsymbol{\mathcal{J}}_1$ as well as the expansion of $\hat{\boldsymbol{r}}$ we get:

$$\boldsymbol{\mathcal{J}}_1 = \frac{1}{2}\frac{G}{c^2}R\sigma \int_0^{2\pi} \mathrm{d}\phi \int_0^{\pi} \sin\theta \mathrm{d}\theta (a\sin\theta\cos\phi)(\sin\theta\cos\phi\hat{\boldsymbol{x}} + \sin\theta\sin\phi\hat{\boldsymbol{y}} + \cos\theta\hat{\boldsymbol{z}}). \tag{B.3}$$

For each term the integrals over ϕ are as follows:

$$1^{\text{st}}\text{Term} \rightarrow \int_0^{2\pi} \mathrm{d}\phi \cos^2\phi\hat{\boldsymbol{x}} = \pi\hat{\boldsymbol{x}}, \tag{B.4}$$

$$2^{\text{nd}}\text{Term} \rightarrow \int_0^{2\pi} \mathrm{d}\phi \cos\phi\cos\sin\hat{\boldsymbol{y}} = \boldsymbol{0}, \tag{B.5}$$

$$3^{\text{rd}}\text{Term} \rightarrow \int_0^{2\pi} \mathrm{d}\phi \sin\phi\hat{\boldsymbol{z}} = \boldsymbol{0}. \tag{B.6}$$

From Appendix A.3, the integral over θ in the first term is simply:

$$\int_0^{\pi} \sin^3\theta \mathrm{d}\theta = \frac{4}{3}. \tag{B.7}$$

All told, the solution for this term is:

$$\boxed{\boldsymbol{\mathcal{J}}_1 = \frac{2}{3}\frac{G}{c^2}R\sigma\pi a\hat{\boldsymbol{x}}}. \tag{B.8}$$

B.2 Coriolis Case:2 $\boldsymbol{\mathcal{C}}$ Term

For the $\boldsymbol{\mathcal{C}}_2$ term we require $\boldsymbol{v}_A \cdot \boldsymbol{v}$. This is given as:

$$\boldsymbol{v}_A \cdot \boldsymbol{v} = -v_A R\omega \sin\theta(\hat{\boldsymbol{x}} \cdot \hat{\boldsymbol{\phi}}) \tag{B.9}$$

$$= -v_A R\omega \sin\theta[\hat{\boldsymbol{x}} \cdot (-\sin\phi\hat{\boldsymbol{x}} + \cos\phi\hat{\boldsymbol{y}})] \tag{B.10}$$

$$= -v_A R\omega \sin\theta\sin\phi. \tag{B.11}$$

Inputting this into the $\boldsymbol{\mathcal{C}}_2$ term we get:

$$\boldsymbol{\mathcal{C}}_2 = -4\frac{G}{c^2}\int_\epsilon^\infty d^3\bar{x}\frac{\rho(\bar{\mathbf{x}})[\mathbf{v}_A\cdot\mathbf{v}(\bar{\mathbf{x}})]}{\bar{r}^2}\hat{\mathbf{r}} \tag{B.12}$$

$$= 4\frac{G}{c^2}\int_\Omega \mathrm{d}\Omega\frac{\sigma v_A R\omega\sin\theta\sin\phi}{R^2}\hat{\boldsymbol{r}} \tag{B.13}$$

$$= 4\frac{G}{c^2}\frac{\sigma v_A\omega}{R}\int_\Omega \mathrm{d}\Omega\sin\theta\sin\phi\hat{\boldsymbol{r}} \tag{B.14}$$

$$= 4\frac{Gv_A\omega}{c^2R}\int_0^{2\pi}\mathrm{d}\phi\int_0^\pi \mathrm{d}\theta\sin\theta R^2\sin\theta\sin\phi(\sin\theta\cos\phi\hat{\boldsymbol{x}}+\sin\theta\sin\phi\hat{\boldsymbol{y}}+\cos\theta\hat{\boldsymbol{z}}) \tag{B.15}$$

$$= 4\frac{Gv_A\omega R}{c^2}\int_0^{2\pi}\mathrm{d}\phi\int_0^\pi \mathrm{d}\theta\sin^2\theta\sin\phi(\sin\theta\cos\phi\hat{\boldsymbol{x}}+\sin\theta\sin\phi\hat{\boldsymbol{y}}+\cos\theta\hat{\boldsymbol{z}}). \tag{B.16}$$

The $\hat{\boldsymbol{z}}$ term reduces to zero due to the integration of $\sin\phi$ over a full revolution. Additionally, the $\hat{\boldsymbol{x}}$ term reduces to zero because of the integration over a full revolution in ϕ from the product $\sin\phi\cos\phi$. This leaves only the $\hat{\boldsymbol{y}}$ term remaining as:

$$\boldsymbol{\mathcal{C}}_2 = 4\frac{Gv_A\omega R}{c^2}\int_0^{2\pi}\mathrm{d}\phi\int_0^\pi \mathrm{d}\theta\sin^2\theta\sin^2\phi\hat{\boldsymbol{y}}. \tag{B.17}$$

Using integral number #296 from [Sel75] yields:

$$\int_0^{2\pi}\mathrm{d}\phi\sin^2\phi = \left[\frac{\phi}{2}-\frac{1}{4}\sin 2\phi\right|_0^{2\pi} = \pi. \tag{B.18}$$

And from section A.3 that the integral over θ will reduce to 4/3. So overall for the $\boldsymbol{\mathcal{C}}_2$ term we get:

$$\boxed{\boldsymbol{\mathcal{C}}_2 = \frac{16}{3}\frac{\pi Gv_A\omega R}{c^2}\hat{\boldsymbol{y}}}. \tag{B.19}$$

B.3 Coriolis Case:2 $\boldsymbol{\mathcal{G}}$ Term

Recalling the $\boldsymbol{\mathcal{G}}_2$ term as:

$$\boldsymbol{\mathcal{G}}_2 = -\frac{G}{c^2}\int_\epsilon^\infty d^3\bar{x}\frac{\rho(\bar{\boldsymbol{x}})}{\bar{r}^2}\hat{\boldsymbol{r}}\cdot(4\boldsymbol{v}_A - 3\boldsymbol{v}(\bar{\boldsymbol{x}}))[\boldsymbol{v}_A - \boldsymbol{v}(\bar{\boldsymbol{x}})] \tag{B.20}$$

For the $\boldsymbol{\mathcal{G}}_2$ term we need to determine $\hat{\boldsymbol{r}}\cdot(4\boldsymbol{v}_A - 3\boldsymbol{v})[\boldsymbol{v}_A - \boldsymbol{v}]$. Distributing the dot product over the first parenthesis we get $4\hat{\boldsymbol{r}}\cdot\boldsymbol{v}_A - 3\hat{\boldsymbol{r}}\cdot\boldsymbol{v}$. The second term reduces to zero as $\boldsymbol{v} = v\hat{\boldsymbol{\phi}}$ and $\hat{\boldsymbol{r}}\cdot\hat{\boldsymbol{\phi}} = \boldsymbol{0}$. While the first term becomes $4v_A\hat{\boldsymbol{r}}\cdot\hat{\boldsymbol{x}} = 4v_A\sin\theta\cos\phi$. Making the $\boldsymbol{\mathcal{G}}_2$ term become:

$$\boldsymbol{\mathcal{G}}_2 = -\frac{G}{c^2}\int_\Omega \mathrm{d}\Omega\frac{4v_A\sigma\sin\theta\cos\phi}{R^2}(v_A\hat{\boldsymbol{x}} - \omega R\sin\theta\hat{\boldsymbol{\phi}}). \tag{B.21}$$

Evaluating the left term in the above expression we get:

$$\boldsymbol{\mathcal{G}}_{2,\text{left}} = \frac{4v_A^2\sigma}{R^2}\int_0^{2\pi}\mathrm{d}\phi\int_0^\pi \mathrm{d}\theta\sin^2\theta R^2\cos\phi\hat{\boldsymbol{x}}. \tag{B.22}$$

This of course evaluates to zero due to the integration over ϕ. Therefore:

$$\boldsymbol{\mathcal{G}}_2 = \frac{4Gv_A\sigma\omega}{Rc^2}\int_\Omega \mathrm{d}\Omega\sin^2\theta\cos\phi\hat{\boldsymbol{\phi}} \tag{B.23}$$

$$= \frac{4Gv_A\sigma\omega}{Rc^2}\int_0^{2\pi}\mathrm{d}\phi\int_0^\pi \mathrm{d}\theta\sin\theta R^2\sin^2\theta\cos\phi(-\sin\phi\hat{\boldsymbol{x}} + \cos\phi\hat{\boldsymbol{y}}). \tag{B.24}$$

The integral over θ yields a factor of $\frac{4}{3}$ (for details see section A.3) leaving:

$$\boldsymbol{\mathcal{G}}_2 = \frac{16Gv_A\sigma\omega R}{3c^2}\int_0^{2\pi}\mathrm{d}\phi(-\sin\phi\cos\phi\hat{\boldsymbol{x}} + \cos^2\phi\hat{\boldsymbol{y}}). \tag{B.25}$$

Here the $\hat{\boldsymbol{x}}$ term evaluates to zero and the $\hat{\boldsymbol{y}}$ evaluates to π, so:

$$\boldsymbol{\mathcal{G}}_2 = \frac{16}{3}\frac{Gv_A\sigma\omega\pi R}{c^2}\hat{\boldsymbol{y}}. \tag{B.26}$$

It is worth noting here that the $\boldsymbol{\mathcal{G}}_2$ term is identical in magnitude and direction to the $\boldsymbol{\mathcal{C}}_2$ term. Additionally, hidden between the term is a BAC-CAB rule. Specifically, in the $\boldsymbol{\mathcal{C}}_2$ after some of the terms integrate to zero, the final unit vectors can be written as $\hat{\boldsymbol{r}}(\hat{\boldsymbol{x}} \cdot \hat{\boldsymbol{\phi}})$. Similarly, within the $\boldsymbol{\mathcal{G}}_2$ term we can write it as $\hat{\boldsymbol{\phi}}(\hat{\boldsymbol{x}} \cdot \hat{\boldsymbol{r}})$. All other factors in between the two terms are identical, with the exception that the $\boldsymbol{\mathcal{G}}_2$ term has a negative sign in front. Thus, using the BAC-CAB rule in reverse, we could show that in the end these two integrals could combine to form a single integral that contains the vector triple product $\hat{\boldsymbol{x}} \times (\hat{\boldsymbol{r}} \times \hat{\boldsymbol{\phi}})$. This implies that the Coriolis case is completely governed by gravitomagnetism.

B.4 Centrifugal Case:3 $\boldsymbol{\mathcal{B}}$ Term

We are left to evaluate the following integral for the $\boldsymbol{\mathcal{B}}_3$ term in Case:3:

$$\boldsymbol{\mathcal{B}}_3 = 4\frac{G}{c^2}R^2\sigma s \int_\Omega \mathrm{d}\Omega \sin\theta \cos\phi \hat{\boldsymbol{r}} \tag{B.27}$$

After expanding out $\hat{\boldsymbol{r}}$ and the integral we get:

$$\boldsymbol{\mathcal{B}}_3 = 4\frac{G}{c^2}R^2\sigma s \int_0^{2\pi} \mathrm{d}\phi \int_0^{\pi} \mathrm{d}\theta \sin^2\theta \cos\phi(\cos\phi \sin\theta \hat{\boldsymbol{x}} + \sin\phi \sin\theta \hat{\boldsymbol{y}} + \cos\theta \hat{\boldsymbol{z}}). \tag{B.28}$$

The third term will have an integral over $\cos\phi$ from 0 to 2π. This of course is equal to zero. The second term will have the product of $\sin\phi\cos\phi$ integrated over $\phi = [0, 2\pi]$. Appendix A.6 has details on how this term will also be evaluated to zero.

Therefore, the only term left makes $\boldsymbol{\mathcal{B}}$ equal to:

$$\boldsymbol{\mathcal{B}}_3 = 4\frac{G}{c^2}R^2\sigma s \int_0^{2\pi} \mathrm{d}\phi \cos^2\phi \int_0^{\pi} \mathrm{d}\theta \sin^3\theta \hat{\boldsymbol{x}}. \tag{B.29}$$

The antiderivative of $\cos^2\phi$ is $\frac{1}{2}(\phi + \sin\phi\cos\phi)$, the second term in the antiderivative will be zero because of the sine factor. So the integration over ϕ will yield a

factor of π. For the integration over θ we can once again use Appendix A.3 to yield a factor of 4/3. Replacing s with x_A/R, we have:

$$\boxed{\boldsymbol{\mathcal{B}}_3 = \frac{16\pi}{3}\frac{G\sigma\omega^2 R x_A}{c^2}\hat{\boldsymbol{x}}}. \tag{B.30}$$

B.5 Centrifugal Case:3 $\boldsymbol{\mathcal{D}}$ Term

For the $\boldsymbol{\mathcal{D}}_3$ term in the centrifugal case we have this integral to solve:

$$\boldsymbol{\mathcal{D}}_3 = -\frac{3}{2}\frac{G}{c^2}R^2\sigma\int_\Omega \mathrm{d}\Omega\frac{(s\omega R\sin\theta\sin\phi)^2}{R^2}\hat{\boldsymbol{r}}. \tag{B.31}$$

With $\hat{\boldsymbol{r}} = \cos\phi\sin\theta\hat{\boldsymbol{x}} + \sin\phi\sin\theta\hat{\boldsymbol{y}} + \cos\theta\hat{\boldsymbol{z}}$, the integral will have three terms. Evaluating the integral over ϕ for each of them yields:

$$\boldsymbol{\mathcal{D}}_3 = -\frac{3}{2}\frac{G}{c^2}R^2\sigma s^2\omega^2\int_0^{2\pi}\mathrm{d}\phi\int_0^{\pi}\mathrm{d}\theta\sin^3\theta\sin^2\phi(\cos\phi\sin\theta\hat{\boldsymbol{x}} + \sin\phi\sin\theta\hat{\boldsymbol{y}} + \cos\phi\hat{\boldsymbol{z}}). \tag{B.32}$$

From Appendix A.3 the integrals over ϕ for the first and second terms are simply 0. From the same appendix, we know that for the third term the integral over θ is equal to 4/3. This leaves the term as:

$$\boldsymbol{\mathcal{D}}_3 = -2\frac{G}{c^2}R^2\sigma s^2\omega^2\int_0^{2\pi}\mathrm{d}\phi\sin^2\phi\cos\phi\hat{\boldsymbol{z}}. \tag{B.33}$$

With the u substitutions of $\sin\phi \to u$ and $\cos\phi d\phi \to \mathrm{d}u$ we get:

$$\boldsymbol{\mathcal{D}}_3 = -2\frac{G}{c^2}R^2\sigma s^2\omega^2\int_{\sin 0}^{\sin\pi}u^2\mathrm{d}u\hat{\boldsymbol{z}}. \tag{B.34}$$

Which of course equals zero:

$$\boxed{\boldsymbol{\mathcal{D}}_3 = \mathbf{0}}. \tag{B.35}$$

B.6 Centrifugal Case:3 $\boldsymbol{\mathcal{G}}$ Term

In the centrifugal case, we were able to simplify its $\boldsymbol{\mathcal{G}}_3$ term to be:

$$\boldsymbol{\mathcal{G}}_3 = -3\frac{G}{c^2}\sigma \int_\Omega \mathrm{d}\Omega s\omega R \sin\theta \sin\phi \boldsymbol{v}. \tag{B.36}$$

Now recalling that $\boldsymbol{v} = \omega R(\sin\theta\hat{\boldsymbol{\phi}} + s\hat{\boldsymbol{y}})$, the integral we now need to solve is:

$$\int_\Omega \mathrm{d}\Omega \sin\theta \sin\phi(\sin\theta\hat{\boldsymbol{\phi}} + s\hat{\boldsymbol{y}}) = \int_0^{2\pi} \mathrm{d}\phi \int_0^{\pi} \mathrm{d}\theta \sin^2\theta \sin\phi(\sin\theta\hat{\boldsymbol{\phi}} + s\hat{\boldsymbol{y}}). \tag{B.37}$$

The second term in the integral has an integration over ϕ only of $\sin\phi$ for a full period. This of course is equal to zero. The first term requires an integral of $\sin^2\theta$ over θ. We can use Appendix A.3 to find it equal to 4/3. Now our integral looks like:

$$\int_\Omega \mathrm{d}\Omega \sin\theta \sin\phi(\sin\theta\hat{\boldsymbol{\phi}} + s\hat{\boldsymbol{y}}) = \frac{4}{3}\int_0^{2\pi} \mathrm{d}\phi \sin\phi\hat{\boldsymbol{\phi}}. \tag{B.38}$$

The conversion of $\hat{\boldsymbol{\phi}}$ into rectilinear unit vectors is $\hat{\boldsymbol{\phi}} = -\sin\phi\hat{\boldsymbol{x}} + \cos\phi\hat{\boldsymbol{y}}$ makes the integral:

$$\frac{4}{3}\int_0^{2\pi} \mathrm{d}\phi \sin\phi\hat{\boldsymbol{\phi}} = \frac{4}{3}\int_0^{2\pi} \mathrm{d}\phi \sin\phi(-\sin\phi\hat{\boldsymbol{x}} + \cos\phi\hat{\boldsymbol{y}}). \tag{B.39}$$

The integral over a full period of $\sin^2\phi$ is simply π, while the integral over a full period of $\sin\phi\cos\phi$ is simply zero. This makes the whole integration simply equal to $-4\pi/3\hat{\boldsymbol{x}}$. Altogether, the final form of $\boldsymbol{\mathcal{G}}$ is:

$$\boxed{\boldsymbol{\mathcal{G}}_3 = 4\pi\frac{G\sigma\omega^2 R x_A}{c^2}\hat{\boldsymbol{x}}}. \tag{B.40}$$

B.7 Centrifugal Case:3 $\mathcal{J}$ Term

In the centrifugal case the $\boldsymbol{\mathcal{J}}_3$ term is:

$$\boldsymbol{\mathcal{J}}_3 = -\frac{1}{2}\frac{G}{c^2}R^2\sigma\omega^2 s\int_\Omega \mathrm{d}\Omega \sin\theta\cos\phi\hat{\boldsymbol{r}}. \tag{B.41}$$

Expanding out the $\hat{\boldsymbol{r}}$ and the integral we get:

$$\boldsymbol{\mathcal{J}}_3 = -\frac{1}{2}\frac{G}{c^2}R^2\sigma\omega^2 s\int_0^{2\pi}\mathrm{d}\phi\int_0^{\pi}\mathrm{d}\theta\sin^2\theta\cos\phi(\sin\theta\cos\phi\hat{\boldsymbol{x}}+\sin\theta\sin\phi\hat{\boldsymbol{y}}+\cos\theta\hat{\boldsymbol{z}}). \tag{B.42}$$

The third term has an integral of $\cos\phi$ over a full period and is therefore 0. The second term has an integral over $\sin\phi\cos\phi$ over a full period. By Appendix A.6 this is also zero. What remains is:

$$\boldsymbol{\mathcal{J}}_3 = -\frac{1}{2}\frac{G}{c^2}R^2\sigma\omega^2 s\int_0^{2\pi}\mathrm{d}\phi\int_0^{\pi}\mathrm{d}\theta\sin^3\theta\cos^2\phi\hat{\boldsymbol{x}}. \tag{B.43}$$

From Appendix A.3 we get that the integral over $\sin^3\theta$ is simply $4/3$. Then the integral of $\cos^2\phi$ over a full period is simply equal to π. This brings the total integral to:

$$\boldsymbol{\mathcal{J}}_3 = -\frac{2\pi}{3}\frac{G}{c^2}R^2\sigma\omega^2 s\hat{\boldsymbol{x}} \tag{B.44}$$

Plugging in $s = x_A/R$ we get:

$$\boxed{\boldsymbol{\mathcal{J}}_3 = -\frac{2\pi}{3}\frac{G}{c^2}R\sigma\omega^2 x_A\hat{\boldsymbol{x}}}. \tag{B.45}$$

Appendix C

Analytic Solution for I_R

There is an interesting "bump" in the Radiation curve in Figure 3.3 that happens around $Z \approx 3500$. The aim of this section is to demonstrate that the curve should be flat for all Z, and this bump is nothing but a numerical artifact. The integral (equation 3.2) to generate all the curves in Figure 3.3 was solved numerically for each point on the curves. That integral is:

$$I = 2\int_0^\infty \frac{\mathrm{d}\zeta E(\zeta)}{(1+\zeta)^4} \frac{[\int_0^{\zeta'} \mathrm{d}\zeta/E(\zeta')]^2}{\int_0^\zeta \mathrm{d}\zeta''/(1+\zeta'')E(\zeta'')} \tag{C.1}$$

We can rewrite this a bit for some clarity by recalling that the quantity in square brackets in the numerator is simply the comoving distance, $D_C(\zeta)/D_H$. Additionally, the integral in the denominator is the light travel distance $D_T(\zeta)/D_H$. The factors of the Hubble distance D_H all cancelled with each other, leaving the overall integral dimensionless. Furthermore, the $E(\zeta)$ functions are all given in reference to some epoch Z, and for a single component universe can be written as:

$$E_Z(z) = \sqrt{\Omega_{x,Z}(1+z)^{d_x}} = \sqrt{\Omega_{x,Z}}(1+z)^{d_x/2}. \tag{C.2}$$

For radiation this is simply $E_{R,Z} = \sqrt{\Omega_{R,Z}}(1+z)^4$. Given this simple form of

$E(z)$, we can evaluate the distance integrals analytically. For the comoving distance we have:

$$\frac{D_{C,R}(z)}{D_H} = \int_0^z \frac{\mathrm{d}\zeta}{\sqrt{\Omega_{R,Z}}(1+z)^2} = \frac{1}{\sqrt{\Omega_{R,Z}}}\left(\frac{z}{1+z}\right). \tag{C.3}$$

The light time travel distance becomes:

$$\frac{D_{T,R}(z)}{D_H} = \int_0^z \frac{\mathrm{d}\zeta}{\sqrt{\Omega_{R,Z}}(1+z)^3} = \frac{1}{2\sqrt{\Omega_{R,Z}}}\left[\frac{(1+z)^2-1}{(1+z)^2}\right]. \tag{C.4}$$

Plugging these values into Equation C.1 we get:

$$I_{R,Z} = 2\int_0^\infty \mathrm{d}\zeta \frac{\sqrt{\Omega_{R,Z}}(1+\zeta)^2}{(1+\zeta)^4}\left[\frac{1}{\sqrt{\Omega_{R,Z}}}\left(\frac{\zeta}{1+\zeta}\right)\right]^2\left[\frac{2\sqrt{\Omega_{R,Z}}(1+\zeta)^2}{(1+\zeta)^2-1}\right] \tag{C.5}$$

A number of factors cancel from the integrand, including all factors of $\sqrt{\Omega_{R,Z}}$. The simplified equation is:

$$I_{R,Z} = 4\int_0^\infty \mathrm{d}\zeta \frac{\zeta^2}{(1+\zeta)^2[(1+\zeta)^2]-1]} \tag{C.6}$$

The antiderivative for the integral provided by WolframAlpha is:

$$\frac{1}{1+\zeta} + 2\ln\left(\frac{1+\zeta}{2+\zeta}\right) \tag{C.7}$$

Evaluated at $\zeta = \infty$ the first term is zero while the second term becomes $2\ln(1)$ which is also zero. Evaluated at $\zeta = 0$ the first term is simply 1, while the second term becomes $-\ln 4$. Multiplying by the overall factor of 4 the integral is:

$$\boxed{I_{R,Z} = 4(\ln 4 - 1) \approx 1.55}. \tag{C.8}$$

This is constant for the integral as evaluated from any epoch Z. Because this is a constant, the bump in Figure 3.3, must be the result of the numerical integration. Furthermore, since a similar integration technique was used to generate the $\xi(Z)$

function as presented in Figure 4.1, it is reasonably assumed that the "glitch" in that plot is the result of a numerical instability in that region.

Bibliography

[AAA+20] N. Aghanim, Y. Akrami, M. Ashdown, J. Aumont, C. Baccigalupi, M. Ballardini, A. J. Banday, R. B. Barreiro, N. Bartolo, S. Basak, R. Battye, K. Benabed, J.-P. Bernard, M. Bersanelli, P. Bielewicz, J. J. Bock, J. R. Bond, J. Borrill, F. R. Bouchet, F. Boulanger, M. Bucher, C. Burigana, R. C. Butler, E. Calabrese, J.-F. Cardoso, J. Carron, A. Challinor, H. C. Chiang, J. Chluba, L. P. L. Colombo, C. Combet, D. Contreras, B. P. Crill, F. Cuttaia, P. de Bernardis, G. de Zotti, J. Delabrouille, J.-M. Delouis, E. Di Valentino, J. M. Diego, O. Doré , M. Douspis, A. Ducout, X. Dupac, S. Dusini, G. Efstathiou, F. Elsner, T. A. Enßlin, H. K. Eriksen, Y. Fantaye, M. Farhang, J. Fergusson, R. Fernandez-Cobos, F. Finelli, F. Forastieri, M. Frailis, A. A. Fraisse, E. Franceschi, A. Frolov, S. Galeotta, S. Galli, K. Ganga, R. T. Génova-Santos, M. Gerbino, T. Ghosh, J. González-Nuevo, K. M. Górski, S. Gratton, A. Gruppuso, J. E. Gudmundsson, J. Hamann, W. Handley, F. K. Hansen, D. Herranz, S. R. Hildebrandt, E. Hivon, Z. Huang, A. H. Jaffe, W. C. Jones, A. Karakci, E. Keihänen, R. Keskitalo, K. Kiiveri, J. Kim, T. S. Kisner, L. Knox, N. Krachmalnicoff, M. Kunz, H. Kurki-Suonio, G. Lagache, J.-M. Lamarre, A. Lasenby, M. Lattanzi, C. R. Lawrence, M. Le Jeune, P. Lemos, J. Lesgourgues, F. Levrier, A. Lewis, M. Liguori, P. B. Lilje, M. Lilley, V. Lindholm, M. López-Caniego, P. M. Lubin, Y.-Z. Ma, J. F. Macías-Pérez, G. Maggio, D. Maino, N. Mandolesi, A. Mangilli, A. Marcos-Caballero, M. Maris, P. G. Martin, M. Martinelli, E. Martínez-González, S. Matarrese, N. Mauri, J. D. McEwen, P. R. Meinhold, A. Melchiorri, A. Mennella, M. Migliaccio, M. Millea, S. Mitra, M.-A. Miville-Deschênes, D. Molinari, L. Montier, G. Morgante,

A. Moss, P. Natoli, H. U. Nørgaard-Nielsen, L. Pagano, D. Paoletti, B. Partridge, G. Patanchon, H. V. Peiris, F. Perrotta, V. Pettorino, F. Piacentini, L. Polastri, G. Polenta, J.-L. Puget, J. P. Rachen, M. Reinecke, M. Remazeilles, A. Renzi, G. Rocha, C. Rosset, G. Roudier, J. A. Rubiño-Martín, B. Ruiz-Granados, L. Salvati, M. Sandri, M. Savelainen, D. Scott, E. P. S. Shellard, C. Sirignano, G. Sirri, L. D. Spencer, R. Sunyaev, A.-S. Suur-Uski, J. A. Tauber, D. Tavagnacco, M. Tenti, L. Toffolatti, M. Tomasi, T. Trombetti, L. Valenziano, J. Valiviita, B. Van Tent, L. Vibert, P. Vielva, F. Villa, N. Vittorio, B. D. Wandelt, I. K. Wehus, M. White, S. D. M. White, A. Zacchei, and A. Zonca. Planck 2018 results VI. cosmological parameters. *Astronomy &Astrophysics*, 641:A6, sep 2020.

[ABB+23] C. Altucci, F. Bajardi, A. Basti, N. Beverini, S. Capozziello, G. Carelli, D. Ciampini, G. De Luca, R. Devoti, G. Di Stefano, A.D.V. Di Virgilio, F. Fuso, U. Giacomelli, A. Govoni, E. Maccioni, P. Marsili, A. Ortolan, A. Porzio, A. Simonelli, G. Terreni, and R. Velotta. *The GINGER Project – Preliminary Results*, pages 3956–3962. World Scientific Publishing Company, 2023.

[Abr90] M. A. Abramowicz. Centrifugal force - a few surprises. *Monthly Notices of the Royal Astronomical Society*, 245:733, August 1990.

[aPARAAAC+14] and P. A. R. Ade, N. Aghanim, C. Armitage-Caplan, M. Arnaud, M. Ashdown, F. Atrio-Barandela, J. Aumont, C. Baccigalupi, A. J. Banday, R. B. Barreiro, J. G. Bartlett, E. Battaner, K. Benabed, A. Benoî t, A. Benoit-Lévy, J.-P. Bernard, M. Bersanelli, P. Bielewicz, J. Bobin, J. J. Bock, A. Bonaldi, J. R. Bond, J. Borrill, F. R. Bouchet, M. Bridges, M. Bucher, C. Burigana, R. C. Butler, E. Calabrese, B. Cappellini, J.-F. Cardoso, A. Catalano, A. Challinor, A. Chamballu, R.-R. Chary, X. Chen, H. C. Chiang, L.-Y Chiang, P. R. Christensen, S. Church, D. L. Clements, S. Colombi, L. P. L. Colombo, F. Couchot, A. Coulais, B. P. Crill, A. Curto, F. Cuttaia, L. Danese, R. D. Davies, R. J. Davis, P. de Bernardis, A. de Rosa, G. de Zotti, J. Delabrouille, J.-M. Delouis, F.-X. Désert, C. Dickinson, J. M. Diego, K. Dolag, H. Dole, S. Donzelli, O. Doré, M. Douspis, J. Dunkley, X. Dupac, G. Efstathiou, F. Elsner, T. A. Enßlin, H. K. Erik-

sen, F. Finelli, O. Forni, M. Frailis, A. A. Fraisse, E. Franceschi, T. C. Gaier, S. Galeotta, S. Galli, K. Ganga, M. Giard, G. Giardino, Y. Giraud-Héraud, E. Gjerløw, J. González-Nuevo, K. M. Górski, S. Gratton, A. Gregorio, A. Gruppuso, J. E. Gudmundsson, J. Haissinski, J. Hamann, F. K. Hansen, D. Hanson, D. Harrison, S. Henrot-Versillé, C. Hernández-Monteagudo, D. Herranz, S. R. Hildebrandt, E. Hivon, M. Hobson, W. A. Holmes, A. Hornstrup, Z. Hou, W. Hovest, K. M. Huffenberger, A. H. Jaffe, T. R. Jaffe, J. Jewell, W. C. Jones, M. Juvela, E. Keihänen, R. Keskitalo, T. S. Kisner, R. Kneissl, J. Knoche, L. Knox, M. Kunz, H. Kurki-Suonio, G. Lagache, A. Lähteenmäki, J.-M. Lamarre, A. Lasenby, M. Lattanzi, R. J. Laureijs, C. R. Lawrence, S. Leach, J. P. Leahy, R. Leonardi, J. León-Tavares, J. Lesgourgues, A. Lewis, M. Liguori, P. B. Lilje, M. Linden-Vørnle, M. López-Caniego, P. M. Lubin, J. F. Macías-Pérez, B. Maffei, D. Maino, N. Mandolesi, M. Maris, D. J. Marshall, P. G. Martin, E. Martínez-González, S. Masi, M. Massardi, S. Matarrese, F. Matthai, P. Mazzotta, P. R. Meinhold, A. Melchiorri, J.-B. Melin, L. Mendes, E. Menegoni, A. Mennella, M. Migliaccio, M. Millea, S. Mitra, M.-A. Miville-Deschênes, A. Moneti, L. Montier, G. Morgante, D. Mortlock, A. Moss, D. Munshi, J. A. Murphy, P. Naselsky, F. Nati, P. Natoli, C. B. Netterfield, H. U. Nørgaard-Nielsen, F. Noviello, D. Novikov, I. Novikov, I. J. O'Dwyer, S. Osborne, C. A. Oxborrow, F. Paci, L. Pagano, F. Pajot, R. Paladini, D. Paoletti, B. Partridge, F. Pasian, G. Patanchon, D. Pearson, T. J. Pearson, H. V. Peiris, O. Perdereau, L. Perotto, F. Perrotta, V. Pettorino, F. Piacentini, M. Piat, E. Pierpaoli, D. Pietrobon, S. Plaszczynski, P. Platania, E. Pointecouteau, G. Polenta, N. Ponthieu, L. Popa, T. Poutanen, G. W. Pratt, G. Prézeau, S. Prunet, J.-L. Puget, J. P. Rachen, W. T. Reach, R. Rebolo, M. Reinecke, M. Remazeilles, C. Renault, S. Ricciardi, T. Riller, I. Ristorcelli, G. Rocha, C. Rosset, G. Roudier, M. Rowan-Robinson, J. A. Rubiño-Martín, B. Rusholme, M. Sandri, D. Santos, M. Savelainen, G. Savini, D. Scott, M. D. Seiffert, E. P. S. Shellard, L. D. Spencer, J.-L. Starck, V. Stolyarov, R. Stompor, R. Sudiwala, R. Sunyaev, F. Sureau, D. Sutton, A.-S. Suur-Uski, J.-F. Sygnet, J. A. Tauber, D. Tavagnacco, L. Terenzi, L. Toffolatti, M. Tomasi, M. Tris-

tram, M. Tucci, J. Tuovinen, M. Türler, G. Umana, L. Valenziano, J. Valiviita, B. Van Tent, P. Vielva, F. Villa, N. Vittorio, L. A. Wade, B. D. Wandelt, I. K. Wehus, M. White, S. D. M. White, A. Wilkinson, D. Yvon, A. Zacchei, and A. Zonca. Planck 2013 results. XVI. cosmological parameters. *Astronomy & Astrophysics*, 571:A16, oct 2014.

[AS14] A. Avilez and C. Skordis. Cosmological constraints on Brans-Dicke theory. *Physical Review Letters*, 113(1), jul 2014.

[BD61] C. Brans and R. H. Dicke. Mach's principle and a relativistic theory of gravitation. *Physical Review*, 124(3):925–935, November 1961.

[BGF17] Simen Braeck, Øyvind G. Grøn, and Ivar Farup. The cosmic causal mass. *Universe*, 3(2), 2017.

[BH18] Gianfranco Bertone and Dan Hooper. History of dark matter. *Rev. Mod. Phys.*, 90:045002, Oct 2018.

[BP95] Julian B. Barbour and Herbert Pfister, editors. *Mach's Principle: From Newton's Bucket to Quantum Gravity*. Birkhäuser, Boston, Basel, Berlin, 1995.

[Bra14] C. H. Brans. Jordan-Brans-Dicke Theory. *Scholarpedia*, 9(4):31358, 2014. revision #151619.

[BS97] Hermann Bondi and Joseph Samuel. The Lense-Thirring effect and Mach's principle. *Physics Letters A*, 228(3):121–126, apr 1997.

[BSG+19] S. Böhm, M. Schartner, A. Gebauer, T. Klügel, U. Schreiber, and T. Schüler. Earth rotation variations observed by VLBI and the Wettzell "G" ring laser during the CONT17 campaign. *Advances in Geosciences*, 50:9–15, 2019.

[CN15] L Filipe O Costa and José Natário. Inertial forces in general relativity. *Journal of Physics: Conference Series*, 600(1):012053, mar 2015.

[CS70] Jeffrey Mark Cohen and William J. Sarill. Centrifugal force and general relativity. *Nature*, 228:849–849, 1970.

[DLCI68] V. De La Cruz and W. Israel. Spinning shell as a source of the Kerr metric. *Phys. Rev., 170: 1187-92(June 25, 1968).*, 170(5), 1 1968.

[DSZ21] Guido D'Amico, Leonardo Senatore, and Pierre Zhang. Limits on wCDM from the EFTofLSS with the PyBird code. *Journal of Cosmology and Astroparticle Physics*, 2021(01):006, jan 2021.

[DV20] Angela D. V. Di Virgilio. Sagnac gyroscopes and the GINGER project. *Frontiers in Astronomy and Space Sciences*, 7, 2020.

[EIH38] A. Einstein, L. Infeld, and B. Hoffmann. The gravitational equations and the problem of motion. *Annals of Mathematics*, 39(1):65–100, 1938.

[Gos17] Gopi Kant Goswami. Cosmological parameters for spatially flat dust filled universe in brans-dicke theory. *Research in Astronomy and Astrophysics*, 17(3):27, 2017.

[Gre68a] G. S. Greenstein. Brans-Dicke cosmology. *Astrophysical Letters*, 1:139, January 1968.

[Gre68b] George S. Greenstein. Brans-Dicke cosmology, II. *Astrophysics and Space Science*, 2(2):155–165, October 1968.

[Hog99] David W Hogg. Distance measures in cosmology. *arXiv preprint astro-ph/9905116*, 1999.

[Jon06] Rickard M. Jonsson. An intuitive approach to inertial forces and the centrifugal force paradox in general relativity. *American Journal of Physics*, 74(10):905–916, oct 2006.

[Kee02] William C. Keel. *The Road to Galaxy Formation*. Praxis Publishing, Cornwall, 2002.

[KR22] Marc Kamionkowski and Adam G Riess. The Hubble tension and early dark energy. *arXiv preprint arXiv:2211.04492*, 2022.

[Kra78] Andrzej Krasiński. Ellipsoidal space-times, sources for the Kerr metric. *Annals of Physics*, 112(1):22–40, 1978.

[KRA+08] M. Kowalski, D. Rubin, G. Aldering, R. J. Agostinho, A. Amadon, R. Amanullah, C. Balland, K. Barbary, G. Blanc, P. J. Challis, A. Conley, N. V. Connolly, R. Covarrubias, K. S. Dawson, S. E. Deustua, R. Ellis, S. Fabbro, V. Fadeyev, X. Fan, B. Farris, G. Folatelli, B. L. Frye, G. Garavini, E. L. Gates, L. Germany, G. Goldhaber, B. Goldman, A. Goobar, D. E. Groom, J. Haissinski, D. Hardin, I. Hook, S. Kent, A. G. Kim, R. A. Knop, C. Lidman, E. V. Linder, J. Mendez, J. Meyers, G. J. Miller, M. Moniez, A. M. Mourã o, H. Newberg, S. Nobili, P. E. Nugent, R. Pain, O. Perdereau, S. Perlmutter, M. M. Phillips, V. Prasad, R. Quimby, N. Regnault, J. Rich, E. P. Rubenstein, P. Ruiz-Lapuente, F. D. Santos, B. E. Schaefer, R. A. Schommer, R. C. Smith, A. M. Soderberg, A. L. Spadafora, L.-G. Strolger, M. Strovink, N. B. Suntzeff, N. Suzuki, R. C. Thomas, N. A. Walton, L. Wang, W. M. Wood-Vasey, and J. L. Yun and. Improved cosmological constraints from new, old, and combined supernova data sets. *The Astrophysical Journal*, 686(2):749–778, oct 2008.

[KT90] Edward W. Kolb and Michael S. Turner. *The Early Universe*. Addison-Wesley Publishing Company, Reading, 1990.

[Maj17] Fatemeh Zahra Majidi. Another kerr interior solution. *arXiv preprint arXiv:1705.00584*, 2017.

[Mau12] Tim Maudlin. *Philosophy of Physics: Space and Time*. Princeton University Press, 2012.

[MNT07] T. W. Murphy, K. Nordtvedt, and S. G. Turyshev. Gravitomagnetic influence on gyroscopes and on the lunar orbit. *Physical Review Letters*, 98(7), feb 2007.

[MTW73] C. W. Misner, K. S. Thorne, and J. A. Wheeler. *Gravitation*. 1973.

[Nar83] J.V. Narlikar. Cosmologies with variable gravitational constant. *Foundations of Physics*, 13(3), mar 1983.

[OOKH75] Hiroshi Okamura, Tadayuki Ohta, Toshiei Kimura, and Kichiro Hiida. Einstein's theory of relativity and Mach's principle. *Progress of Theoretical Physics*, 54(6):1872–1878, 12 1975.

[PAG+99] S. Perlmutter, G. Aldering, G. Goldhaber, R. A. Knop, P. Nugent, P. G. Castro, S. Deustua, S. Fabbro, A. Goobar, D. E. Groom, I. M. Hook, A. G. Kim, M. Y. Kim, J. C. Lee, N. J. Nunes, R. Pain, C. R. Pennypacker, R. Quimby, C. Lidman, R. S. Ellis, M. Irwin, R. G. McMahon, P. Ruiz-Lapuente, N. Walton, B. Schaefer, B. J. Boyle, A. V. Filippenko, T. Matheson, A. S. Fruchter, N. Panagia, H. J. M. Newberg, W. J. Couch, and The Supernova Cosmology Project. Measurements of Ω and Λ from 42 high-redshift supernovae. *The Astrophysical Journal*, 517(2):565–586, jun 1999.

[PB86] H Pfister and K H Braun. A mass shell with flat interior cannot rotate rigidly. *Classical and Quantum Gravity*, 3(3):335, may 1986.

[Pee76] P. J. E. Peebles. *Principles of Physical Cosmology*. Princeton University Press, Princeton, 1976.

[PFWB21] Ryan S. Park, William M. Folkner, James G. Williams, and Dale H. Boggs. The JPL planetary and lunar ephemerides DE440 and DE441. *The Astronomical Journal*, 161(3):105, feb 2021.

[PGVdCPMP19] Joan Solà Peracaula, Adrià Gómez-Valent, Javier de Cruz Pérez, and Cristian Moreno-Pulido. Brans–Dicke gravity with a cosmological constant smoothes out ΛCDM tensions. *The Astrophysical Journal*, 886(1):L6, nov 2019.

[PS22] L. Perivolaropoulos and F. Skara. Challenges for ΛCDM: An update. *New Astronomy Reviews*, 95:101659, dec 2022.

[PSKK19] Vivian Poulin, Tristan L. Smith, Tanvi Karwal, and Marc Kamionkowski. Early dark energy can resolve the Hubble tension. *Physical Review Letters*, 122(22), jun 2019.

[RCY+19] Adam G. Riess, Stefano Casertano, Wenlong Yuan, Lucas M. Macri, and Dan Scolnic. Large Magellanic cloud cepheid standards provide a 1% foundation for the determination of the Hubble constant and stronger evidence for physics beyond ΛCDM. *The Astrophysical Journal*, 876(1):85, may 2019.

[RFC+98] Adam G. Riess, Alexei V. Filippenko, Peter Challis, Alejandro Clocchiatti, Alan Diercks, Peter M. Garnavich, Ron L. Gilliland,

Craig J. Hogan, Saurabh Jha, Robert P. Kirshner, B. Leibundgut, M. M. Phillips, David Reiss, Brian P. Schmidt, Robert A. Schommer, R. Chris Smith, J. Spyromilio, Christopher Stubbs, Nicholas B. Suntzeff, and John Tonry. Observational evidence from supernovae for an accelerating universe and a cosmological constant. *The Astronomical Journal*, 116(3):1009–1038, sep 1998.

[Rin94] Wolfgang Rindler. The Lense-Thirring effect exposed as anti-Machian. *Physics Letters A*, 187(3):236–238, 1994.

[RSC+07] Adam G. Riess, Louis-Gregory Strolger, Stefano Casertano, Henry C. Ferguson, Bahram Mobasher, Ben Gold, Peter J. Challis, Alexei V. Filippenko, Saurabh Jha, Weidong Li, John Tonry, Ryan Foley, Robert P. Kirshner, Mark Dickinson, Emily MacDonald, Daniel Eisenstein, Mario Livio, Josh Younger, Chun Xu, Tomas Dahlén, and Daniel Stern. New Hubble space telescope discoveries of type Ia supernovae at $z \geq 1$: Narrowing constraints on the early behavior of dark energy. *Astrophysical Journal*, 659(1):98–121, April 2007.

[SAS+22] Nils Schöneberg, Guillermo Franco Abellán, Andrea Pérez Sánchez, Samuel J. Witte, Vivian Poulin, and Julien Lesgourgues. The H_0 olympics: A fair ranking of proposed models. *Physics Reports*, 984:1–55, oct 2022.

[Sch09] Bernard Schutz. *A First Course In General Relativity*. Cambridge University Press, Cambridge, 2009.

[Sci53] D. W. Sciama. On the origin of inertia. *Monthly Notices of the Royal Astronomical Society*, 113(1):34–42, 02 1953.

[Sel75] Samuel M. Seleby, editor. *Standard Mathematical Tables*. CRC Press, Inc., Cleveland, 1975.

[ST21] Toyokazu Sekiguchi and Tomo Takahashi. Early recombination as a solution to the H_0 tension. *Physical Review D*, 103(8), apr 2021.

[VTB+22] A. D. V. Di Virgilio, G. Terreni, A. Basti, N. Beverini, G. Carelli, D. Ciampini, F. Fuso, E. Maccioni, P. Marsili, J. Kodet, and K. U. Schreiber. Overcoming 1 part in 10^9 of earth angular rotation rate

measurement with the G Wettzell data. *The European Physical Journal C*, 82(9), sep 2022.

[Wei08] Steven Weinberg. *Cosmology*. Oxford University Press, New Delhi, 2008.

[Wil95] C. M. Will. *Theory and Experiment in Gravitational Physics*. University Cambridge, Cambridge, 1995.

[Wil11] Clifford M. Will. On the unreasonable effectiveness of the post-Newtonian approximation in gravitational physics. *Proceedings of the National Academy of Sciences*, 108(15):5938–5945, mar 2011.

[WND96] J. G. Williams, X. X. Newhall, and J. O. Dickey. Relativity parameters determined from lunar laser ranging. *Phys. Rev. D*, 53:6730–6739, Jun 1996.